Corrosion Initiation of Concrete Bridge Elements Exposed to De-icing Salts

Robert Wolofsky

November 2011

Department of Civil Engineering and Applied Mechanics
McGill University
Montreal, Canada

A thesis submitted to the
Faculty of Graduate Studies and Research
in partial fulfillment of the requirements for the
Degree of Master of Engineering

Corrosion Initiation of Concrete Bridge Elements Exposed to De-icing Salts

Abstract

A large portion of bridges in North America was built 50 to 75 years ago, designed with a similar service lifespan. As a result, many existing bridges require full inspections, repairs, retrofitting or decommissioning. With limited resources available, it is crucial that maintenance strategies and rehabilitations are planned accordingly. To do so, designers, engineers and owners must be informed on the timeframe of the degradation process. Deterioration of reinforced concrete bridges is strongly associated with corrosion of steel caused by the application of deicing salts. In Montreal, the severity and duration of the winter period is a major concern. Motorists require safe roads to commute, thus large quantities of salt are spread each winter season to achieve bare pavement. The chlorides from the deicing salt enter the concrete and destroy the passive oxide layer protecting the reinforcing steel, making the steel vulnerable to corrosion. In this work, the "TransChlor" computer software was used to simulate chloride ion ingress into concrete cover. A climatic model for Montreal weather was used in the simulations to accurately portray real life environmental conditions. Cumulative probability distributions for corrosion initiation with respect to time and embedment depths were produced for mist, direct, and splash exposure conditions.

Key words: Montreal, Quebec, TransChlor model, reinforced concrete structure, bridge, maintenance, climate, exposure, deicing salt, chloride ion ingress, corrosion.

Résumé

Une grande partie des ponts en Amérique du Nord a été construite il y a 50 à 75 ans, et conçus avec une durée de vie de service similaire. En conséquence, de nombreux ponts existants requièrent des inspections complètes, des réparations, lune modernisation ou un déclassement. Avec les ressources limitées disponibles, il est essentiel que des stratégies de maintenance et de réhabilitation soient planifiées. Pour ce faire, les concepteurs, les ingénieurs et les propriétaires doivent être informés sur les processus de dégradation. La détérioration des ponts en béton armé est fortement associée à la corrosion de l'acier par l'application de sels de déglaçage. À Montréal, la sévérité et la durée de la période hivernale est un problème majeur. Les automobilistes ont besoin des routes sûres et, une grande quantité de sel est utilisée chaque hiver pour déglacer les routes. Les chlorures provenant du sel de déglaçage pénètrent le béton et détruisent la couche d'oxyde passive qui protège l'acier d'armature, et rend l'acier plus vulnérable à la corrosion. Dans ce travail, le logiciel "TransChlor" a été utilisé pour simuler la pénétration des ions chlorures dans la couverture de béton. Un modèle climatique de Montréal pour la météorologie a été utilisé dans les simulations pour représenter exactement les conditions réelles de l'environnement. Les distributions de probabilité cumulative du temps requis pour l'initiation de la corrosion ont été obtenus en fonction de la couverture de béton pour des conditions d'exposition de brouillard, d'exposition directe, et par éclaboussures.

Mots clés: Montréal, Québec, le modèle "TransChlor", structure en béton armé, pont, maintenance, le climat, l'exposition, le sel de déglaçage, l'infiltration des ions chlorure, la corrosion.

Acknowledgements

I would like to express my sincerest gratitude to Professor Chouinard for his support and guidance, who helped me achieve my goals and reach my absolute potential. Professor Chouinard is an expert in the field of probabilistic and statistical science, and as such, has shown me that problems affecting a concrete structure, which is a topic with much inherent variability, can be successfully modeled.

I would also like to express my deepest thankfulness to David Conciatori, who contributed a lot of his time and energy in developing the TransChlor model as well as aiding me in completing this dissertation. I could not have done it without his help and wish him all the success in his career.

I would like to thank the entire McGill civil engineering department who has assisted in the success of this thesis. It is an honor to have had the privileged to be educated by some of the finest Professors this nation has to offer and I take great pride in having been both an undergraduate and a postgraduate student under their guidance.

I would like to acknowledge the research grant provided by the NSERC CREATE program, data provided by the MTQ and Environment Canada, and resources from Laval University and École Polytechnique, which supported the completion of this thesis.

Most importantly, I would like to express my most heartfelt thanks and love to my entire family and friends, who has shown me immensurable support and encouragement throughout this lengthy and demanding process. Without there influences, I would not be the man I am today.

To all engineering students everywhere, always strive forward for your goals and never give up because as hard as the road might be, you can succeed. I always say, if someone else can do it, so can you!

Table of Contents

List of Figures

List of Tables

Chapter 1

Introduction

1.1 Background

Reinforced concrete is the most widely used construction material around the world. It is the most durable and versatile composite material, and can be used for almost any structural member, ranging from small streets to large bridges to tall buildings. It can also be used to make poles, pipes, retaining walls, etc. The concrete, which resists compression forces, coupled with reinforcing steel bars, which resists tension forces, allows reinforced concrete to be able to withstand almost any force. The concrete cover also protects the steel from harsh conditions, from oil rigs in the deep ocean to severe sand storms in the desert.

Even though reinforced concrete is a very resilient construction material, the concrete is still susceptible to deterioration and the reinforcing steel to corrosion. Occasionally, the structure degrades faster than originally assumed. This can be caused by incorrect expectations in the design phase, inadequate specifications or construction and sometimes due to more undesirable conditions than originally assumed. Unfortunately, many concrete structures in the field are experiencing major damage from corrosion (Revie 2000).

All over the world, concrete bridges are extensively used in the transportation infrastructures. Citizens depend on these structures for their daily commutes and interruption in their service, for even one day, can cost society dearly. In this thesis, the major focus was on deterioration of concrete bridges exposed to de-icing salts.

Over the years, trillions of dollars and thousands of man-hours have been spent building concrete structures. As is the case of any physical material, reinforced concrete structures break down and need repairs. This requires more time, money, and energy to be spent repairing damaged highway bridges and the cost is increasing at a rate of $500 million per year (Huang and Yang 1997). In the United States, it has been estimated that the cost of damage caused only by deicing salts is between $325 and $1000 million per year to reinforced concrete bridges and car parks (Revie 2000).

As can be seen, deterioration of concrete structures is inevitable. It is therefore necessary to account for this unavoidable disturbance. Through superior maintenance strategies and planning, inconveniences to owners and impacts on society can be mitigated. Furthermore, maintenance strategies coupled with effective rehabilitation programs will require less time, money and resources compared with new construction (Pakvor 1995).

It is important that every structure has a maintenance strategy. With general inspections, maintenance and repairs, the service life of a degrading structure can drastically increase. Owners can also insure a higher structural reliability and have more confidence that the structures in service are being used safely. This is best illustrated in Figure 1.1.

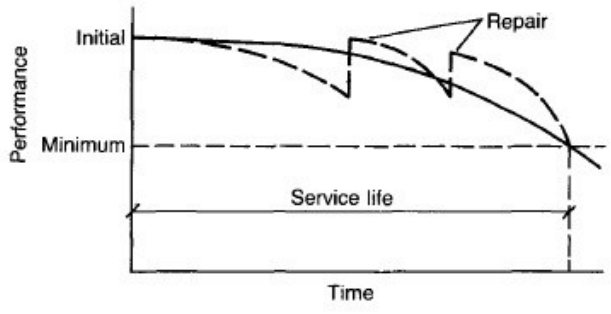

Figure 1.1: Relationship of Concrete Performance with respect to Time (CEB 1992)

The solid line represents the theoretical service life of the structure and the dotted line represents the actual state of the structure throughout its life. With regular inspections and repairs to a deteriorating structure, the minimum safety performance can be achieved for the entire service life.

Unfortunately, maintenance programs are highly neglected or are applied passively and not proactively. Inspections are only used when significant signs of deterioration occur and, thus, are already in an advanced stage of deterioration (Pakvor 1995). Even more so, advanced warning signs such as cracking and spalling are not always present. For that reason, maintenance should be done systematically at set intervals. Having a fixed schedule reduces the chance of problems becoming too severe and is the most effective preventative solution against degradation of concrete structures.

1.2 Objective and Thesis Layout

Degradation of our infrastructure is becoming a major concern. With so many structures deteriorating, it is important that old structures are analyzed for structural capacity, safety and reliability, and that newly constructed structures are designed with the future in mind. Hence, it is necessary to give designers and owners the tools necessary to produce maintenance strategies that highlight critical times in the structures service life.

As was mentioned, the main purpose of this work was on degradation of concrete overpasses subjected to deicing salts. With any chemical reaction, aggressive substances are carried from one place to the reactive component in the concrete (i.e. chloride ions from the deicing salts spread on the concrete surface move toward the reinforcing steel found in the interior). Nevertheless, even if the aggressive substance is found in the concrete, it must travel towards the reactive substance for

a reaction to occur. Hence, if no transport takes place, the reaction will not occur (CEB 1992). Therefore, understanding the transportation of aggressive agent is critical and as such, is the main objective of this dissertation.

The transport phenomenon in concrete is best illustrated in Figure 1.2. The transport of gases, water and dissolved agents depend mostly on the presence of cracks, the pore structure, and the environment conditions. However, the presence of water or moisture is by far the most important factor controlling the deterioration process (CEB 1992). For instance, the cracks and pore structure can be analogous to the roadway, whereas water can be compared to the vehicle that transports the ions and molecules. Without water, those substances will not travel very far even if there are large cracks and open pores. An exception to this analogy is carbonation-induced corrosion, which does not rely on water for transportation.

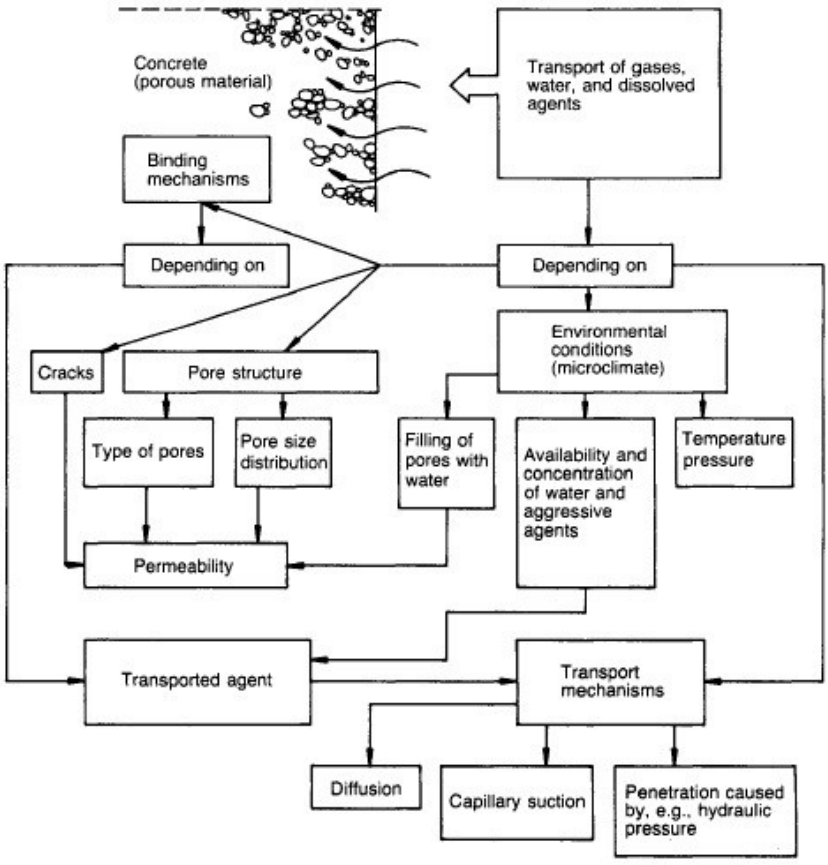

Figure 1.2: Transport of Substances in Concrete (CEB 1992)

There are two main transport processes in water, diffusion and capillary suction, which are depicted in Figures 1.3 and 1.4, respectively. Diffusion is a process that occurs in a porous material. The driving force for diffusion is the difference in concentration of an aqueous solution, and the tendency for these two concentrations to reach equilibrium. Capillary suction is more kinematic in nature. Free surfaces of the pore walls in the cement paste show a surplus of energy due to a lack of binding components to the adjacent molecules. Capillary suction drives on the surface energy produced by the pore surface (CEB 1992).

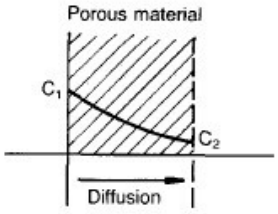

Figure 1.3: Diffusion Process

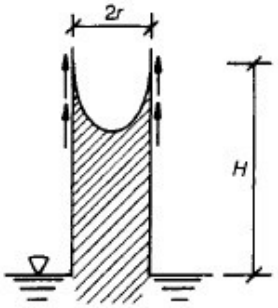

Figure 1.4: Capillary Suction Process

Chloride ion ingress is caused by both transport mechanisms discussed. Due to the binding effect of cement, some chlorides will be bounded to the paste and some will remain free in the aqueous solution. It is the free chloride ions that are of concern. When a sufficient amount of free chloride ions reach the steel reinforcement, the passive film can be destroyed. The critical chloride ion concentration needed to start depassivation depends on several parameters, such as type of steel and pH of concrete. When the oxide layer is removed, the corrosion protection will be lost and corrosion can begin.

Using the TransChlor computer software, the time to corrosion initiation of reinforcing steel subjected to chloride ions was determined. The model simulates both capillary suction and diffusion transport mechanisms. Thermal effects and carbonation reactions are also integrated in the model, and probabilities for these parameters are included to take into consideration the variability associated with concrete properties. Furthermore, the model distinguishes between exposure conditions: mist, direct and splash.

However, the major feature of TransChlor is the incorporation of real climatic data, which significantly affects the transport properties. Data for Montreals' climate was obtained from Environment Canada for the last 45 years.

The primary objective of this thesis is to provide engineers and owners with the tools needed to produce reliable maintenance strategies, and plan inspections or repairs accordingly and efficiently. To do so, one must determine the time to corrosion initiation. This is because the steel will begin corroding after this point in time and the structural capacity will start to decrease. Thus, the corrosion initiation time is a critical point in the service life a structure. The TransChlor model is perfect for this task since the main function of the simulation is the production of cumulative probability distribution curves with respect to corrosion initiation and time. To produce these curves, the model compares the chloride ion profile produced for a particular exposure condition with the depth and type of steel used. Using the cumulative probability distribution created, the time to corrosion initiation for that condition can be determined and used to estimate the life expectancy of that particular reinforcing bar under consideration.

Many different disciplines were introduced and used in this dissertation. An overview of the deterioration process of a reinforced concrete element is presented in chapter 2. This chapter focuses on the deterioration of concrete and the corrosion of reinforcement subjected to deicing salts. . Since corrosion of the reinforcing steel

is the major concern when subjected to deicing salt, it is important to understand the corrosion process. Topics in chapter 2 include critical chloride ion concentration, corrosion initiation, corrosion propagation, and structural reliability.

In chapter 3, deicing salt usage in the United States and Canada are presented. How salts function as well as the impact they have on society is discussed as well. Deicing salts are important since they keep the roadways clean and safe for motorist. However, the chloride ions in the salt attack the reinforcing steel and cause corrosion. Therefore, it was necessary to research and review salt application on the roadways.

Chapter 4 gives an overview of the modeling techniques used in this work. The core work was performed with the TransChlor computer program. TransChlor is a novel model that simulates chloride ion ingress into the concrete cover. What makes TransChlor unique is the fact that it uses real climate conditions in the simulation. Furthermore, the model distinguishes between exposure conditions. Hence, the climate, exposure and TransChlor computer model are all discussed in this chapter.

To run the simulations, climatic data sets were needed to be input into the program. Data was provided from Environment Canada, which included hourly temperature, relative humidity, solar radiation, and precipitation. In addition, data on the concrete overpass under investigation were needed. All the data sets are displayed in chapter 5.

Once all the models and data sets were in order, simulations with the TransChlor model were ready to begin. This is discussed in chapter 6. The input parameters are discussed and the TransChlor analytical process is presented. The probabilistic analyses were performed and the results are displayed as graphs showing chloride ion profiles with respect to depth or time, as well as the cumulative probability distributions curves with respect to corrosion initiation.

The discussion and conclusion are presented in chapters 7 and 8, respectively. Final thoughts, remarks and observations are presented in both chapters. A list of recommendations for future work is also provided in the final chapter.

Chapter 2

Deterioration of Reinforced Concrete Elements

2.1 General

Reinforced concrete is one of the most commonly used construction materials around the world because of its high durability. With so many structures exposed to the environment, buildings and bridges require a material that can withstand its multiple attacks. This is not to say concrete is not susceptible to deterioration. There are many different modes of attack on concrete: sulfate attack on the cement paste, alkali-silica reaction of the aggregates, freeze-thaw cycles, corrosion of the reinforcing steel, etc. Corrosion of the reinforcement is reported to be the most common degradation mechanism in concrete highways. In this thesis, the focus will be on deterioration of reinforced concrete structures caused by the corrosion of reinforcement subjected to deicing salts.

Trillions of dollars have been spent building concrete structures over the years. Just like cars break down and need repairs, so do these reinforced concrete structures. This requires more money to be spent repairing damaged highway bridges and the cost is increasing at a rate of $500 million per year (Huang and Yang 1997).

Most failures in highway structures are the result of strength degradation caused by environmental stressors. The most common environmental stressors are chemicals (i.e. chlorine ions, sulfates, carbon dioxide), moisture, and cycles of extreme temperatures. These stressors over time reduce the overall strength of the structure. The aggressiveness of the environment, the concrete and steel properties, the

amount of concrete cover, and the geometry of each section control the extent of this resistance loss (Enright and Frangopol 1998; Enright and Frangopol 2000).

The most common damaged members on a bridge are the beams, pier caps, columns and abutments. The location of damage is dependent on the structural member type, the location of the element on the structure, and lastly the source or stressor which is causing the damage (Enright and Frangopol 2000).

The reliability of a reinforced concrete structure is dependent not just on the degradation of the structural elements but also on the applied loads. If a structure does not loose its strength, its reliability can be accurately predicted with a time-variant vehicle live load model. However, this is not the case since bridges undergoes environmental attack and its resistance deteriorates over time (Enright and Frangopol 1998).

2.2 Concrete Deterioration

As was mentioned, deterioration of concrete structures caused by corrosion of reinforcement exposed to deicing salts will be discussed extensively. Carbonation also plays a small role in the deterioration of concrete structures exposed to the atmosphere and was incorporated in the model used. When analyzing the chloride induced deterioration process, there are two main stages. These two stages are corrosion initiation and corrosion propagation.

Corrosion initiation is the time frame where the steel becomes depassivated when a sufficient amount of chloride ions accumulate around the steel and corrosion is just about to begin (Kirkpatrick, Weyers et al. 2002a). This “sufficient amount of chloride ions” is referred as the critical chloride concentration and will be discussed in a later section. Corrosion propagation is the time period after corrosion has begun. During

this period there is a loss of steel and a reduction in bond between steel and concrete. Corrosion of the steel produces expansive rust products, which will cause cracking of the concrete. These cracks will continue to grow and cause subsequent spalling and delamination from the expansive pressures. Generally, there are visual signs of corrosion-induced deterioration of the concrete elements. These include rust staining, cracking, and delamination or spalling of the concrete cover. A schematic of the deterioration process can be seen in Figure 2.1.

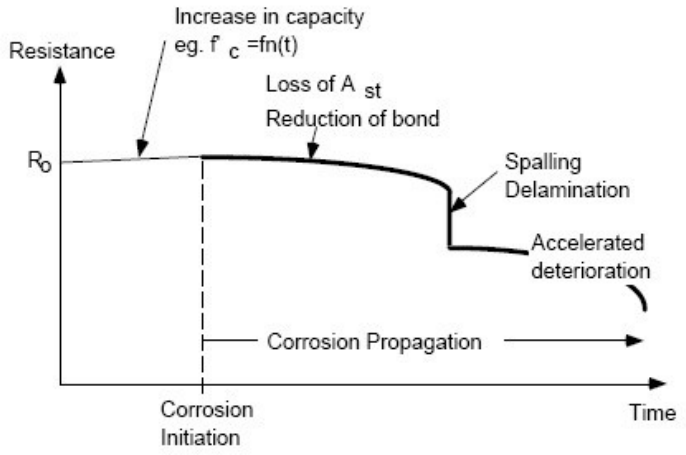

Figure 2.1: Schematic of Deterioration Process for a RC Structural Member (Stewart 2003)

As can be seen, corrosion propagation will significantly affect the long-term performance of reinforced concrete structures. The loss of steel area and debonding will cause a decrease in resistance over time, eventually causing spalling and delamination. Spalling and delamination will cause a sudden loss of resistance followed by an accelerated deterioration process. This is because the loss of the concrete cover allows easier ingress of chloride ions, moisture and oxygen (which are the main products needed to initiate and fuel corrosion) to other portions of the steel that have not began to corrode. Reduced concrete cover, low quality concrete unsuitable for the particular exposure and poor compaction and curing will often intensify the deterioration process (Stewart and Rosowsky 1998).

2.3 Corrosion of Reinforcement

The corrosion of reinforcement is the most severe problem in reinforced concrete elements. The steel reinforcement is consumed in the corrosion process, therefore lowering the amount of steel available to carry the tensile forces. The consumption of steel bars also generates corrosion products with volumes several times greater than the original steel bars. This increase in volume causes expansive pressures to build up in the concrete and tensile cracks to form. For that reason, it is important to understand how the corrosion process takes place.

Corrosion of ferrous reinforcing steel requires both moisture and oxygen to be present. Since concrete is a porous construction material, it will allow moisture and oxygen to travel through the pores and microcracks in the concrete towards the steel. Once there are sufficient amounts of oxygen and moisture, the iron in the reinforcing steel will corrode.

Corrosion of reinforcing steel in concrete is an electrochemical process that requires an electrical current to flow between an anode and cathode location (Revie 2000; Boyd 2010). The corrosion process is illustrated in Figure 2.2 and the chemical reactions are as follows:

Anode Reaction:

$$Fe \rightarrow Fe^{2+} + 2e^{-}$$

Cathode Reaction:

$$\tfrac{1}{2} O_2 + H_2O + 2e^{-} \rightarrow 2OH^{-}$$

The products from the anode and cathode combine to form:

$$Fe^{2+} + 2OH^{-} \rightarrow Fe(OH)_2$$

This new product further reacts with water and oxygen to form:

$$2Fe(OH)_2 + {}^{1}/_{2}\, O_2 + H_2O \rightarrow 2Fe(OH)_3 \rightarrow Fe_2O_3 \cdot nH_2O \ (RUST)$$

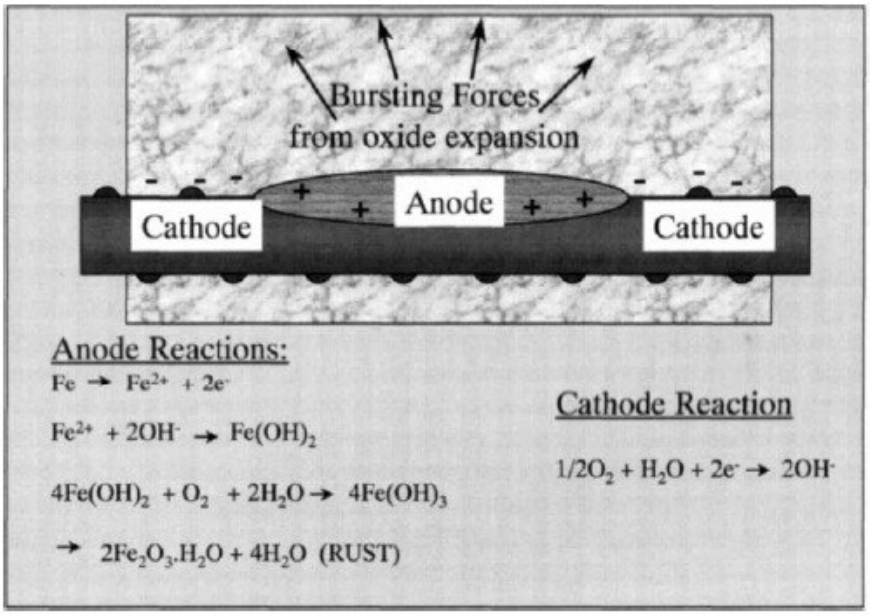

Figure 2.2: The Corrosion Process for Steel in Concrete (Revie 2000)

However, corrosion does not occur right away because the high pH of the concrete protects the steel by creating a passive oxide layer. The passivated steel is composed of a dense, stable gamma ferric oxide layer which is tightly adhering to the steel surface (Revie 2000; Boyd 2010). This protective layer limits the access of oxygen and moisture to the steel and prevents corrosion (Revie 2000; Boyd 2010).

Chloride ions and carbon dioxide are two chemicals that can enter the concrete and destroy the passive layer without first causing significant deterioration to the concrete (Revie 2000). Chloride ions are found in the deicing salts applied to bridges during the winter periods. Carbonic acid is created in concrete by reacting carbon dioxide and moisture, which are both found in the atmosphere. When dealing with bridge structures, chloride ions are more critical since they will cause depassivation of the steel much quicker than carbonation.

The passivation of the steel reinforcement can be seen in the following chemical reaction:

$$Fe(OH)_2 + O_2 \rightarrow \gamma \cdot FeOOH + H_2O$$

This reaction only occurs in a highly alkaline environment that can be found in concrete. The iron hydroxide formed at the anode is oxidized to γ•ferric hydroxide, which is the passivation film. However, if the pH drops to low, roughly 11.5, the passivation film is destroyed and corrosion can resume (Revie 2000; Boyd 2010).

As was already mentioned, depassivation of the reinforcement is caused by carbonation of the concrete and by chloride ion ingress. During carbonation, the calcium hydroxides in concrete react with the carbonic acid and convert into calcium carbonates. This will result in a drop of pH in the pore solution, which will cause the passive oxide layer to become unstable and break down. During a chloride-induced attack, the chlorides take the iron ions out of the passivation film to form rust. The chloride ions are then released in the process to continue attacking the passive oxide layer.

The depassivation of the steel reinforcement from the chloride ions is shown in the following chemical reactions:

$$Fe^{2+} + Cl^- \rightarrow [FeCl]^- + 2OH^- \rightarrow Fe(OH)_2 + Cl^-$$

Analyzing the chemical reactions, one can see that the chlorides are not consumed in the process. Furthermore, the chloride ions are not used in the formation of rust. Therefore, once there are sufficient chlorides present, the chemical reaction will not require additional chloride ions and the process will continue until the steel has been completely depassivated.

Once the protective oxide layer has been consumed, corrosion can commence. The accumulation of corrosion products at the anodic site causes a substantial increase in volume and pressures, which will subsequently cause cracking and spalling of the concrete. This will induce delaminations of the concrete cover. However, lack of sufficient oxygen at the anode will cause the ferrous ions to remain aqueous, diffuse away and deposit somewhere else in the pores of the concrete. This is referred to as

green or black rust. This situation is very dangerous since it will lead to substantial corrosion of the reinforcement without the advanced warning signs given by the cracking and spalling of the concrete (Revie 2000).

2.4 Chlorides in Concrete

Chloride ions found in deicing salts have been found to be the most detrimental substance applied to reinforced concrete bridge elements since they initiate corrosion in the steel reinforcement. The durability of bridge decks, beams, columns, and abutments are significantly affected by the ingress of chloride ions. There are two main sources of chlorides ions in concrete: internal chlorides and external chlorides. Common sources for internal chlorides are calcium chloride containing admixtures, contaminated aggregates, and seawater. Common sources for external chlorides are seawater exposure, deicing salts, fire, and chloride contaminated groundwater or soils (Jefremczuk 2005). Generally, external chloride ion sources are the dominant contributor to corrosion initiation and internal chloride sources are often negligible. Jefremczuk (2005) provides more information on chloride ion sources.

There are also two main classes of chlorides in concrete as well. They are total chlorides and free chlorides. Total chlorides are the total amount of chloride ions in the concrete including the bounded chloride ions in the cement paste and the free chloride ions in the pores. Free chloride ions are the chloride ions in the pores. It is the free chloride ions that are able to react with the steel reinforcement and cause the destruction of the passive oxide layer.

2.5 Critical Chloride Concentration

When reinforcing steel is placed in concrete, the concrete's high pH causes an oxide film to form on the surface of the steel. The corrosion process of the reinforcement can only begin once this passive oxide layer has been destroyed. Reactions with chloride ions, as well as moisture and oxygen, destroy the oxide film. The concentration of chloride ions needed to destroy the oxide film is referred to as the critical or threshold chloride ion concentration. Carbonation of the concrete also destroys the oxide film by lowering the pH of the concrete (Huang and Yang 1997; Enright and Frangopol 1998; Stewart and Rosowsky 1998; Akgul and Frangopol 2005; Val and Stewart 2005; Duprat 2007).

There have been numerous researches into the critical chloride concentration and there is a large variability in the values obtained. This variation is caused by the many different factors that influence the critical chloride ion concentration. These factors include concrete mix type and proportions, pH, C_3A content, w/c, relative humidity, and temperature (Stewart and Rosowsky 1998; Duprat 2007). It has been assumed that because of the large variation in concrete properties, the critical chloride concentration is found within a large range, estimated to be roughly to be 0.2-3% by weight of cement (Duprat 2007).

Furthermore, the research performed has had much variation in its testing and measurements procedures. Some have performed tests on mortar specimens, some on paste specimens, and others on concrete specimens. These will all have very different critical chloride ion concentration values. Moreover, it is unclear if the chloride concentration is compared with the total or free chloride ions (Stewart and Rosowsky 1998). As was mentioned, it is the free chloride ions that are able to react with the steel reinforcement, but this value is difficult to determine when testing concrete specimens. Usually, the total chloride ion content is provided in the results.

It has also been understood that the pH of the concrete pores influences the stability of the passivation film. This relationship is shown in Figure 2.3.

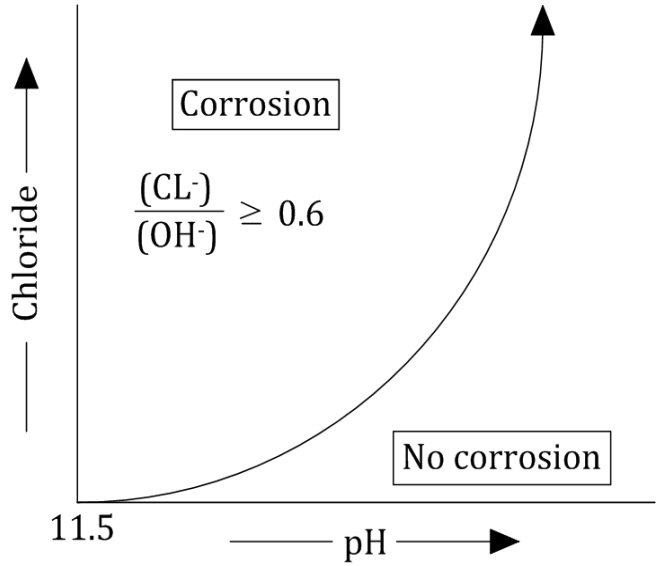

Figure 2.3: Influence of pH and Chloride Ions on the Corrosion Initiation of Steel (Boyd 2010)

The amount of chloride ions needed to destroy the passive layer is dependant on the amount of hydroxide ions in contact with the steel reinforcement. A higher pH in the pore solution requires more chlorides to destabilize the passive oxide layer. If the pH falls below 11.5, no chloride ions are needed and the passivation film will break down. The general equation to determine if corrosion will occur is also depicted in Figure 2.3.

In this thesis, we will use the same critical chloride ion concentration that was assumed for the work done by Laval University (Conciatori 2005). Tables were provided from research done by Laval University comparing their work with research performed by Black Steel, Canada (Henocq et al. 2007).

In Table 2.1, the chloride threshold values found in their work are compared with those found in the literature. In Table 2.2, the chloride threshold given by the (Cl-) / (OH) is compared with their literature review.

Table 2.1: Chloride threshold values used in this work, in comparison with literature

References	Exposure	Sample	Total Cl (wt % cem.)
This work	Laboratory	Mortar	0.50 ± 0.05
Elsener and Böhni	Laboratory	Mortar	0.25 – 0.50
Petterson	Laboratory	Mortar	0.50 – 1.80
Hansson and Sorensen	Laboratory	Mortar	0.60 – 1.40
Alonso et al.	Laboratory	Mortar	1.24 – 3.08
Page et al.	Laboratory	Paste	0.40
Locke and Siman	Laboratory	Concrete	0.60
Tuutti	Laboratory	Concrete	0.50 – 1.40
Thomas	Outdoors	Concrete	0.50 – 0.70
Henriksen	Outdoors	Structures	0.30 – 0.70
Fedaral Highway (FHWA)	-	Concrete	0.30

Table 2.2: Chloride threshold given by $[Cl^-]/[OH^-]$ used in this work, in comparison with literature

References	Exposure	Sample	
This work	Laboratory	Mortar	1.27 ± 0.09
Petterson	Laboratory	Mortar	1.70 – 2.60
Alonso et al.	Laboratory	Mortar	1.17 – 3.98
Page et al.	Laboratory	Mortar	0.22
Goni et al.	Laboratory	Solution and mortar	0.66 – 1.45

2.6 Corrosion & Deterioration Process

2.6.1 Corrosion Initiation

The main focus of this thesis is to accurately model and predict corrosion initiation and the probability that corrosion has started. The corrosion initiation period is the time it takes for the steel reinforcement to begin corroding. This duration is dependant on the length of time it takes for the substances needed for corrosion, such as water, oxygen, chloride ions and carbon dioxide, to penetrate the concrete clear cover and reach the depth of reinforcing steel in a sufficient amount to begin corrosion of the steel. Therefore, the transport process of these substances into the concrete as well as the various chemical reactions that take place characterizes the corrosion initiation process (Conciatori, Sadouki et al. 2008; Conciatori, Laferrière et al. 2010).

As was just mentioned, the movement of these substances is the key factor in determining when corrosion will initiate. There have been many computer models and simulation programs that were created to estimate the ingress of chloride ions. Examples of such models are Duramodel, Life365, Stadium, TransChlor, among many others. In the early stages of computer simulations, simple models were used which were based on Fick's Diffusion law since diffusion usually dominates the transport process in the ingress of chloride ions. By re-arranging and modifying Fick's diffusion law for the corrosion initiation time, the following equation is obtained (Enright and Frangopol 2000):

$$T_1 = \frac{X^2}{4D_c}\left[erf^{-1}\left(\frac{C_0 - C_{cr}}{C_0}\right)\right]^{-2} \qquad [2.1]$$

where:

T_1 = corrosion initiation time (year)

X = concrete cover (cm)

D_c = chloride diffusion coefficient (cm^2/year)

C_o = Cl^- concentration at the concrete surface (% weight of concrete)

C_{cr} = Critical Cl^- concentration at which corrosion begins (% weight of concrete)

There are four variables in this equation that influence the corrosion initiation time: the diffusion coefficient and thickness of the concrete cover, the chloride ion concentration at the surface and the critical chloride ion concentration to initiate corrosion.

If the concrete cover is increased, the corrosion initiation time will increase as well, meaning it will take longer for corrosion to begin. This is because the chloride ions must travel into the concrete to reach the reinforcing steel and the larger the thickness of the concrete cover, the longer it will take for chloride ions to reach the reinforcement. Furthermore, a thick concrete cover will also slow down the corrosion rate once corrosion begins because there will be a lower availability of oxygen in the vicinity of the reinforcement (Duprat 2007). Acknowledging the importance of concrete cover, it is expected that reinforcing steel closest to the surface of a structural member will be the first to begin corroding (Kirkpatrick, Weyers et al. 2002). Therefore, shear reinforcement is especially vulnerable to chloride-induced corrosion since it is closest to the surface.

The chloride diffusion coefficient represents the amount of chloride ions diffusing into the concrete as a function of time. This coefficient varies widely from concrete to concrete because the chloride diffusion coefficient is greatly influenced by parameters such as mix proportions, curing time and conditions, compaction, environmental exposure and time effects (Stewart 2003). A low chloride diffusion coefficient significantly increases the time until the initiation of corrosion (Kirkpatrick, Weyers et al. 2002a).

The surface chloride concentration is generally considered at a depth of half an inch (12.7mm) below the deck surface because the chloride ion concentration are relatively constant as a function of time at this depth (Kirkpatrick, Weyers et al. 2002). At the surface, chloride ion concentration fluctuates rapidly because of the quick response to capillary suction (Conciatori, Sadouki et al. 2008). The surface concentration also changes with the seasons because the concentration is influenced by the amount of de-icing salts applied at the surface, as well as by the drainage efficiency and the water tightness of expansion and construction joints (Stewart 2003). The chloride ion concentration decreases in the spring, summer, and fall when no salts are applied onto the surface and increases in the winter when de-icing salts are used (Kirkpatrick, Weyers et al. 2002).

The simple model does not account for many other factors that influence the transportation of chloride ions in concrete, such as capillary suction. Upgraded and updated models began to improve on the simple diffusion model, including various transport mechanisms such as capillary suction, aqueous water transport with and without chlorides, thermal transfer, vapor transfer, carbon dioxide diffusion, etc. Some models, such as Stadium®, include advanced chemical interactions and changes within the concrete, while others focus more on the environment and atmosphere around the structures, such as TransChlor. There are also models that take into account cracking of the concrete (Jefremczuk 2005). To date, however, there is not a computer program, which accounts simultaneously for complex chemical reactions, environmental conditions, and cracking of concrete.

2.6.2 Corrosion Propagation

Corrosion of steel occurs when the surface layer is depassivated. The corrosion of the reinforcement reduces the cross sectional area of the steel and produces corrosive products (i.e. rust). Rust has a much larger volume than the original steel material and will cause expansive stresses in the concrete. This leads to cracking, delamination and spalling of the concrete cover. Furthermore, the bond between the concrete and reinforcement is also negatively affected. All these factors contribute to reduce the overall strength and ductility of the structure (Lounis, International et al. 2003).

The key substances needed for corrosion are iron, moisture, oxygen and electron flow. As such, the rate of corrosion is dependant on the availability of water and oxygen in the vicinity of the reinforcement (Duprat 2007). These substances penetrate into concrete through the pore spaces in the cement paste matrix or micro-cracks. The rate of ingress depends mostly on the quality and condition of concrete and mainly on the water-cement ratio of the concrete mix (Lounis, International et al. 2003).

It is very difficult to estimate corrosion rates since the availability of moisture and oxygen varies greatly from structure to structure and even at different locations within the same structure. Therefore, the estimation of corrosion rates is very difficult at the design stage. Some models of the corrosion process convert oxygen diffusion rates in the concrete into corrosion rates of the steel by using molecular equations of the corrosion reactions (Vu and Stewart 2000). However, the corrosion rate is most accurately determined from field studies and experiments using the corrosion current density (Stewart and Rosowsky 1998).

Several field methods can be used to evaluate corrosion-related damage of a structure. Three widely used methods are the half-cell method, the DC polarization method, and the AC impedance method. The half-cell method produces corrosion potential contour lines across the structure. The disadvantage of this method is that it indicates corrosion probabilities but not corrosion rates. The DC polarization method can estimate corrosion rates but it does not consider the IR drop effect (i.e. the loss in voltage as a current passes through a resistor) and therefore the corrosion rates may be under-estimated. The AC impedance method is the most precise in estimating corrosion rates (Huang and Yang 1997).

Using either the DC linear polarization method or the AC impedance method, the polarization resistance, Rp, can be determined. Once the polarization resistance has been determined, the corrosion current density, i_{corr} (amp/cm^2), can be determined by the Stern-Geary equation as expressed in Equation 2.2 (Huang and Yang 1997; Val, Stewart et al. 1998):

$$i_{corr} = \left(\frac{\beta a \beta b}{2.303(\beta a + \beta b)} \right) = \frac{B}{R_p} \qquad [2.2]$$

where:

βa = Tafel's slopes of anodic polarization curve

βb = Tafel's slopes of cathodic polarization curve

B = 26 mV for steels in an alkaline environment

After obtaining the corrosion current density, the instantaneous corrosion rate can be calculated using Faraday's law (Huang and Yang 1997):

$$\Gamma_{corr} = \left(\frac{i_{corr}}{nF} \right) \times \left(\frac{W_{Fe}}{D_{Fe}} \right) \qquad [2.3]$$

where:

Γ_{corr} = thickness loss of steel per unit of time (cm/s)

F = Faraday's constant, 96,500 Coulomb/mole

n = 2, valance of the oxidation reaction: $Fe^{2+} + 2e^{-} \rightarrow Fe$

W_{Fe} = atomic weight of steel (55.8 g/mole)

D_{Fe} = density of steel (7.86 g/cm^3)

There have been several studies on corrosion rates on reinforced concrete structures. Akgul and Frangopol (2005) indicate that corrosion rates for steel reinforcement in concrete ranges between 0.013 mm to 0.064 mm per year and for steel exposed to the atmosphere directly or through cracks ranges from 0.051 mm to 0.254 mm per year. Duprat (2007) suggests that corrosion rates vary from 0.013 mm to 0.127 mm per year for ordinary concrete (Duprat 2007).

After corrosion of the steel reinforcement is initiated, the cross sectional area decreases with time with a rate that is dependent on the number of bars actively corroding, the corrosion rate and the diameter of the individual bars.

There are two types of corrosion: general corrosion and pitting corrosion. General corrosion is a process when the outside surface of the steel bar is reduced at a uniform rate. This occurs when water and oxygen have had sufficient time to surround the reinforcement during the corrosion initiation phase. The side of the reinforcement closest to the surface will generally begin corroding before the opposite side of the reinforcement because water and oxygen travels a shorter distance to the steel surface. However, it is often assumed that general corrosion causes a uniform decrease of the cross-sectional area and a gradual decrease in resistance over time. General corrosion is generally associated to ductile-type failures of the steel reinforcement.

Pitting corrosion occurs when a location along the reinforcement is more heavily corroded than others and a pit appears at the surface of the reinforcement. Pitting

corrosion usually occurs in the presence of large cracks in the concrete. These cracks allow quick access and high availability of water and oxygen at that location. Pitting corrosion is very localized and usually more severe in concrete structures because it is often associated with brittle failure due to the sudden failure of the bar (Akgul and Frangopol 2005)

The computer model used for this research does not consider cracking. Therefore, only uniform corrosion of reinforcement is considered in this thesis. For further information on pitting corrosion, refer to (Val, Stewart et al. 1998; Duprat 2007; Stewart and Al-Harthy 2008). For the general case of reinforcing bars of various diameters and different corrosion initiation times, the change of cross-sectional area of steel reinforcement A(t) can be estimated with the following equations (Enright and Frangopol 2000):

$$A(t) = \frac{\pi}{4}\sum_{j=1}^{n}\left[D_j(t)\right]^2 \qquad [2.4]$$

$$D_j(t) = \begin{cases} D_{jo} & for\ t \le T_{1j} \\ D_{jo} - r_{corr}(t - T_{1j}) & for\ T_{1j} < t < T_{1j} + D_{jo}/r_{corr} \\ 0 & for\ t \ge T_{1j} + D_{jo}/r_{corr} \end{cases} \qquad [2.5]$$

where:

$D_j(t)$ = diameter of bar j at time t

n = number of bars

D_{jo} = initial diameter of bar j

r_{corr} = corrosion rate

t = elapsed time

T_{1j} = corrosion initiation time for bar j

These equations estimate the amount of steel that has been corroded at a given time and can be used to estimate the residual service life of a structure. The main difficulty is the selection of the appropriate corrosion initiation times and corrosion

rates for each bar. A simplification is to assume that each bar has the same corrosion rate. The corrosion initiation time can be obtained from simple or complex corrosion initiation models, such as equation 4.1.

2.6.3 Corrosion Products

During the corrosion process, the iron of reinforcing steel is consumed and rust is produced. Several forms of rust can be created, as shown in Figure 2.4. The production of rust is detrimental to reinforced concrete elements because the volume of the rust products is several times that of the original iron (Figure 2.4).

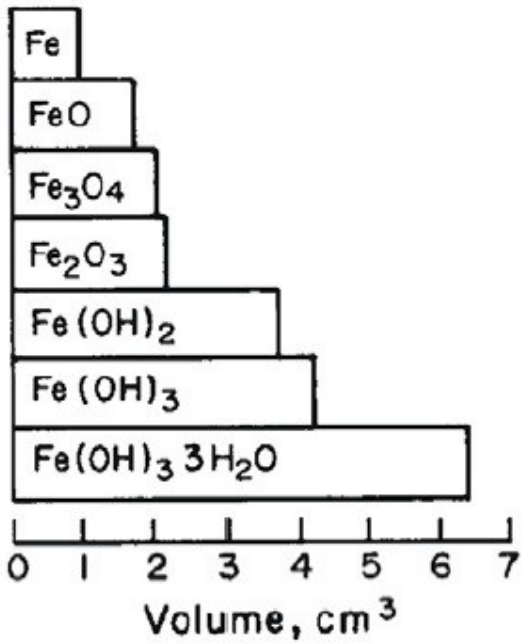

Figure 2.4: Specific Volume of Rust Products (Boyd 2010)

The production of rust is seen to be more than six times the volume of the original iron material. This large increase in volume needs some place to expand but cannot because of the confinement from the surrounding concrete. This causes an increase of internal pressure, which develops tensile stresses in the concrete, which in turn results in cracking of the concrete.

2.6.4 Expansion, Cracking and Spalling of Concrete Cover

The combination of expansion and cracking causes the concrete cover to spall off and expose either new concrete or the steel reinforcement.

Besides corrosion products from the steel, internal pressure can be caused by chemical reactions in the concrete (sulfates), chemical reactions between the cement and aggregate (ASR), and freeze-thaw or heat cycles (Enright and Frangopol 2000).

The cracking and spalling of the concrete cover will lead to a new boundary condition for the concrete or expose the steel reinforcement. This will lead to accelerated corrosion, which is discussed in the next section.

2.6.5 Accelerated Corrosion and Deterioration

With spalling, it is easier for chloride ions to reach the interior bars. Oxygen and moisture are also more readily available to fuel the corrosion process as well. Furthermore, the interior concrete will usually have a higher permeability than surface concrete because it does not have a surface treatment, such as finishing, making ingress more likely. Reinforcing steel may also be directly exposed to the environment, making that steel susceptible to severe corrosion and a much higher corrosion rate.

Structural strength is also decreased because spalling or delamination of the concrete cover reduces the concrete compression zone. Therefore, spalling of the top cover leads to delamination of the upper surface, which will reduce the effective depth and subsequently the moment arm used for flexural resistance. Spalling or delamination of the top and bottom cover will also produce a decrease in shear

capacity because of the reduction in the concrete cross section (Vu and Stewart 2000).

Models can be used to predict the time for initial cracking and spalling and therefore the time until accelerated corrosion and deterioration (Liu, Weyers et al. 1996). The time for initial cracking and spalling is influenced by many parameters, such as reinforced concrete material and section properties, time to corrosion initiation, traffic loading and rupture capacity. There is considerable uncertainty in the model and experiments have shown that this model may under-estimate the actual time to spalling (Vu and Stewart 2000).

2.7 Structural Reliability

Safety and reliability analysis of our structures is very important since it can be used to minimize risks to its users. In the previous section, initiation and propagation of corrosion was described. In this section, that information is introduced in structural analysis procedures to determine the residual life of these structures.

When analyzing a structure, various design limits must be checked and satisfied. Generally, moment and shear resistance are the most important, but tension, compression, bearing, development bond, reinforcement spacing and deflection must be checked as well. The loss of bond at the steel/concrete interface is also critical since a loss of bond will impair the composite behavior.

Formulas for moment and shear resistance of a rectangular concrete beam are given in Equation 2.6 and Equation 2.7, respectively.

$$M_f = A_s f_y \left(d - \frac{1}{2} \frac{A_s f_y}{0.85 f_c^{'} b} \right) \quad [2.6]$$

where:

A_s = Area of tension reinforcement

f_y = Specific yield strength of reinforcing bars

d = Distance from the extreme compression fiber to the centroid of tensile steel

f'_c = Specified compressive strength of concrete at 28 days

b = Width of the compression face of the member.

$$V_f = 0.0316 \cdot 2\sqrt{f_c^{'} b_v d_v} + \frac{A_v f_y d_v}{s} \quad [2.7]$$

where:

b_v = effective web width

d_v = effective shear depth

A_v = area of shear reinforcement

s = shear stirrup spacing

These equations indicate that the area of reinforcement and the depth of concrete affect both the shear and moment capacities of the reinforced concrete element. Before the initiation of corrosion, the steel reinforcement and the effective depth remain constant and the resistance usually increases because of the gain in compressive strength of concrete with time. After the initiation of corrosion, the structural resistance decreases with the reduction in cross sectional area of the steel reinforcement. This decrease in resistance progresses at a uniform rate until cracking and spalling of the concrete cover occurs. This coincides with beginning of accelerated corrosion. There is an immediate drop in resistance because of the reduced concrete depth and a larger corrosion rate applies from that point in time.

It is generally considered that the shear resistances of bridge structure elements are the controlling features relative to failure mechanisms (Enright and Frangopol 2000). The most common source of damage on a reinforced concrete bridge is water

infiltration through deck joints. Therefore, the most heavily damaged locations are in the vicinity of these joints close to the supports, which are areas of high shear stresses.

Considering that shear reinforcement is placed on the outside of the flexural reinforcement, shear-reinforcing steel has a smaller concrete cover. As a result, the corrosion initiation time for shear reinforcement is significantly lower than that for flexural reinforcement. The normalized loss of area is also much greater for shear reinforcement than flexural reinforcement because of the much smaller diameter that is used for shear reinforcement. The smaller diameter bar has a larger specific surface area. Consequently, this causes the smaller steel bar to corrode more rapidly since a larger surface area is exposed compared with its volume. Thus, shear reinforcement will begin corroding before the flexural steel and will also corrode and be consumed much more quickly (Enright and Frangopol 2000).

Combining these factors together, shear resistance and degradation at the support joints is determined to be the most critical location on a bridge. To summarize, it is because support joints are the most susceptible to corrosion, corrosion of shear reinforcement is found to be more sever than flexural reinforcement, and lastly because supports are the locations with maximum shear demand for a simply supported bridge. Hence, shear failure is likely to dominate for concrete bridges that undergo corrosion of the reinforcement.

When dealing with the structural analysis of the structure, it is important to determine not only the residual strength of the entire structure but also the new loading conditions it is subjected to. When a bridge is first designed, there is uncertainty on the future vehicle usage. Predictions are made but these are inherently inaccurate and can be substantially underestimated. Updated vehicle live load and dead load of the structure, as well as any retrofit or repair of the structure, should be incorporated in the calculation and design checks of the residual life of the structure.

Chapter 3

Deicing Salts

3.1 General

Sodium chloride salt is recognized as the best deicer because it works fast, it is cheap and is very easy to use. There are numerous products on the market, but none has matched the cost effectiveness of salt (Salt Institute 2009).

On the downside, deicing salts have been found to be detrimental to reinforcing steel and subsequently to reinforced concrete structures. Chloride ions found in deicing salts destroy the passive film around the steel, exposing the steel to oxygen and moisture, causing corrosion to begin.

Although deicing salts are harmful to reinforcing bars, their benefits to society cannot be overlooked. Deicing salt is used to prevent or destroy the snow/ice bond to the pavement so that traffic action and/or snowplows can clear the road, a road surface condition known as a "bare pavement" (Salt Institute 2009). This notion of a "bare pavement" policy provides a level of safety that allows secure driving conditions on our roadways and became a useful concept for roadway maintenance because it was a simple and self-evident guideline for highway crews (EPA 1999).

In this chapter, deicing salts are discussed, specifically their usage in North America, their impact on society, how they function, how they are applied and lastly, how they are stored.

3.2 Deicing Salts in the United States

In the United States, salt was first used on roads for snow and ice control in the 1930s (Salt Institute 2009). It was only after World War II that road salt usage began to soar. This is because the expanding highway system became essential to the public and the economy.

The "bare pavement" concept, where roadways after a storm are free of snow and ice, quickly became a policy in most cities. As a result, salt use doubled every 5 years during the 1950s and 1960s growing from 1 million tons in 1955 to nearly 10 million tons less than 15 years later (National Research Council 1991). This can be seen in Figure 3.1.

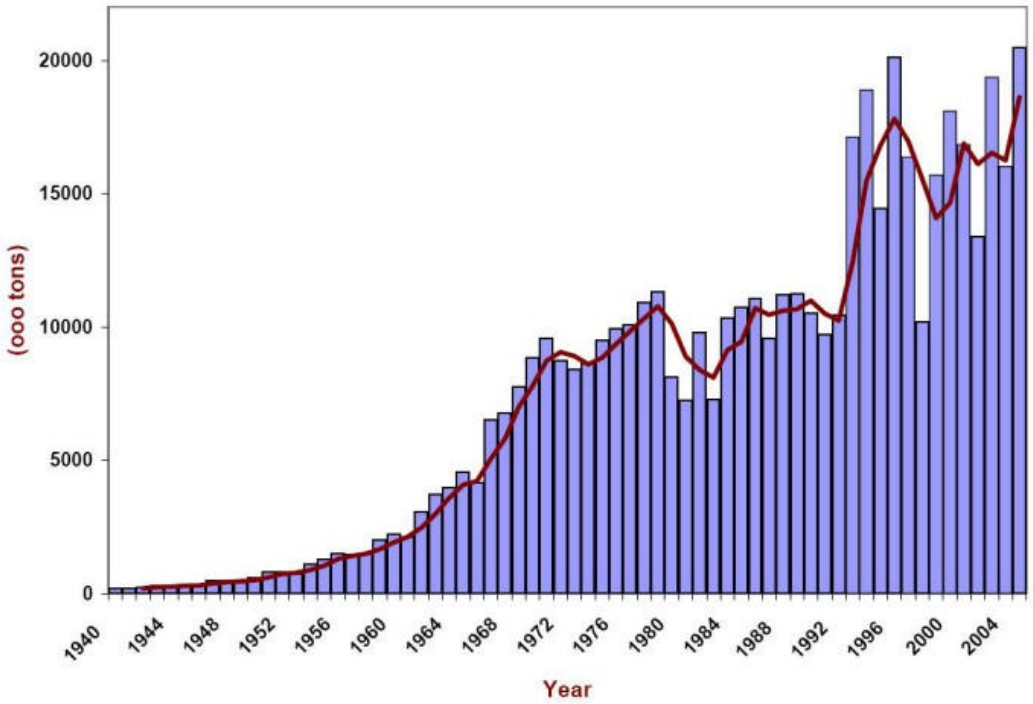

Figure 3.1: Usage of Rock Salt for Deicing in the U.S. in Thousands of Tons (Salt Institute 2009)

Road-salt use in the United States ranges from 8 million to 12 million tons of NaCl per year. However, a substantial increase in salt usage after 1993 has occurred and can be seen in Figure 3.1 to have almost doubled in value. Official salt application rates for several states are listed in Table 3.1 (National Research Council 1991).

Table 3.1: Official Salt Use Policies in Various States

Region and State	Summary of General Policy
New England	
Connecticut	Salt applied at 215 lb/lane-mi on multilane roads; no more than 150 lb/lane-mi on two-lane state highways
Massachusetts	Salt applied at less than 300 lb/lane-mi on state highways
New Hampshire	Salt application guideline of 250 to 300 lb/lane-mi on state highways
Middle Atlantic	
Maryland	Salt application guideline of 300 to 500 lb/lane-mi on state highways
West Virginia	Salt application guideline of 100 to 250 lb/lane-mi, usually mixed with abrasives, except in cities
Great Lakes	
Michigan	Salt applied at 225 lb/lane-mi on primary highways. Salt and sand mixtures used on lower-priority roads, depending on storm temperature and severity
Ohio	Salt applied at 200 to 300 lb/lane-mi on Interstate and primary highways; 100 to 200 lb/lane-mi, with abrasives on secondary roads; no more than 100 to 200 lb/lane-mi on low-priority roads
Wisconsin	Salt application rates of 100 to 300 lb/lane-mi recommended; additional salt use restrictions related to pavement temperature in place
Plains	
Iowa	Salt applied at 150 lb/lane-mi (mixed with sand) on Interstates and other arterials; 100 lb/lane-mi on collectors; no salt used on local roads
Kansas	Salt applied at 100 to 250 lb/lane-mi (mixed with sand on Interstates, freeways, and other roads with 2,500+ ADT; less on roads with 750 to 2,500 ADT; no salt used on roads with < 750 ADT
West	
Colorado	Salt only with abrasives; rates not defined
California	Salt applied at 500 lb/Lane-mi on some mountain highways

NOTE: Although policies often identify an ideal salt application rate for equipment calibration, they seldom regulate the timing and frequency of applicatiosn. Application timing and frequency are typically determined by maintenance engineer in charge during the storm. Data in the table are from states that responded to relevant questions in survey.
ADT = average daily traffic
SOURCE: TRB survey of state highway agencies.

Average annual salt loadings for several states are also determined and listed in Table 3.2 (National Research Council 1991). Each state averaged more than 10 tons per lane-mile per year on state maintained highways. Out of all the states, Massachusetts, New Hampshire, and New York report the highest annual road salt loadings, with Massachusetts being the highest at 19.94 tons per lane-mile per year (Wegner and Yagi 2001).

Table 3.2: Average Annual Salt Loadings on State Highways

Region and State	Average Annual Loading (tons/lane-mile)
New England	
Maine	8.0
Massachusetts	19.4
New Hampshire	16.4
Vermont	17.1
Middle Atlantic	
Delaware	9.0
Maryland	7.1
New Jersey	6.7
New York	16.6
Virginia	3.0
West Virginia	6.3
Great Lakes	
Illinois	6.6
Indiana	9.0
Michigan	12.9
Ohio	9.1
Wisconsin	9.2
Plains	
Iowa	3.8
Minnesota	5.0
Missouri	1.0
Nebraska	1.5
Oklahoma	1.5
South Dakota	1.0
Mountain and West	
Alaska	1.2
California	3.0
Idaho	0.3
Nevada	1.9
New Mexico	0.5

NOTE: Date are from only those states that responded to relevant questions in survey.
SOURCE: TRB survey of state highway agencies

The concept “more is better” led to practices of high application rates of salt. By the late 1950s, however, damage to vegetation, contamination to drinking water near unprotected salt storage, and pitting and “rust out” of automobiles and corrosion of highway structures, especially bridge decks, were becoming apparent (EPA 1999).

It became evident that research was needed to determine the corrosivity of deicing salts. One of the very first such maps was produced to summarize many years of results obtained by exposing bare steel coupons attached to different vehicles in the north-eastern U.S. and Canada. This corrosivity map is shown in Figure 3.2 in which the Snowbelt region is circled. The higher level of vehicle corrosion in the Snowbelt region when compared to adjacent non-marine regions can only be attributed to the use of deicing salts (Roberge 1999).

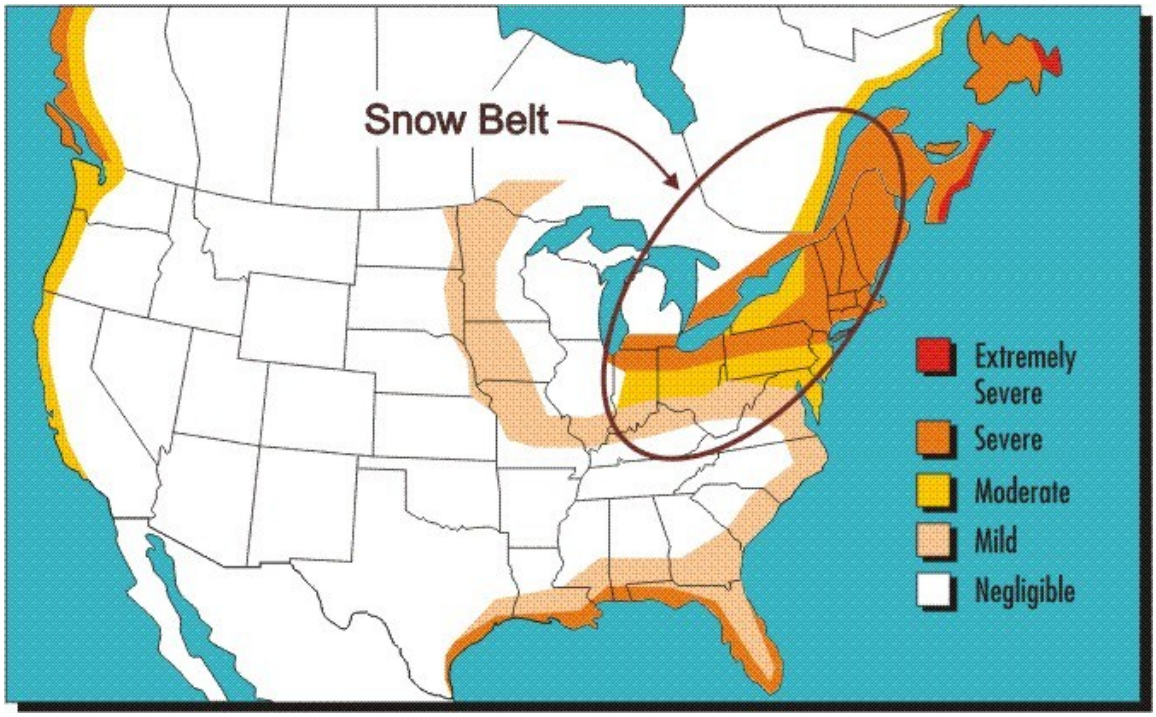

Figure 3.2: Corrosivity Map of North America Showing the Particular Aggressiveness of the Snowbelt Region (Roberge 1999)

3.3 Deicing Salts in Canada

Canada has been using road salts (mostly NaCl) for ice melting since the 1940s. Environment Canada estimates that on average, five million metric tons are used annually in Canada (Smith 2009).

In Canada, salt has become more heavily regulated by the federal environmental agency, Environment Canada. In 1995, Environment Canada initiated a five-year comprehensive assessment of road salts. This was done to determine whether conventional deicers should be considered toxic substances under the Canadian Environmental Protection Act. The assessment included sodium chloride (NaCl), calcium chloride ($CaCl_2$), magnesium chloride ($MgCl_2$) and potassium chloride (KCl), as well as ferrocyanide additives used for anti-caking (Rush 2009; Smith 2009). The study found that high concentrations of road salts commonly enter the environment through roadway melt water and through seepage from mismanaged salt storage facilities and snow disposal sites (Environment Canada 2000). The Canadian Ministers of the Environment and of Health therefore recommended adding road salt to Schedule 1 of Canada's Environmental Protection Act of 1999 (Brink and Auen 2004).

In December of 2001 Canada's Environmental Protection Act (CEPA) Priority Substance List Assessment Report was released, stating that road salts were affecting freshwater ecosystems, soils, vegetation and wildlife. Therefore, it was concluded that road salts that contain inorganic chloride salts with or without ferrocyanide salts are 'toxic' as defined in Section 64 of the Canadian Environmental Protection Act of 1999 (Canadian Environmental Protection Act 1999; Environment Canada 2000; Brink and Auen 2004; Rush 2009; Smith 2009).

In response, Environment Canada proposed management strategies to minimize the impacts of deicing salt on the environment in late 2003 (Brink and Auen 2004).

Included in the Priority Substance List Assessment Report were recommended provincial application rates as well as municipal application rates for deicing salts. This is shown in Figures 3.3 and 3.4, respectively. The recommended application rate for Montréal is found to be 300 kg salt per 2-lane km, which is also the maximum recommended rate for Quebec (Environment Canada 2000).

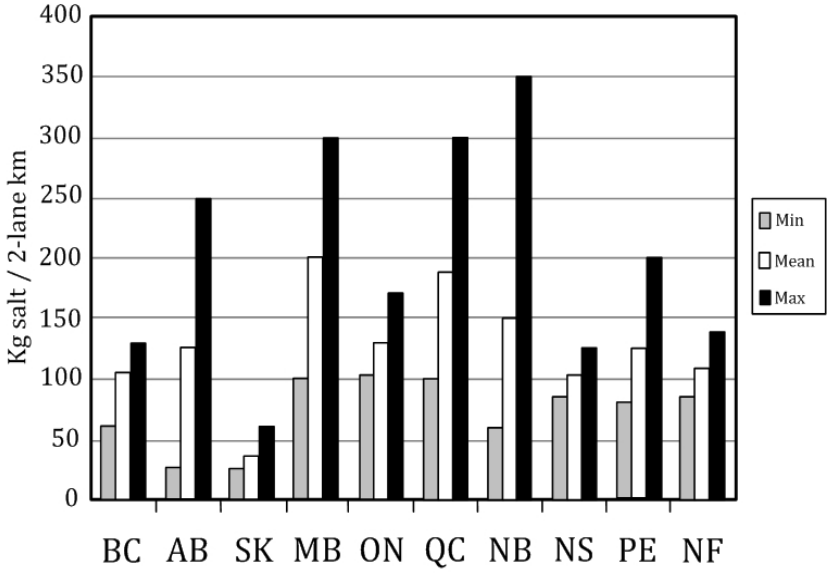

Figure 3.3: Recommended Provincial Application Rates for Sodium Chloride Road Salts, 1998 (Morin and Perchanok 2000)

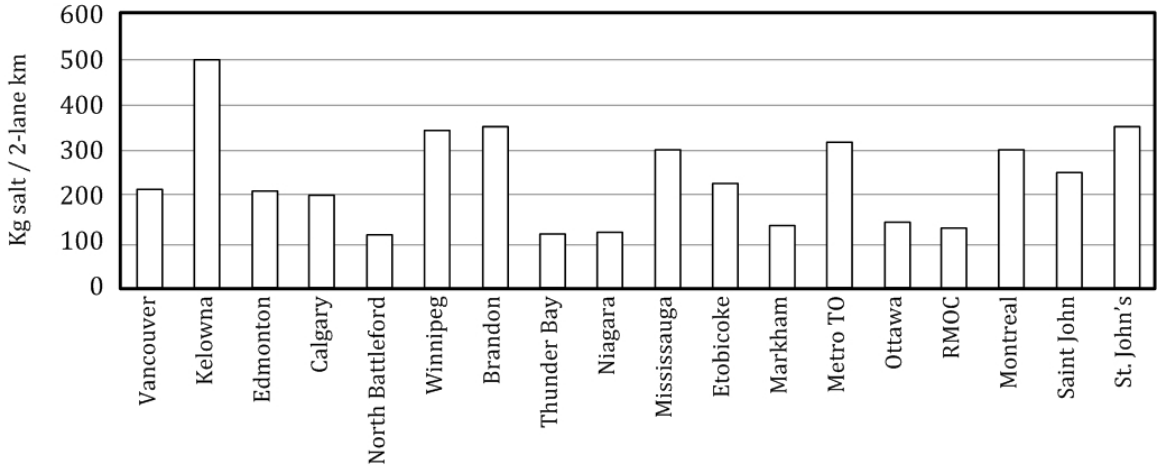

Metro TO = Metropolitan Toronto prior to amalgamation

RMOC = Regional Municipality of Ottawa-Carleton

Figure 3.4: Average Recommended Municipal Application Rates for Sodium Chloride Road Salts, 1998 (Morin and Perchanok 2000)

Industry estimates show that Ontario and Quebec use the most amount of deicing salt, but Nova Scotia has the highest loading per unit area of land. The lowest uses of road salts are in the western provinces (Smith 2009). The amount of deicing salts used in each province is listed in Table 3.3 (Morin and Perchanok 2000).

Table 3.3: Total Loading of Sodium Chloride Road Salt, winter 1997-1998

Province	Loading of sodium chloride road salt (tons)				
	Provincial	Estimated county + municipal	Total provincial + county + municipal	Estimated commercial + industrial[1]	Total
British Columbia	83 458	48 199	131 657	9 874	141 531
Alberta	101 063	67 870	168 933	12 670	181 603
Saskatchewan	44 001	4 844	48 845	3 663	52 508
Manitoba	36 780	28 256	65 036	4 878	69 914
Ontario	592 932	1 123 653	1 716 585	128 744	1 845 329
Quebec	609 550	827 205	1 436 755	107 757	1 544 512
New Brunswick	189 093	75 826	264 919	19 869	284 788
Prince Edward Island	23 051	4 300	27 351	2 051	29 402
Nova Scotia	270 105	77 761	347 866	26 090	373 956
Newfoundland	159 200	47 558	206 758	15 507	222 265
Yukon	1 791	120	1 911	143	2 054
Northwest Territories[2]	1 846	0	1 846	138	1 984
Total	**2 112 870**	**2 305 592**	**4 418 462**	**331 385**	**4 749 847**

[1]Commercial and industrial road salt use is assumed to be at 7.5% of provincial and municipal use (7.5% based on estimate by Cheminfo, 1999).
[2]Including Nunavut.

As mentioned before, Ontario and Quebec use the most chlorides out of all the provinces. This can be seen in Figure 3.5. In Ontario, the two main users of deicing salts are the MTO and the City of Toronto. In Quebec, the largest user of deicing salts is the MTQ.

The Province of Quebec has a total road network of 135,000 km. Out of this, the Ministère des Transports du Québec (MTQ) manages 31,000 km. On average, 60000 tons of salts are spread on Québec roads every winter (Transport Québec 1994; Smith 2009)

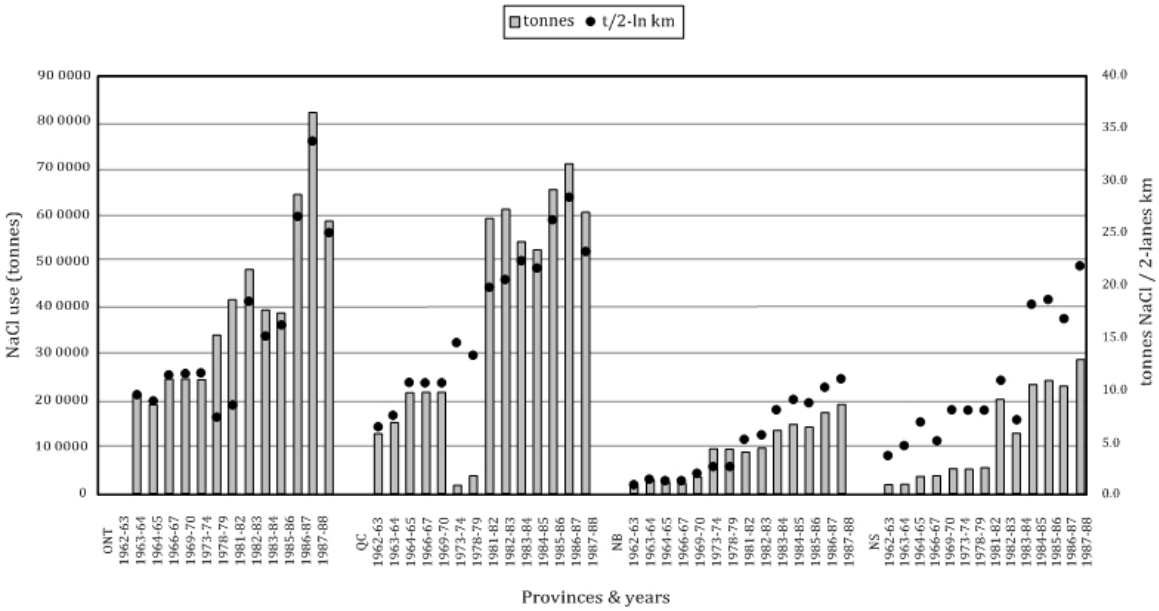

Figure 3.5: Historical Salt Use by Provincial Agencies
(Morin and Perchanok 2000; Salt Institute 2009)

3.4 Impact on Society

Winter roadway maintenance is very important to our society. Benefits of usable highways are evident since our normal lives as well as our economy depend on them. Society pays a huge penalty even if one day is lost to snowbound conditions (Salt Institute 2009).

It has been estimated that the MTQ spent $170 million on winter maintenance in 2005. In one report, Environment Canada provided the associated costs and benefits of using deicing salts on our roadways. An overview of the sections described by the

report has been reproduced in Table 3.4 (Environment Canada 2006). The reference provided includes more detail on each section as well as monetary estimations.

Table 3.4: Breakdown of Costs and Benefits of Winter Maintenance, Using Road Salts as a Deicer

Costs	Benefits
Direct: • Material Cost (salts) • Equipment Cost • Labor Cost	Direct: • Fuel savings • Travel time savings • Avoided fatality, injury, and vehicle damage
Indirect: • Cost to Infrastructures • Cost to motor vehicles (on-road • Cost to Environment	Indirect: • Reduction in liability claims to road authority (associated to hazardous driving conditions). • Maintain the economic activity (production, transportation, and earnings) • Maintain access to social activities.

It has also been found that fuel savings are earned with "bare pavements". The roughness of road ice and slippage of wheels can cause an increase in fuel consumption by 35% and as much as 50% when there is 5 cm of snow on the road (Roberge 1999).

In 1976, a report by the Institute for Safety Analysis listed the following cost-benefits of using salt in the U.S. to deice the highways (Roberge 1999):

- Reduces wages lost due to lateness to work by $7.6 billion
- Saves $3 billion in wage loss because of absenteeism
- Reduces production losses by $7 billion
- Reduces losses in goods shipment by $600 million
- Saves 1.4 to 4.5 billion liters of fuel
- Has an 18:1 benefit/cost ratio

In 2004, the Salt Institute commissioned Global Insight, Inc. to model and project the impact of a day when snow and ice closed down the roadways. The study found enormous costs associated with blizzards, which might shut down roadways in a state or province. The methodology was conservative, considering only three variables, not including crash data or personal injuries. The survey included 12 U.S. states and two Canadian provinces. The results of there findings are shown in Table 3.5 (Salt Institute 2009).

Crashes have a large impact on society since they lead to injuries and can sometimes be fatal. One study of Iowa freeways found that snowstorms could increase the crash rate to an astounding 1,300%. Applying salt immediately after a snowfall can dramatically reduce traffic crashes. Intuition tells us that salting and clearing roadways of snow and ice make roads safer and this has been confirmed by studies in both Europe and North America. Within a few hours of spreading salt, a study from Marquette University found an 85% reduction in crashes and an 88.3% reduction in injury-causing accidents (Salt Institute 2009). This is seen in Figure 3.6.

From a scientific point of view, removing snow and ice from the roadway restores a higher coefficient of friction to the road and as such vehicles will have more traction. This will improve a drivers' ability to maintain control. Enhancing traction through winter maintenance, plowing and spreading salt, is one of the proven safety countermeasures in our roadway safety plans (Salt Institute 2009).

Table 3.5: Cost Associated with a One-Day Snowstorm

State/Province	Lost wages	Lost retail sales	Lost tax revenues	**Total per day**
	($Millions)	($Millions)	($Millions)	**($Millions)**
Iowa	38.35	19.91	4.51	**62.67**
Illinois	220.66	98.48	30.43	**349.57**
Indiana	88.23	41.18	10.94	**140.35**
Michigan	165.33	71.5	21.65	**258.48**
Minnesota	97.79	40.32	13.35	**149.46**
Missouri	90.7	39.05	10.45	**140.19**
New Jersey	174.44	80.66	25.77	**280.87**
New York	381.63	161.76	54.18	**597.57**
Ohio	179.29	79.07	23.14	**281.5**
Pennsylvania	214.17	93.17	29.37	**336.7**
Virginia	130.39	56.95	17.64	**204.98**
Wisconsin	84.82	38.78	10.76	**134.36**
Ontario	272.02	33.33	51.79	**357.14**
Quebec	142.77	19.23	28.01	**190.01**

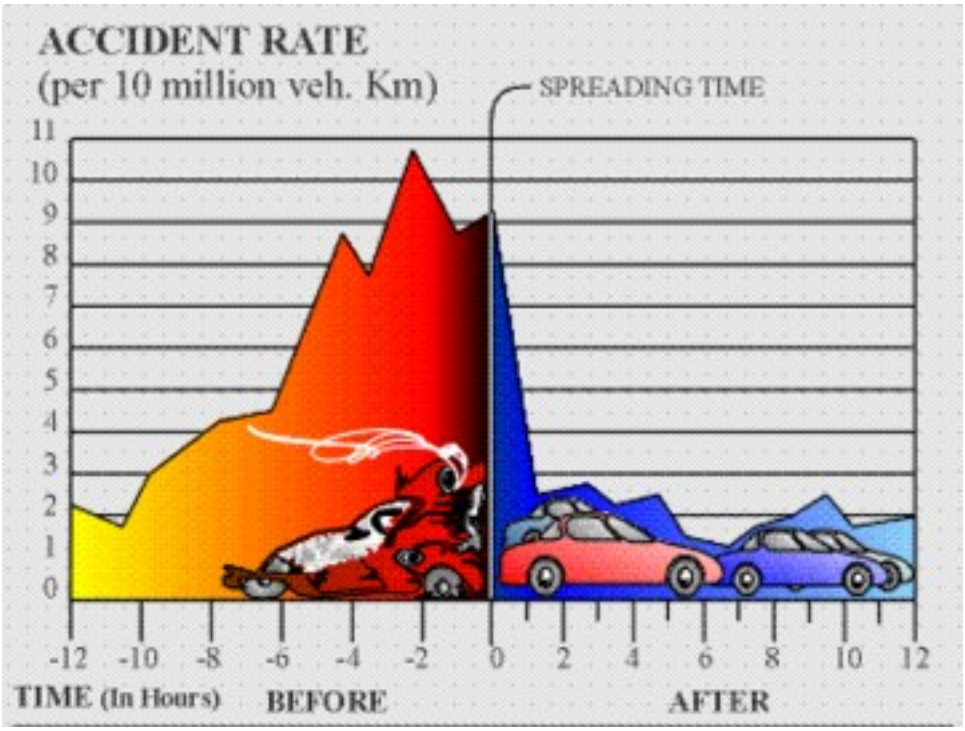

Figure 3.6: Accident Rate Before and After Salt Spreading (Salt Institute 2009)

3.5 Deicing Salts Functions

Salt is usually applied dry but it does not begin its snow-fighting job until it dissolves into brine. This occurs when salt is mixed with water. The concentration of the brine and the temperature of the pavement are the important variables, determining whether and how quickly salt will work (Salt Institute 2009).

When salt first dissolves in water, the resulting brine is at the saturation level, which is around 25 percent. The brine is then quickly diluted by the snow, ice or rain it is in contact with. As the solution becomes more diluted, there is less salt to depress the water's freezing point, assuming the temperature is constant. If the temperature lowers, the loss of melting power accelerates. Intense storms may require multiple applications, so that the brine concentration does not become too dilute and not function as it was initially intended for. The phase diagram for deicing salt is shown in Figure 3.7.

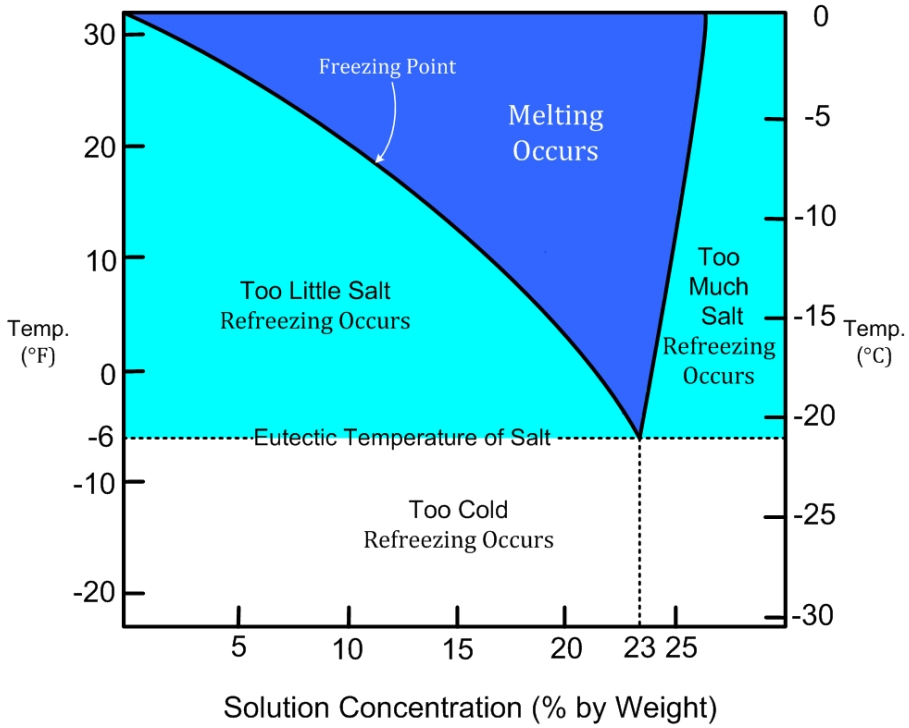

Figure 3.7: Phase Diagram for Salt (Salt Institute 2009)

When salt dissolves in water, the freezing point is depressed in proportion to the concentration of ions in the solution. Sodium chloride is very soluble in water and it also yields a large number of ions per unit weight which makes it especially effective as a freezing point depressant (National Research Council 1991).

As was already mentioned, the addition of salt to water lowers the freezing point of the resulting solution until the concentration reaches about 25 percent. This threshold concentration marks the eutectic point, which means that the addition of more salt past this concentration will not lower the freezing temperature any further. The eutectic temperature for NaCl salt solution is -21˚C (National Research Council 1991; Salt Institute 2009).

Ice melting is too slow near the eutectic temperature to be of any use. At pavement temperatures below -12˚C, sodium chloride is seldom used, and highway agencies rely more on sanding or salt mixed with calcium chloride, which remains effective in cold conditions (National Research Council 1991). Fortunately, most snowstorms occur when the air temperature is between 0° C and -7° C, the temperature range where sodium chloride salt is very effective (Salt Institute 2009).

The formation of ice on a roadway depends on the air temperature, relative humidity, temperature of precipitation, temperature and heat capacity of the infrastructure, wind speed and lastly the concentration of salt products on the highway (Conciatori, Brühwiler et al. 2009).

The objective of deicing application is not to melt the snow and ice entirely off the roadway but to prevent the formation or break up the interface between the pavement and the ice or snow. If applied properly, small amounts of salt usually produce partial melting and flowing brines that break the bond between pavement and ice, and thereby allow accumulations to be removed by the action of traffic or plowing (National Research Council 1991; Salt Institute 2009).

3.6 Salt application

The United States and Canada spend over $2 billion dollars each year on snow and ice control (EPA 1999). Critical bridges and highways are typically treated most intensely, through higher application rates and with more frequent treatments. Lower-priority streets and secondary roads are often left untreated for longer periods of time or not treated at all. (National Research Council 1991)

In North America, there are four main materials that are used for deicing salt application. The four materials used are sodium chloride, calcium chloride, magnesium chloride and blended chlorides. Their properties are summarized in Table 3.6 (National Cooperative Highway Research Program 2007).

Table 3.6: Materials Used for Deicing Salt Application

Material	Chemical Formula	Forms Used	Optimum Eutectic Temperature °C (°F) @ % Concentration [1]	Common Sources	Approximate Annual usage Tonnes (Tons) North America	Median Cost (USD) per Ton (survey of Internet contracts)[2]
Sodium Chloride	NaCl	Primarily solid, but increasing use of liquid	-21 (-5.8) @ 23.3%	Mined from natural deposits, solarization of natural brines	21'080'000 (22'291'000) (Salt Institute)	$36
Calcium Chloride	$CaCl_2$	Mostly liquid brine, some solid flake	-51 (-60) @ 29.8%	Natural well brines, by-product of the Solvay process	Not Available	$120
Magnesium Chloride	$MgCl_2$	Mostly liquid brine, some solid flake	-33 (-28) @ 21.6%	Solarization of natural brines, natural well brines, by-product of metallurgical process	Not Available	$95
Blended Chlorides	Varies with product	Solid and liquid	Varies with product	Natural well brines, solarization of natural brines, mined from natural deposits	Not Available	$142

[1] Source: (Ketcham and et al. 1996)
[2] as of October 2003

Salt is applied onto highways using two main strategies. The first is the traditional deicing strategy, which applies dry salt or pre-wet salt onto the roadway to remove snow and ice bonded to the surface. This is considered a reactive strategy. The second strategy is referred to as anti-icing. Salt is applied before a bond between the ice and roadway can occur. This is done by spraying brine or applying pre-wet solids

on the pavement before a storm occurs. This is considered a pro-active strategy (Salt Institute 2009).

The difficulty with anti-icing programs is that it is tough to predict if a storm will occur in advance. To complement anti-icing strategies, road weather information systems (RWIS) for highway snow and ice control should be used. Components of the RWIS include meteorological sensors, pavement sensors, site-specific forecasts, temperature profiles of roadways, a weather advisor, communications, and planning. RWIS can warn highway agencies if a storm is about to take place as well as maximize the effectiveness of icing and plowing efforts by pinpointing and prioritizing roadways that need attention. RWIS technologies can improve efficiency and effectiveness of deicing as well as reducing the costs of highway winter maintenance (EPA 1999).

In 1967, Salt Institute initiated a "sensible salting" program. The main focus of this program was on proper planning, personnel training, equipment maintenance, spreader calibration, proper storage, proper maintenance around chemical storage areas, and environmental awareness. (Salt Institute 2009)

With the growing concern of salt discharges to the environment in Canada, the Transportation Association of Canada has recognized best practices in planning for salt management (Transportation Association of Canada 2003). The Oregon DOT (Oregon Dept. of Transportation 1999) and NYSDOT (NYSDOT 2001) also makes best practice recommendations for reducing salt usage. For more detail on salt application practices, it is recommended to visit the website, "Center for Environmental Excellence" by the American Association of State Highway and Transportation Officials (AASHTO 2009). Further information can also be found in report 577 written for the National Cooperative Highway Research Program (National Cooperative Highway Research Program 2007).

3.7 Salt Storage

Salt storage has become a major concern since improper storage might allow salt to enter the environment. If properly stored, salt will not be lost by wind or precipitation. Storage piles should never be left exposed to rain or snow. A permanent covered storage facility is the best solution but if this is not possible, then outside piles should be placed on impermeable pads and covered with a waterproof material (Salt Institute 2009).

Storage in a roofed enclosure will:

- Prevent formation of lumpy salt that is difficult to handle with loaders and move through spreaders
- Eliminate the possibility of contaminating streams and wells with salt runoff
- Eliminate salt loss through dissolving and runoff

Salt storage facilities also allows agencies to be sure that they will have access to salt when a storm hits and everything is chaotic. The winter maintenance crews will have the salt needed to keep the roads safe and accessible. A good guideline for salt storage capacity is to have enough salt in your storage facility for a full, average winter (Salt Institute 2009).

It should be noted that salt never loses its capability to melt snow and ice no matter how long it is stored. Rock salt is already between 210 and 320 million years old when it is mined. Carrying over salt on storage piles to the next year or even longer does not diminish the salt's melting power (Salt Institute 2009).

Chapter 4

Modeling

4.1 General

Modeling chloride ion ingress is no easy task. There has been an assortment of programs on the market, as well as technical papers and dissertations, each focusing on different aspects of the transport process. Generally, two types of models are used to simulate the movement of chloride ions: microscopic and macroscopic models.

Microscopic models describe the flow of chloride ion movements and their chemical balance in the concrete. This includes models such as Stadium, Ms Diff, Masi, by-Shin, and Schmidt-Döhl (Conciatori, Sadouki et al. 2008; Conciatori, Laferrière et al. 2010). Macroscopic models take into account the overall chemical effect on transport by considering the various thermal variations as well as the hydrous and ionic movements. The chemical reactions are not directly involved in the macroscopic model and are only considered through parameters simulating the chemical effects on transport. Such macroscopic models include TransChlor, Roelfstra, ClincConc, Saetta, by-Meijers, and Ishida (Conciatori, Sadouki et al. 2008; Conciatori, Laferrière et al. 2010). Even though the microscopic models simulate phase changes and chemical interactions more precisely as well as take into account porosity changes, they require extensive testing to calibrate the model parameters, which can be unfeasible financially and also time consuming (Conciatori, Sadouki et al. 2008; Conciatori, Laferrière et al. 2010).

The model used in this work is the TransChlor model. The TransChlor model is an original program that simulates chloride ion movements in concrete and also considers microclimates created from real climatic data. The data is obtained from meteorological stations. The model also considers the exposure level of the various reinforced concrete structural elements. In the model, vapor movement is characterized by the diffusion process. Capillary suction, which is described as the acceleration of water movement by the adhesive forces between the liquid water and the pore structure of the concrete, is also implemented in the model. The movement of liquid water and water vapor are treated separately (Conciatori, Sadouki et al. 2008; Conciatori, Laferrière et al. 2010).

4.2 Exposure Model

On a structure, each element is exposed to different exposure conditions. Whether it is climatic or chemical exposure, some elements will be more exposed than others and therefore undergo a more severe deterioration process.

The microclimate of the structure depends on its geographical location in the world. A bridge in eastern Canada will have a very different microclimate than a bridge in western Canada. The microclimate includes air temperature, relative humidity, solar radiation and precipitation. The climatic model used in the simulations is discussed in more detail in the next chapter.

The location of the element on the structure is also crucial, bearing in mind that a column will have a different exposure then a beam or slab. The borders, the exterior face of the slab and the bridge deck joints are the most exposed locations to aggressive agents and stagnation of water and are thus most likely affected by deterioration damage caused by corrosion (Conciatori, Sadouki et al. 2008).

On a bridge, the exposure of the structure has been classified into three categories: (i) stagnant water, (ii) splash water, and (iii) spray. It has been seen in past research that chloride ingress takes longer under mist exposure compared with stagnant or splash water exposure. Therefore, chloride ion ingress in the concrete cover is much more significant for zones exposed to stagnant and splash water than for mist exposure zones. Hence, deterioration occurs a lot quicker in zones that are in direct contact with water and aggressive agents (Conciatori, Sadouki et al. 2008).

4.2.1 Stagnant water

In the case of stagnant water exposure, precipitated water accumulates and makes direct contact with the structural elements. The wetting time is the time period when droplets of water are formed on the concrete surface. Wetting time is very short, usually only a couple of minutes if precipitation is interrupted and depends on precipitation intensity.

Once the storm ceases, drying of the structures surface can begin. This is achieved by drainage systems, evaporation, and absorption of water into the concrete. The drying time depends on the quantity of water, likelihood of water stagnation on the surface, the amount of solar radiation, air temperature, wind speed, flow of traffic and type of surface coating. The drying phase can range from half an hour to several hours (Conciatori, Brühwiler et al. 2009).

4.2.2 Splash Water

Rainwater during a storm creates a 1 to 2 mm layer of water on the roadway surface. Part of this water film is driven over by vehicles and droplets are projected laterally from the roadway. The height and distance of the projected droplets depends

mainly on the speed of the vehicles as well as the water film thickness on the road. Areas exposed to splashing depend on the elements spatial location relative to the roadway (Conciatori, Brühwiler et al. 2009).

4.2.3 Spray Water

Certain parts of the structure can be completely protected from precipitation and only exposed to humidity in the air or spray composed of moisture and salt products. The moisture content increases somewhat with the passage of vehicles on the roadways since the vehicles kinetic energy causes suspension of fine water droplets in the air. The movement of the air masses caused by wind and the flow of traffic transports this fine mist over the roadway.

Studies of water spray using real traffic have been done on road sections in Canada. The speeds were studied at 50, 60, 80 and 100 km/h. Snow samples were collected at several locations on a line transverse to the direction of traffic and were analyzed. The results indicate a decrease in the concentration of chloride ions with distance from the roadway. Other studies have shown that 90% of sodium chloride, contained in the mist water, settles over a distance of 20 meters when no wind is observed. Wind is an important parameter for the transportation of these droplets since the wind can carry it over long distances, amounting to several kilometers (Conciatori, Brühwiler et al. 2009).

4.2.4 Structural exposure

The variability in microclimates and environmental stresses is taken into account by considering the different exposure conditions of the structure. The terminologies adopted in Figure 4.1 for the different zones of exposure is S for stagnant water

exposure, E for splash water exposure, B for spray water exposure, and CL for exposure to chloride ions during the winter period. The letters are derived from the French translation of each exposure class and are adopted in this thesis.

In the case of a bridge, different components of the structure are subjected to different exposure conditions as well as risks of chloride ion ingress. This is illustrated in Figure 4.1. The deck slab of the bridge, if no seal is under the asphalt or if the seal is defective, will be exposed to stagnant water. Some areas, where the joints are failing or where drainage is defective, may also be exposed to stagnant water. The borders are usually subjected to splashing, including the outside vertical faces of the borders that can be reached by splash or drips flowing down a vertical surface by gravity. Protected elements, such as bridge piers and the area under the slab, are exposed to salt spray. The exposure condition in the caissons is that of mist but without the presence of chloride ions if no penetration is noted (Conciatori, Brühwiler et al. 2009).

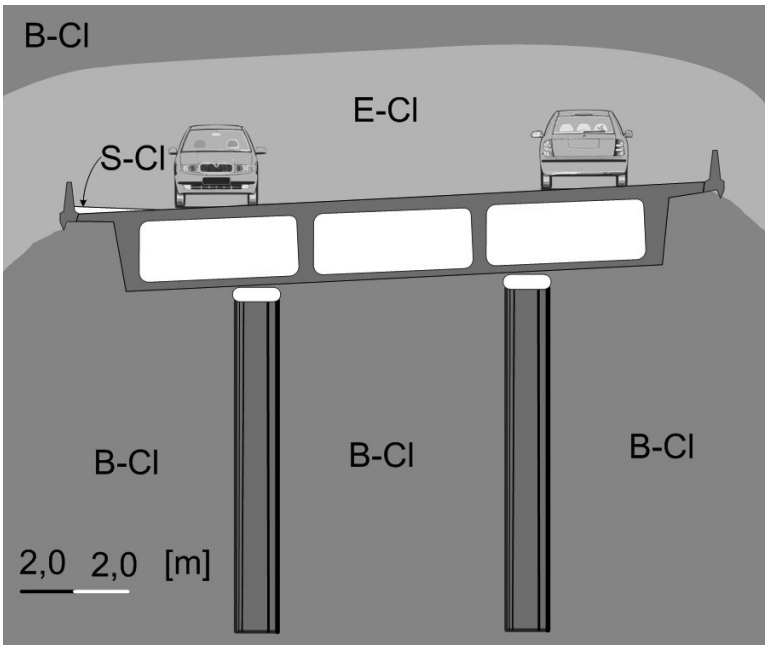

Figure 4.1: Profile of a Bridge with Different Exposure Zones
(Conciatori, Brühwiler et al. 2009)

Sources of damage reported on concrete bridge overpasses is water leaking through the transverse and longitudinal joints, water leaking through the bridge deck, water running off the edge of the deck, traffic spray, and collision damage. The most common damaged members are the beams, pier caps, columns, and abutments. The location of damage is dependent on three factors; the member type (beam, column), the location of the element (interior beam, exterior beam), and the source of damage (chloride-laden water leaking through joints, salt spray) (Enright and Frangopol 2000).

Most bridges are found to have damage due to water leaking through the transverse deck joints. As can be seen in Figure 4.2, water leaks through these joints over the pier caps and abutments. This causes damage to the beams, pier caps, and columns (Enright and Frangopol 2000).

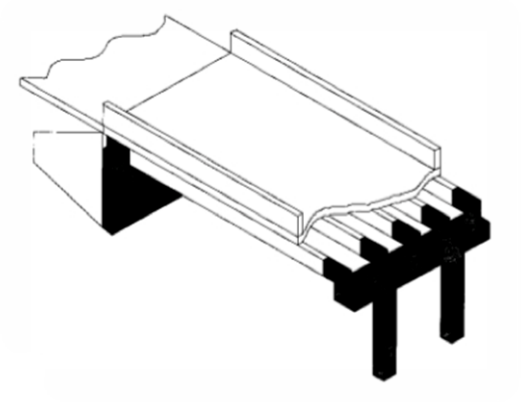

Figure 4.2: Structural Members Affected by Leaking Water
(Enright and Frangopol 2000)

Another possible source of damage is water runoff onto the exterior beams. Chloride-laden water from the application of deicing salts is carried over the edge of the bridge deck. This causes damage to the exterior beams, pier caps, and columns. Figure 4.3 shows this type of damage scenario (Enright and Frangopol 2000).

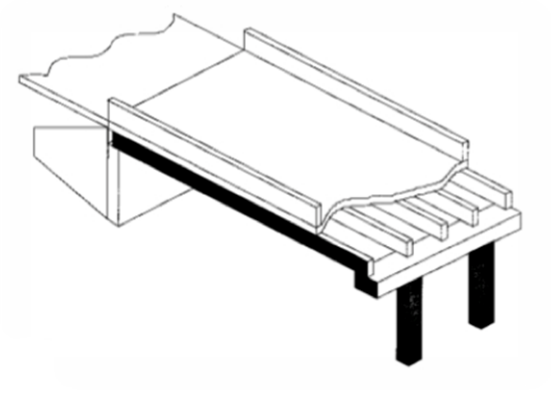

Figure 4.3: Structural Members Affected by Water Runoff
(Enright and Frangopol 2000)

A third source of damage is traffic spray from vehicles passing underneath an overpass. In this scenario, chloride-laden water becomes airborne from the splashing and spraying action caused by the vehicular traffic. This causes damage to the underside of an overpass and mostly affects the sides and bottom of the beams, the pier caps and the columns (Figure 4.4).

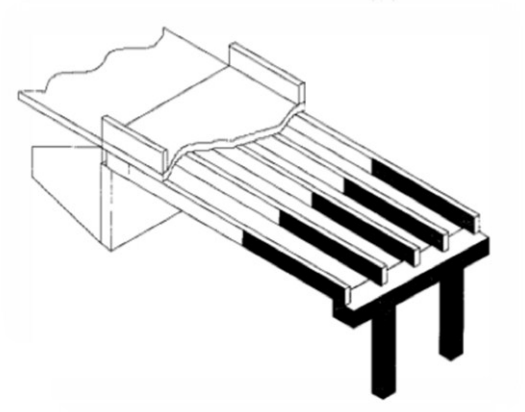

Figure 4.4: Structural Members Affected by Traffic Spray
(Enright and Frangopol 2000)

4.3 Climatic Model

A major feature of the TransChlor model is that it uses real life climate data in its simulations. Therefore, this model takes into account the actual environmental conditions affecting the bridge. A climatic model using historical climate data was created for the structure being analyzed.

The microclimate in the model considers the climatic environment of the various elements of a structure. It is a function of the structural element's exposure to solar radiation, carbon dioxide concentration and the weather conditions (Conciatori, Laferrière et al. 2010). The model distinguishes between shaded areas, sunny areas, areas exposed to precipitation water, protected areas, areas of rapid drying and areas of stagnant water. The microclimate parameters are composed of the air temperature, relative humidity of air, precipitation, and stagnation of water. The severity of a winter period in one year is defined as the number of days where the hourly temperature never surpasses 0°C. Wind intensity and direction have not been considered in the model. The effect of wind was taken into account indirectly in the creation of the TransChlor model by monitoring a structures' exposure and calibrating the model with the results. Comparison of the weather station above the bridge and monitors in the caissons considered the effect of wind since the sensors on the bridge are exposed to wind while the sensors in the caissons are not. The difference found in temperature and relative humidity between the weather station and the various sensors on the bridge were then incorporated into the TransChlor model. (Conciatori, Brühwiler et al. 2009)

To get the precision needed, hourly data was required from the beginning of the service life of the structure. It was assumed that the bridge considered for this application was constructed in 1965.

Climate Data Online, which is a branch of Environment Canada (Environment Canada 2010) provided the necessary hourly data. The four types of hourly data needed for the simulation were temperature, relative humidity, precipitation, and solar radiation.

The hourly data provided from Climate Data Online, however, was not complete and work had to be done on the data set. The hourly data provided for one day was fully complete, partially complete or incomplete. Depending on those three situations, different treatments were performed on the data.

It should be noted that most of the data was complete except for the hourly precipitation data, which required the most work. Furthermore, solar radiation data was only provided for the last 22 years. It was seen that there was a general trend in the solar radiation data and that it did not change very much from year to year. Therefore, the 22-year period was used as being representative of long-term trends. Temperature and relative humidity was missing only a few values but estimates of those values were provided by Climate Data Online and as a result, required the least amount of work.

To complete the hourly precipitation data, daily precipitation data was found on the Environment Canada website and was used to make an estimate of the hourly precipitation data for that day. This was done by taking the daily precipitation data, and turning it into an hourly precipitation as will be explained below.

The first step was to determine the distribution of the duration of rain events for the entire data set. The total number of rain events that occur for each storm length is shown in Figure 4.5.

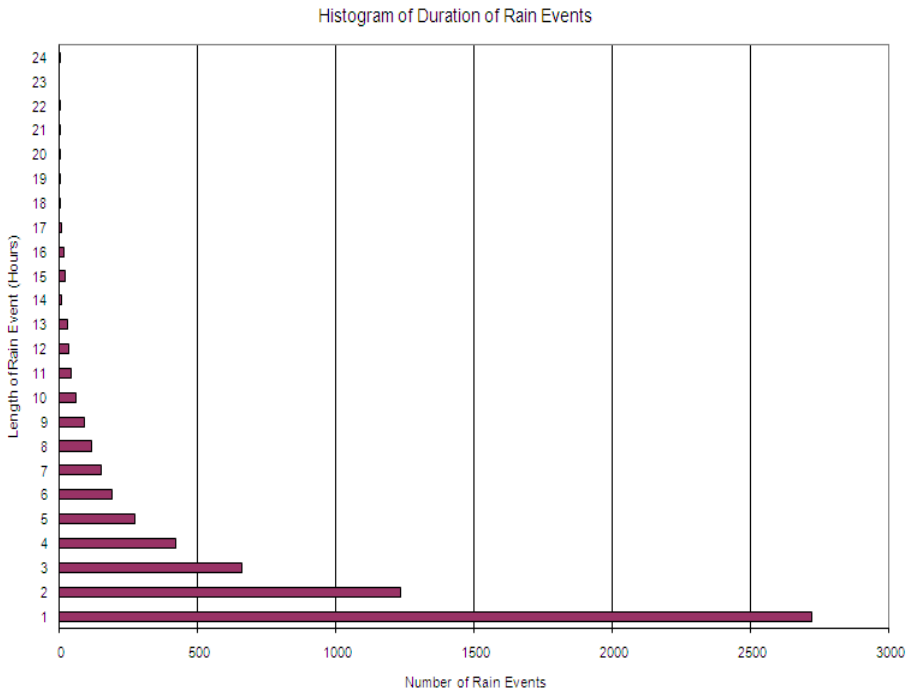

Figure 4.5: Cumulative Histogram of the Duration of Rain Events

The sum of all rain events was then divided by the total number of rain events in each duration class so that the distribution would be from 0 to 1. This is shown in Figure 4.6. An equation for the curve of best fit was determined so that a randomly generated number from 0 to 1 could then establish a random duration for any rain event. Once the duration of storm was randomly determined, the daily precipitation data was evenly distributed over the length of the rain event starting at a random time during that day. To see the results, proceed to the precipitation data section found in chapter 5.

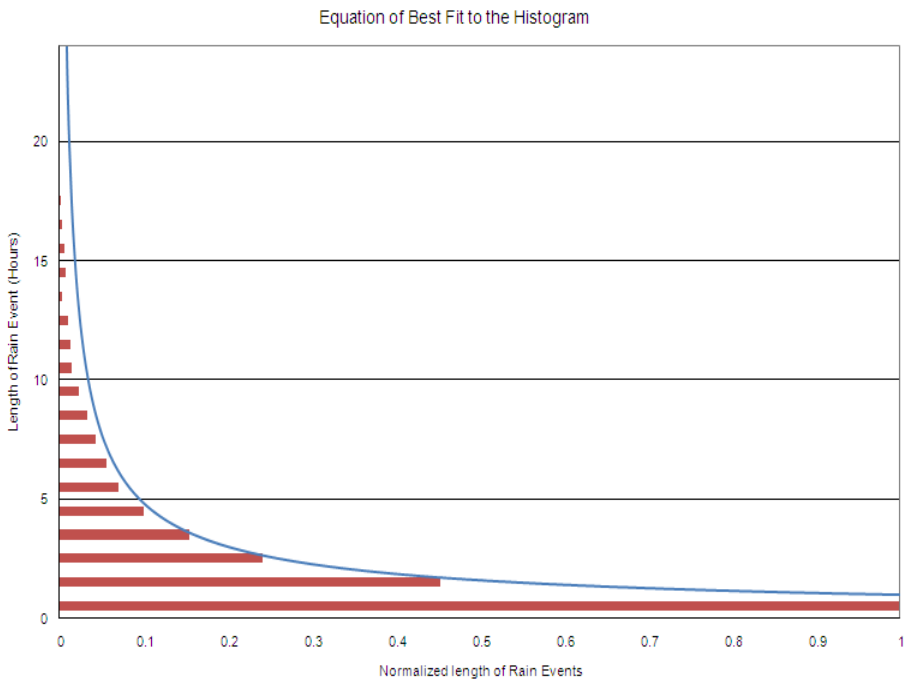

Figure 4.6: Equation of Best Fit to the Cumulative Histogram

Once the climatic model was completed, it was loaded into the TransChlor simulation program. Graphs of the hourly precipitation data are provided in the next chapter. The graphs distinguish between hourly precipitation data given and that which was estimated using the methodology just described.

4.4 Estimation of Salt Usage

Each winter, salt is spread on roadways across North America. A salt estimation for Montreal was not readily available. There were tremendous difficulties in determining the salt utilization because of the many different variables that affect this quantity. The variables to consider include type of salt spreader, salt application policies, local weather, severity of storms and winters, geographical location, type of road and importance, salt management, inventory control, etc. All these factors contribute to fluctuations in the amount of deicing salts applied to roadways.

For the TransChlor model, it is important to know how much salt is being spread over a surface area. Therefore, it is important to know not only how much salt is being spread but also the area of the roadway being treated.

Several surveys provide estimates of the amount of salt used per winter in major Canadian cities (Table 4.1) (Delisle and Dériger 2000). It is estimated that the City of Montreal uses 60,000 tons of salt per winter.

Table 4.1: Estimate of Waste Snow and Salt Usage (per winter)

City	Total snow volume (m^3)[1]	Quantity of salt used (tonnes)
Vancouver	<100 000	2 254
Calgary	320 000	20 428
Regina	150 000	2 067
Winnipeg	175 000	24 525 [2]
Toronto (before amalgamation	1 500 000	17 884
Ottawa-Carleton	1 220 000	68 000
Montreal	11 258 000	60 000 [3]
Quebec City	3 000 000	35 000
Moncton	159 000	12 695
Halifax	N/A	41 679
Charlottetown	N/A	2 300
St. John's	N/A	21 530

[1] These quantities are approximate and vary yearly with snowfall amount, N/A = not available.
[2] Plus 100 000 tonnes of a sand/salt mix containing 5% NaCl.
[3] Plus 39 000 tonnes of a sand/gravel mix (1:9 for sidewalks and 5:5 for streets) during freezing rain.

Annual salt estimation in Montreal was also provided in an email by Service d'Exploitation du Réseau, which is shown in Table 4.2. As can be seen, there is large variation in annual salt application from year to year. The average annual salt estimation might overestimate the amount for some years and underestimate the amount for others.

Table 4.2: Estimated Annual Salt Estimation in Montreal

Year	Quantity of salt (Tons)
2000-2001	62 653
2001-2002	37 655
2002-2003	50 264
2003-2004	44 929
2004-2005	51 230
2006-2007	37 522
2007-2008	57 452
2008-2009	55 844
2009-2010	30 711

(Service d'Exploitation du Réseau, 2010)

However, the last two tables do not indicate how much surface area this salt is spread on. Therefore, other data was needed. It was found that the MTO used an average rate of 34 and 38 tons of salt per two-lane kilometer for the 2007-2008 and 2008-2009 winter seasons, respectively. This estimation is much larger than that reported for Montreal, which is between 20 to 30 tons per 2 lane km (Jefremczuk 2005). This estimation of salt application for Montreal seems reasonable and was confirmed to be realistic when analyzing the boundary conditions of salt application using the TransChlor model.

4.5 Description of the TransChlor Model

In this thesis, the TransChlor model was used to simulate chloride ion ingress into the cover of a reinforced concrete bridge. It is a novel model that was created to take into account real life climate conditions in the chloride ion transportation process. The model uses weather and deicing salt data to predict the spatial and temporal evolution of the chloride ion concentration in the pore structure of the concrete (Conciatori, Laferrière et al. 2010). The objective of the TransChlor model is to

predict the corrosion initiation probability of the steel found in reinforced concrete structural elements.

There are two main transport mechanisms that control chloride ion ingress in the concrete cover, diffusion and capillary suction. Diffusion is the flow of molecules or ions in the interstitial fluid from high to low concentrations. This model incorporates a simplified form of Fick's diffusion law for water vapor transport, thermal diffusion and chloride ion diffusion in water. Surface tension acting in the capillary pores causes liquid water to be transported by capillary suction. Fick's diffusion law does not accurately describe this process. This movement was modeled by considering the kinetic motion of the phenomena. The movement of water is then converted into chloride ion movement by a specific algorithm that simulates chloride ion convection in water (Conciatori, Sadouki et al. 2008; Conciatori, Laferrière et al. 2010).

The TransChlor model only takes into account two primary chemical reactions, carbonation and adsorption of chloride ions by the cement paste. The second chemical reaction is a reversible transformation and therefore can adsorb or release chloride ions into the concrete pore structure (Conciatori, Laferrière et al. 2010).

The TransChlor model assumes a 1-dimensional linear progression into the concrete. The model uses a finite element method to solve for the ion propagation within the concrete cover (i.e. space) and uses a finite differences method to solve for the duration of progression of the propagation front (i.e. time) (Conciatori, Sadouki et al. 2008; Conciatori, Laferrière et al. 2010).

The model uses a numerical approach for the various transport modes. These modes include thermal and vapor transfer, liquid water transport with and without chloride ions, capillary suction, chloride ion diffusion in water, and carbon dioxide diffusion in concrete (Conciatori, Laferrière et al. 2010). Movements of substances in

the concrete depend directly on the concrete permeability for all transport modes, except for thermal transfer (Conciatori, Sadouki et al. 2008).

The important parameters considered are the microclimate and deicing salts. The microclimate and deicing salts were discussed in previous sections. The model considers the thermal and vapor diffusion process as well as the hydrous transport process by capillary suction as a function of the extent of carbonation while it simulates chloride ion ingress. The extent of carbonation is important since it determines the amount of chloride ions bound to the cement paste. The carbonation rate is a function of the molar concentration of calcium hydroxide and calcium silicate hydrate (Conciatori, Sadouki et al. 2008).

The time step used in the simulation was set to 1 hour. This time interval provides sufficient accuracy in the simulation with respect to the temperature profiles, precipitation and water contact with the concrete surface. This interval also takes into account wetting and drying cycles, which have been found to be an important contributor to chloride ion movement in concrete. If this time interval is increased to a few hours, the wet periods become too large and cause an overestimation of the ionic transfer (Conciatori, Laferrière et al. 2010). The time interval can be shortened to gain more precision but it is very difficult to acquire climatic data smaller than one-hour intervals over large periods of time.

In terms of exposure conditions, this model differs from other models since it classifies elements into three distinct categories of exposure instead of assuming a uniform atmosphere over the entire structure. This was described earlier in the exposure model section. The exposure model schematic used in the TransChlor simulations can be seen in Figure 4.7. Shown in the Figure is the occurrence of a rain event as well as the hypothesis the model employs for direct and splash exposure.

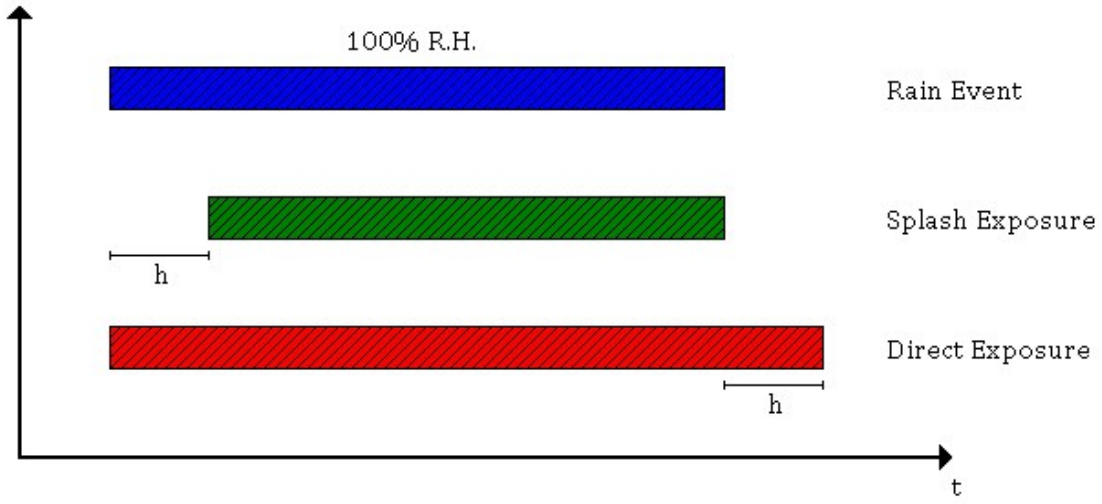

Figure 4.7: Schematic of TransChlor Exposure Model

When a rain event occurs, the surface is saturated with water and the relative humidity reaches 100%. The model assumes that direct exposure starts instantaneously and that splash exposure is delayed by h hours, where h is roughly one hour. This is because it takes some time for a sufficient amount of water to accumulate on the surface before splashing can commence. Direct exposure does not need an accumulation of water and commences as soon as the surface is saturated. Once the rain ceases, drying starts almost immediately and can take some time until the surface is completely dry. The model assumes that it takes one hour after the end of the rain event to become fully dry and therefore, direct exposure is prolonged for that time. Splash exposure on the other hand, ends as soon as the rain stops since it is assumed the water layer on the surface evaporates or is carried off by drainage. Hence, there is an insufficient amount of water on the roadway to accommodate splashing. Mist exposure does not directly relate to the occurrence of a rain event but to the relative humidity and triggers the model when the relative humidity of the air is above 95%.

To generate an intervention of the application of chloride ions to the concrete surface in the TransChlor model (i.e. deicing salts spread on the roadway), four conditions are required:

1. $(T \leq T_{lim})$ + $(H \geq H_{lim})$
2. Rain + $(T \leq T_{lim})$
3. Snow
4. $t_{event} \geq t_{interval}$

where:

T	hourly temperature (°C)
T_{lim}	limiting temperature in the simulation (°C)
H	hourly relative humidity in the concrete pores (-)
H_{lim}	limiting relative humidity in the simulation (-)
t_{event}	Duration of an event (hrs)
$t_{interval}$	Time interval between two passes of a salt truck (hrs)

If any one of the four conditions is met, the model triggers an intervention of a deicing salt truck. The first condition implies that an intervention is triggered if the hourly temperature is less than a limiting temperature and that the relative humidity is greater than a limiting relative humidity. The limiting relative humidity is defined to be 95% since the surface is dangerously close to becoming saturated and can cause freezing of the roadway. The limiting temperature must be less than or equal to 5°C, since that is the maximum temperature when snow and freezing precipitation can occur. This limiting temperature is determined through an iterative procedure. The iterative procedure involves computing the total amount of annual interventions based on the total amount of salt spread per year divided by the amount spread per intervention and then calculates the limiting temperature needed to satisfy the number of interventions determined.

The second condition for an intervention occurs when there is precipitation and the temperature is less than the limiting temperature. This combination would allow for freezing rain to occur and cause ice to form on the concrete surface. The third condition takes place when there is snow. Unfortunately, snow was not taken into account in our simulations. The data provided for precipitation did not specifically distinguish between snow and rain. The last condition implies that if the duration of a winter event that required an intervention (i.e. any of the other conditions) is longer than the time interval determined between the passages of two deicing salt trucks, another intervention must occur. For our simulation, it was assumed that the time interval between two consecutive trucks on the same section of highway must be 8 hours. This means that a deicing salt truck can only spread more salt 8 hours after the previous application so that efficient and effective use of deicing salts are employed and to also lower the environmental footprint on our ecosystem.

The program also incorporates a probabilistic analysis for four variables in the simulation. The four variables considered are water vapor transport, liquid water transport by capillary suction, chloride ion transport, and carbonation. The model uses a two point Rosenblueth method instead of a Monte Carlo simulation method to limit computing times. It was found that the Rosenblueth method is an acceptable approach in the analysis compared with the Monte Carlo simulation (Conciatori, Brühwiler et al. 2009a).

The general formula, Equation 4.1, used in the simulation takes into account all transport modes: thermal diffusion, carbonation, hydrous transport and chloride ion transport. The first term in the formula performs calculations according to Fick's law of diffusion, while the second term is tailored for capillary suction. The parameter z, Equation 4.2, found in the third term is used only for the carbonation reaction (Conciatori, Laferrière et al. 2010).

$$\frac{\partial}{\partial t}\begin{Bmatrix} T \\ [CO_2] \\ H \\ C(B,T) \end{Bmatrix} = div\left(A \cdot \begin{Bmatrix} \overrightarrow{grad(T)} \\ \overrightarrow{grad[CO_2]} \\ \overrightarrow{grad(H)} \\ \overrightarrow{grad(C(B,T)} \end{Bmatrix} \right) - E \cdot \begin{Bmatrix} \overrightarrow{grad(T)} \\ \overrightarrow{grad[CO_2]} \\ \overrightarrow{grad(H)} \\ \overrightarrow{grad(C(B,T)} \end{Bmatrix} - \begin{Bmatrix} 0 \\ z \\ 0 \\ 0 \end{Bmatrix} \quad [4.1]$$

$$z = -(\varepsilon_{ini} \cdot f_w \cdot r_{CH} + 3 \cdot r_{CSH} + 3 \cdot r_{C3S} + 2 \cdot r_{C2S}) \quad [4.2]$$

where:

t	time (s)
T	temperature (°C)
$[CO_2]$	carbon dioxide molar concentration (mol/m^3 air)
H	relative humidity in the concrete pores (-)
C	total Cl^- concentration with respect to the concrete volume (kg/m3)
B	carbonation extent constant
A	matrix composed of the various diffusion and other coefficients
E	matrix composed of the convection and other coefficients
z	a carbonation parameter
ε_{ini}	initial porosity prior to hydration and carbonation (-)
fw	ratio of pore and film water volume to the pore volume (-)
r_{CH}	carbon dioxide reaction rate with portlandite (mol/s m^3 concrete)
r_{CSH}	mean tricalcium and dicalcium silicate forming calcium silicate hydrates (mol/s m^3 concrete)
r_{C3S}	tricalcium silicate reaction rate (mol/s m^3 concrete)
r_{C2S}	dicalcium silicate reaction rate (mol/s m^3 concrete)

The matrix A, Equation 4.3, is composed of the various Fick's diffusion law coefficients. The 4x4 matrix contains coefficients for thermal, carbon dioxide, vapor and chloride ion diffusion as well as the relationships between vapor and chloride ion diffusion (Conciatori, Laferrière et al. 2010).

$$A = \begin{bmatrix} \frac{\lambda_T(T,f)}{c_T(w)} & 0 & 0 & 0 \\ 0 & \frac{D_B(\varepsilon, H_{ext})}{\varepsilon \cdot (1-f)} & 0 & 0 \\ 0 & 0 & D_h(T,H) & 0 \\ 0 & 0 & R_{Cl} \cdot c_f(B) \cdot D_h(T) & D_{Cl} \end{bmatrix} \quad [4.3]$$

where:

λ_T	concrete thermal conductivity (W/(m K))
f	water content with respect to the water density (-)
c_T	unit concrete heat-storage capacity (kJ/(m^3 K))
w	concrete water content per cubic meter of concrete (kg/m^3)
D_B	carbon dioxide diffusion coefficient in concrete (mm^2/s)
ε	pore volume with respect to the total concrete volume (-)
H_{ext}	average atmospheric relative humidity between the concrete fabrication and current simulation time (-)
D_h	water vapor diffusion coefficient (mm^2/s)
R_{Cl}	delay coefficient
c_f	free chloride ion concentration in the concrete interstices with respect to the solution volume (kg/m^3)
D_{Cl}	free chloride ion diffusion coefficient (mm^2/s)

The matrix E, Equation 4.4, is composed of the material movement equations, the

liquid water movement and the suction of chloride ions by liquid water (Conciatori, Laferrière et al. 2010).

$$E = \begin{bmatrix} 0 & 0 & 0 & 0 \\ 0 & 0 & 0 & 0 \\ 0 & 0 & D_{cap} & 0 \\ 0 & 0 & R_{Cl} \cdot c_f(B) \cdot D_{cap} & 0 \end{bmatrix} \qquad [4.4]$$

where:

D_{cap} capillarity coefficient (mm/s)

For more information on each variable shown in the previous equations as well as a more thorough examination of the computation involved in the simulation, refer to Conciatori, Laferrière et al. (2010).

Chapter 5

Data Set

5.1 General

The TransChlor model requires two types of data sets for the simulation to proceed. The first data set is all data related to the bridge structure. This data set includes the age, specifications, drawings, concrete specifications, and any relevant reports or information associated to that structure. The second data set is related to the climate. This data set includes the temperature, relative humidity, precipitation and solar radiation for the region around the structure. This section will present the two data sets needed for the analysis of a Montreal bridge structure using the TransChlor model.

5.2 Bridge Data

In this work, data from actual bridges located in the Montreal area were used. The reports had chloride ion samples, as well as concrete parameters, which were used in the TransChlor simulations.

A large portion of the major bridges found in Montreal were constructed in 1965 and completed in time for the 1967 Montreal Expo. Therefore, these structures are roughly 45 years old. Cement Type I was used and roughly 350 kg/m^3 of cement material was used in the mixture. The w/c was not determined or easily found. Therefore, a w/c of 0.5, which was the norm in 1965, was assumed to be acceptable.

Three different investigations were performed on major bridge structures by taking concrete samples at various locations. Due to confidentiality agreements with the engineering firms involved, the identification of the bridge structures and the exact highway segments analyzed will be omitted. Table 5.1, Table 5.2, and Table 5.3 have also been provided to give a summary of all three reports.

In the first report, a total of 19 samples were taken, and chloride ion concentrations for each sample were obtained at two different depths, 25 and 50 mm. The samples were removed from the outside wall of the caissons.

In the second report, three samples were taken in 2000 and four more were taken in 2010 close to the original cores. The concrete samples were taken from the concrete slab to analyze the maximum chloride ion concentration from the surface.

In the last report, a total of 6 concrete samples were taken. The concrete samples were also taken from the concrete slab.

Table 5.1: Chloride Ion Content of Samples (Report 1)

Sample	Chloride ion content			
	(% of cement)		(Kg/m^3)	
	@surface (2010)	@surface (2000)	@surface (2010)	@surface (2000)
C1 / E4	0.302	0.060	1.057	0.210
C3 / E8	0.197	0.069	0.690	0.242
C5 / E11	0.103	0.049	0.361	0.172
C8	0.018	---	0.063	---

Table 5.2: Chloride Ion Content of Samples (Report 2)

Sample	Chloride ion content	
	(% of cement)	(Kg/m^3)
	@surface	@surface
B1	0.004	0.014
B2	0.038	0.133
B3	0.250	0.875
B4	0.003	0.011
B5	0.002	0.007
B6	0.200	0.700

Table 5.3: Chloride Ion Content of Samples (Report 3)

Sample	Chloride ion content			
	(% of cement)		(Kg/m^3)	
	@25mm	@50mm	@25mm	@50mm
E5-E6 CHA-1	0.080	0.060	0.280	0.210
E5-E6 AEA-1	0.090	0.070	0.315	0.245
E5-E6 AES-1	0.070	0.050	0.245	0.175
E5-E6 CHA-2	1.390	1.110	4.865	3.885
E7-E8 AES-5	0.040	0.030	0.140	0.105
E7-E8 AEA-9	1.930	1.890	6.755	6.615
E7-E8 CHA-4	2.930	2.930	10.255	10.255
E18-E17 CHA-2	0.070	0.050	0.245	0.175
E18-E17 AES-3	0.050	0.050	0.175	0.175
E19-E18 AEA-9	0.150	0.090	0.525	0.315
J14-J13 CHA-2	2.150	1.690	7.525	5.915
J14-J13 AEA-2	0.460	1.380	1.610	4.830
J14-J13 AES-1	0.050	0.040	0.175	0.140
J14-J13 AEA-1	0.070	0.050	0.245	0.175
J14-J13 AEA-3	0.890	---	3.115	---
J14-J13 AES-3	0.050	0.040	0.175	0.140
J14-J13 CHA-1	0.580	0.570	2.030	1.995
J15-J14 AES-3	0.050	0.070	0.175	0.245
J16-J15 AEA-7	0.040	0.050	0.140	0.175

Analyzing all the available information, a few observations were made on the exposure of various structural elements of the reinforced concrete overpass. The three main exposures observed are mist, splash and stagnant (direct). Exposure classifications for all core samples at 25 mm and 50 mm depths is shown in Figures 5.1 and 5.2, respectively.

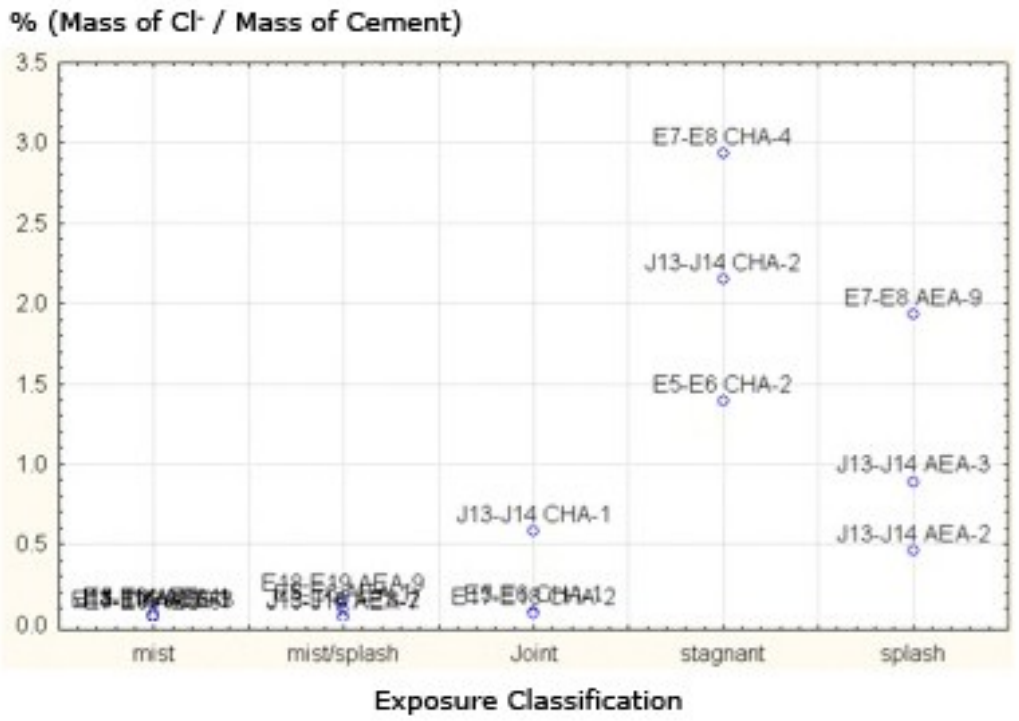

Figure 5.1: Exposure Classification for Samples at 25 mm Depth

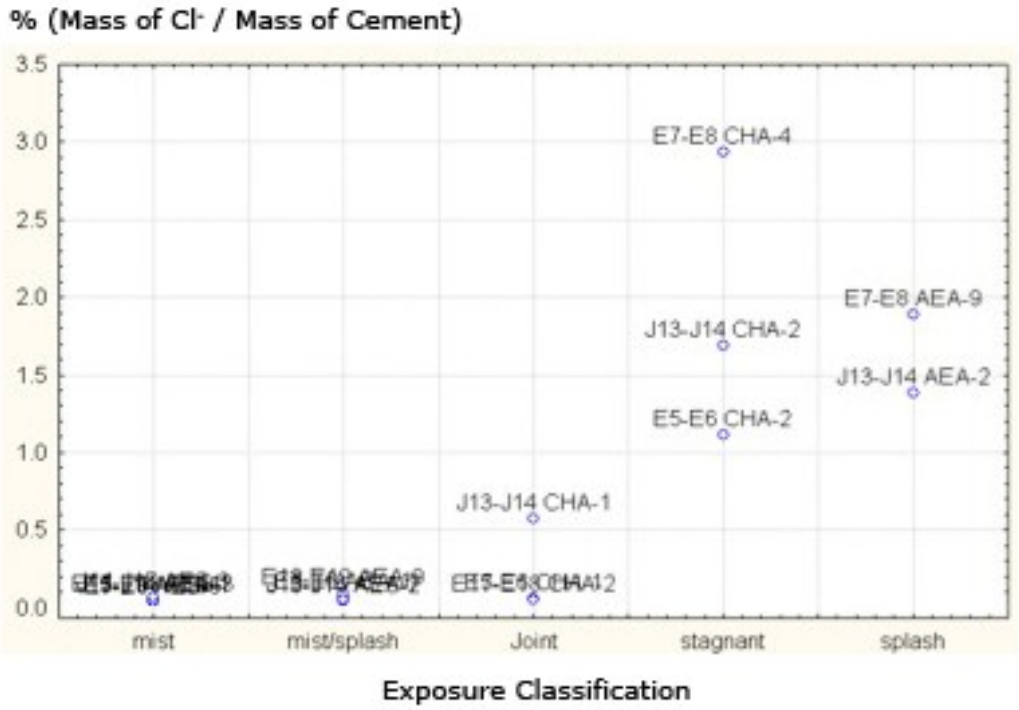

Figure 5.2: Exposure Classification for Samples at 50 mm Depth

Each exposure condition can affect structural members differently, causing a wide range in deterioration experienced. There are several damage scenarios that can occur on a bridge structure under the three main exposure conditions: stagnant water, splashing, and traffic spray.

One of the most critical sections on a bridge is the area situated around and below deck joints. The damaged is caused by water leaking through transverse joints in the deck. The water leaks through these joints over piers and abutments, and this causes the beams, pier caps and columns to be damaged (Enright and Frangopol 2000). Water stains, which are seen as dark spots under the deck joints, can be clearly seen on the underside of bridge decks. Leaking decks can cause similar damage compared to that caused by leaking deck joints. The water passes through the deck and damages the beams and other structural elements below.

Another critical section is the sides of the bridge decks. Embankments magnify the potential risk at these locations because the gradient of the road causes water to flow to one side. As a result, the lower side of the embankment is more susceptible to attack. If the drainage is damaged or clogged, water will accumulate and remain stagnant. This will allow the water to diffuse into the concrete under a pressure head. A more severe situation will occur if the defected or damaged drainage is constructed integrally inside the structure. This is because the chloride-laden water can accumulate inside the structure unnoticed and further collect with time. This would increase the pressure head and cause faster ingress into the concrete.

There is another possible damage scenario that can occur on the side of the bridge. If the drainage is damaged and water is allowed to build up, water runoff can take place on the exterior beams. This would cause chloride ions to be carried over the edges of the bridge deck and cause damage to the exterior beams, pier caps and columns. (Enright and Frangopol 2000) Comparing the lower and upper side of a bridge, the upper side of the bridge embankment shows less water staining than the

lower side. This can suggest that chloride-laden water is more likely to attack this side.

The next critical sections considered are locations of underpasses and overpasses. An underpass and overpass can have many different sources of chloride attack, including all the damage situations just stated above. Water from the decks and joints of an overpass can leak below onto an underpass. Damaged drainage can cause water to accumulate on the sides of the deck and pour over the edge onto the exterior beams or the underpass below. Traffic spray, which is produced by vehicular traffic, can cause chloride ions from the underpass to become airborne and collect on the underside of the overpass. This type of exposure causes damage to the underside of beams, pier caps, and columns (Enright and Frangopol 2000). As can be seen, a structural member can be affected by several forms of attack caused by the three different exposures. There could be a single or a combination of damage source. The harshness of each one determines the extent of degradation. Figure 5.6 illustrates best the exposure conditions of an underpass and overpass section.

Similar to the aforementioned underpass and overpass sections, bridges that are situated near other bridges can raise a reasonable concern as well. As is the case for an underpass causing traffic spray damage to an overpass, splash and spray damage from one bridge can cause damage to another bridge in its vicinity.

5.3 Climatic Data

As stated earlier, Climate Data Online, which is a division of Environment Canada (Environment Canada 2010), supplied the climatic data. The four types of hourly data provided are the temperature, relative humidity, precipitation, and solar radiation.

It is very important to get concise and accurate climatic data to use for the simulation since this is the main advantage of using the TransChlor model. The TransChlor model uses data of the real environment and predicts how chlorides will interact in this setting. If the data is not precise, then the simulation will not truly predict how the chlorides are actually behaving.

Each data set was observed for any general trend or pattern and suggestions were made on how data from the past could be used in analyzing a future bridge project. It was determined that future models could be easily made for the temperature and solar radiation data set but would be more difficult for the relative humidity and precipitation data sets. This is because of the inherent variability associated with these two events.

This is discussed in further detail in the following sections. The data for each category is also represented by graphs since the data files are extremely large and contain nearly half a million data points for each data type.

5.3.1 Temperature Data

In this section, the hourly data provided for the temperature can be seen in Figure 5.3 through 5.11. The data provided from Environment Canada was in 1/10°C. This is the exact format that is needed for the TransChlor model.

It can be seen that the maximum summer and minimum winter temperature for the island of Montreal is roughly 30°C and -30°C, respectively. There is a general trend in the yearly temperature, with the band thickness related to the variation in temperature between night and day. Therefore, it is possible to use past data to create a temperature data set of any length of time, which can then be used with the TransChlor model to estimate the residual life of an existing bridge structure or service life of a potential bridge project.

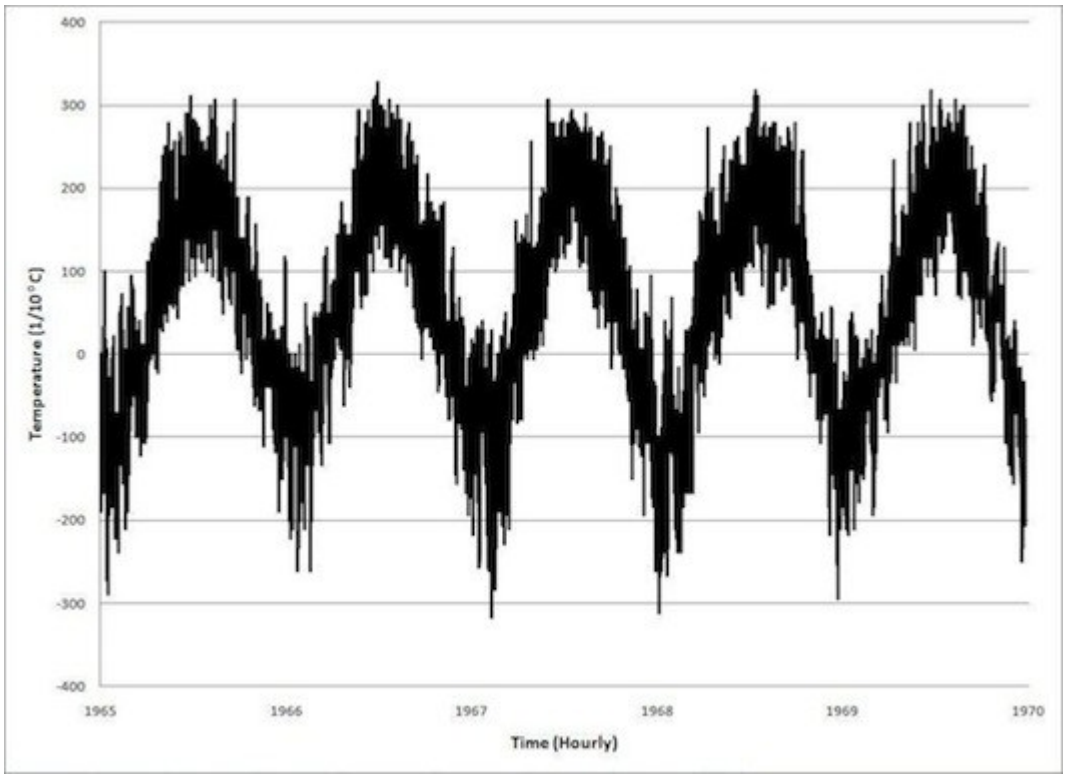

Figure 5.3: Temperature Vs. Time (1965-1970)

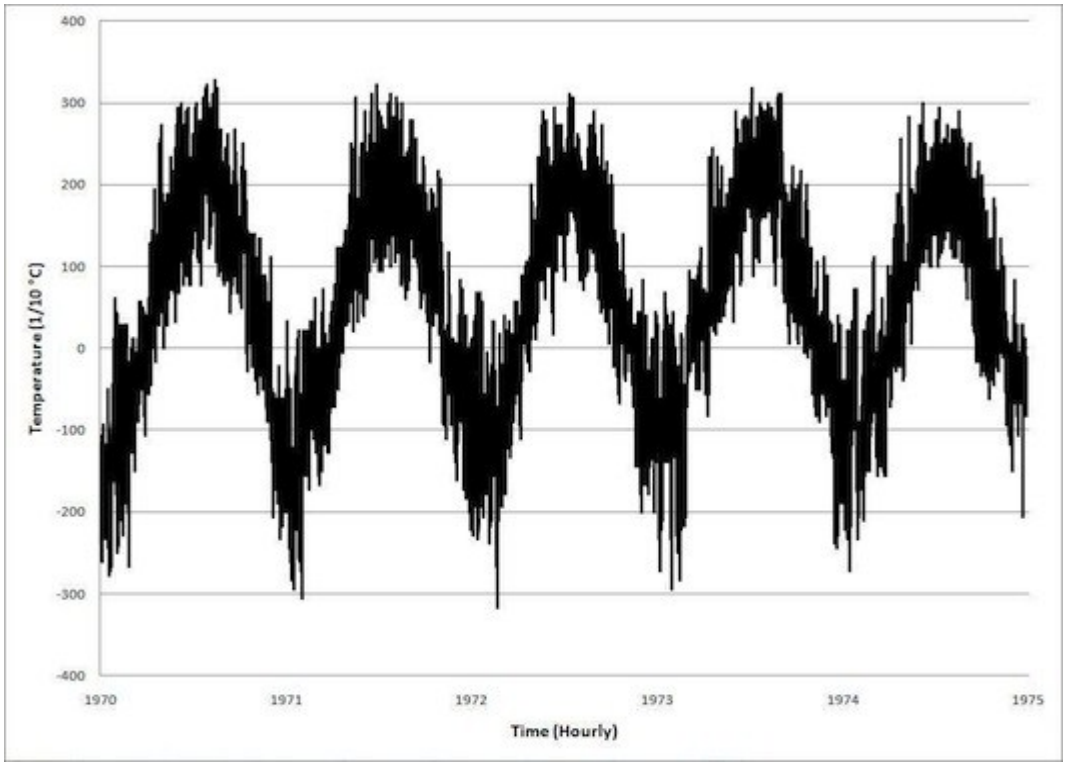

Figure 5.4: Temperature Vs. Time (1970-1975)

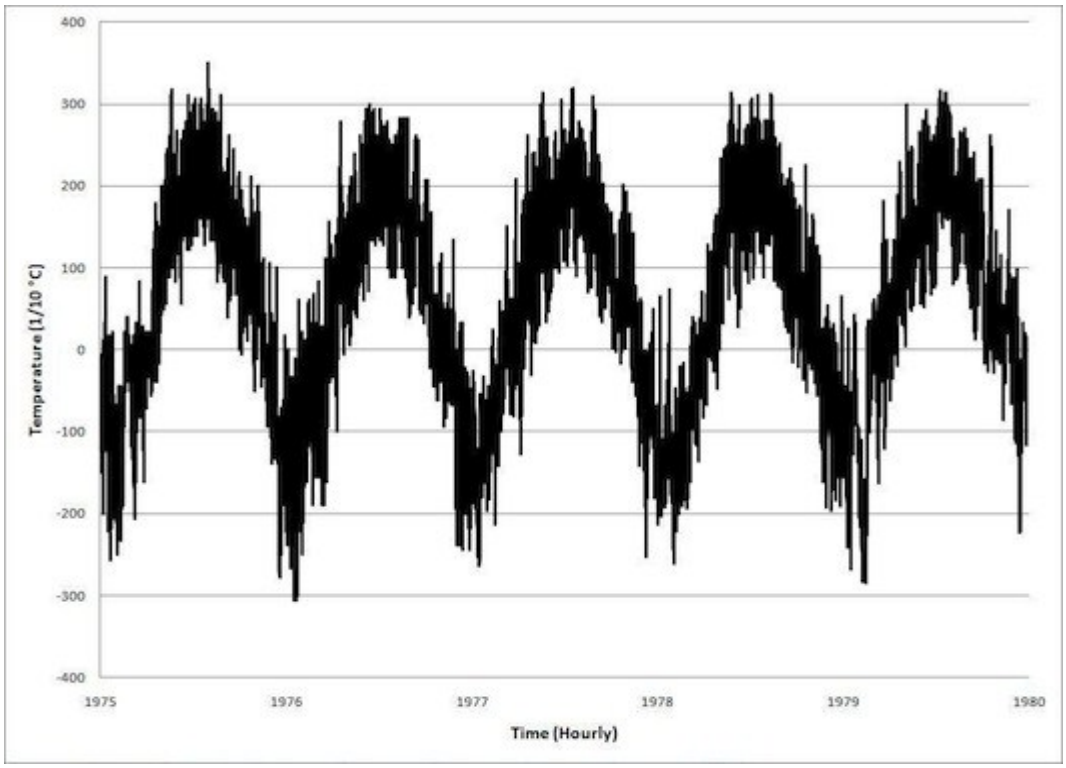

Figure 5.5: Temperature Vs. Time (1975-1980)

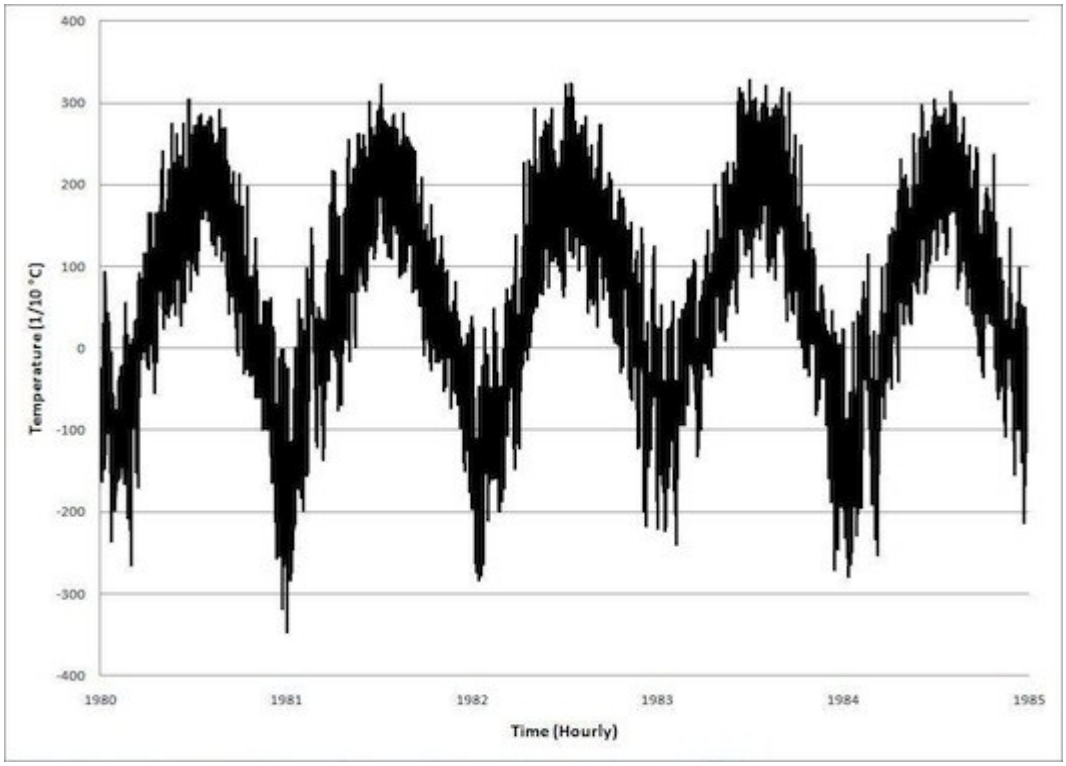

Figure 5.6: Temperature Vs. Time (1980-1985)

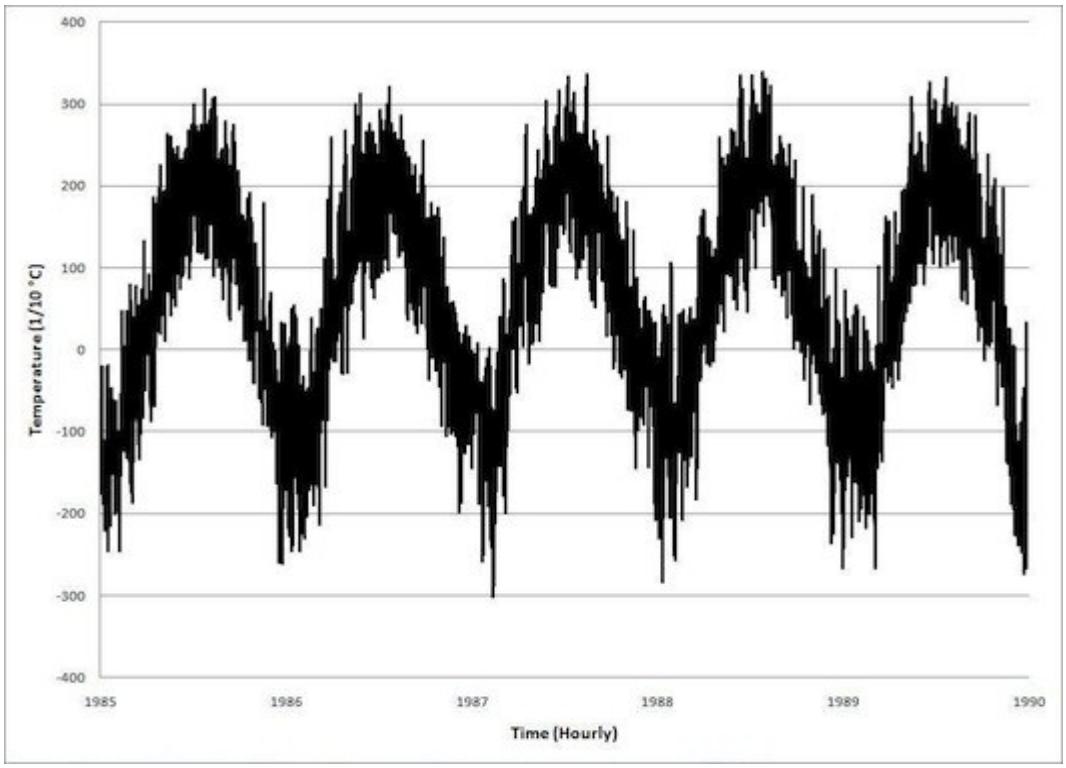

Figure 5.7: Temperature Vs. Time (1985-1990)

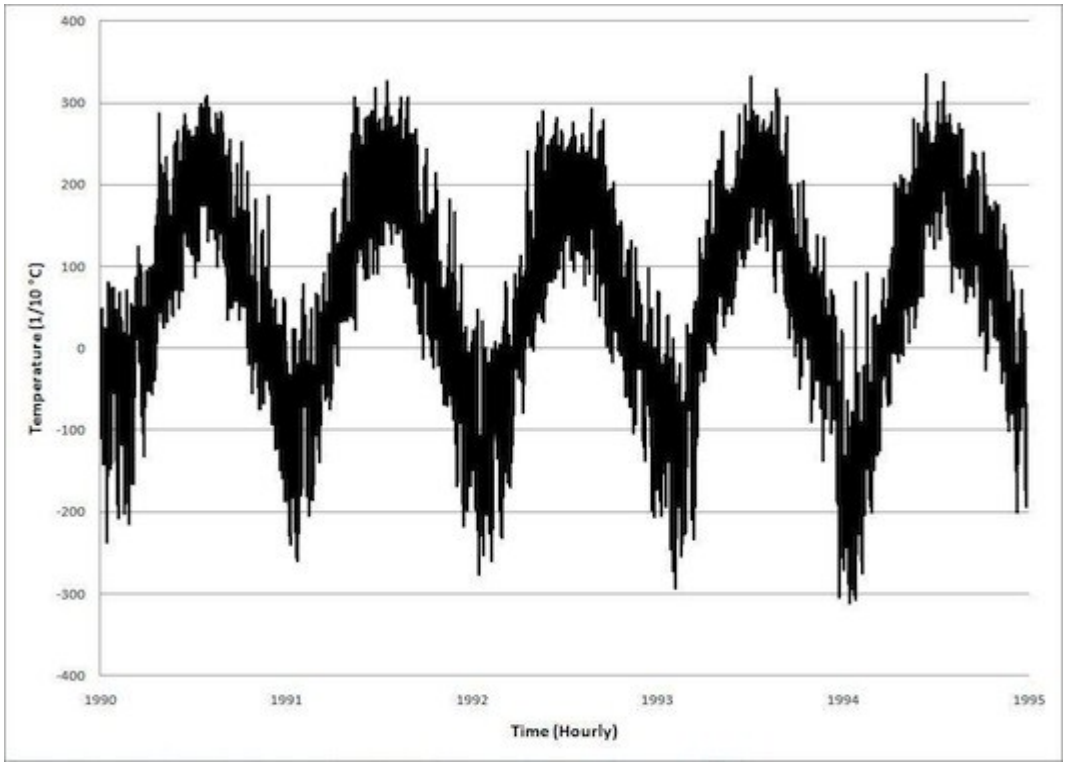

Figure 5.8: Temperature Vs. Time (1990-1995)

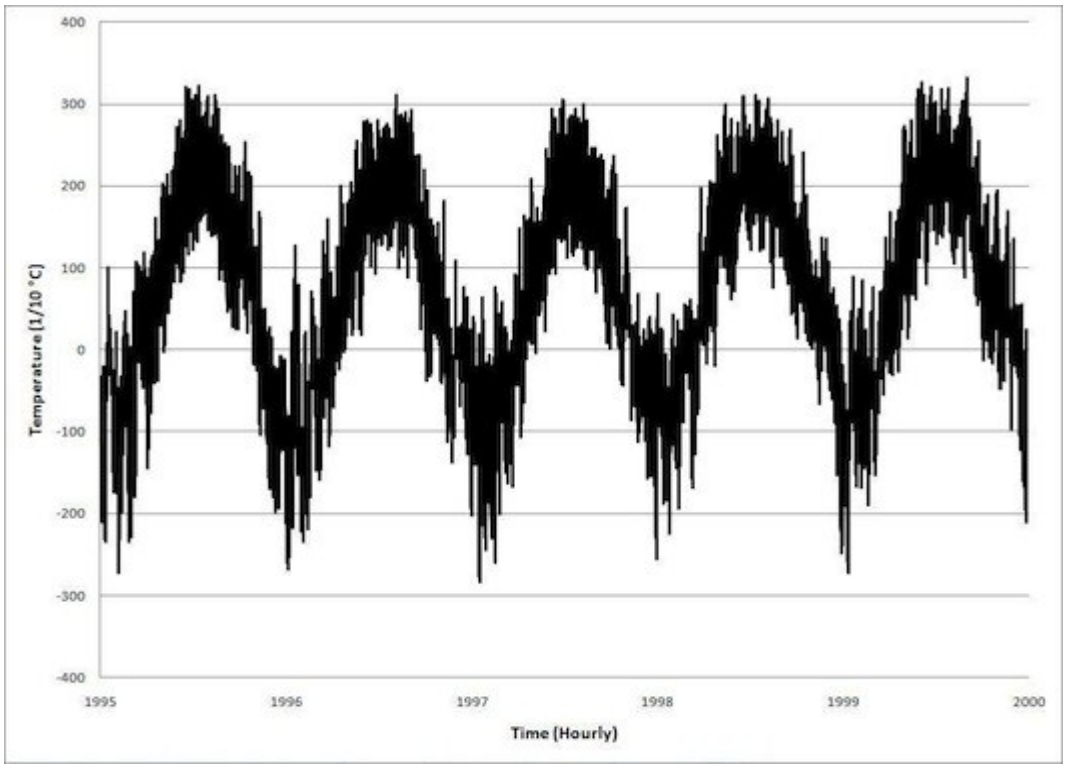

Figure 5.9: Temperature Vs. Time (1995-2000)

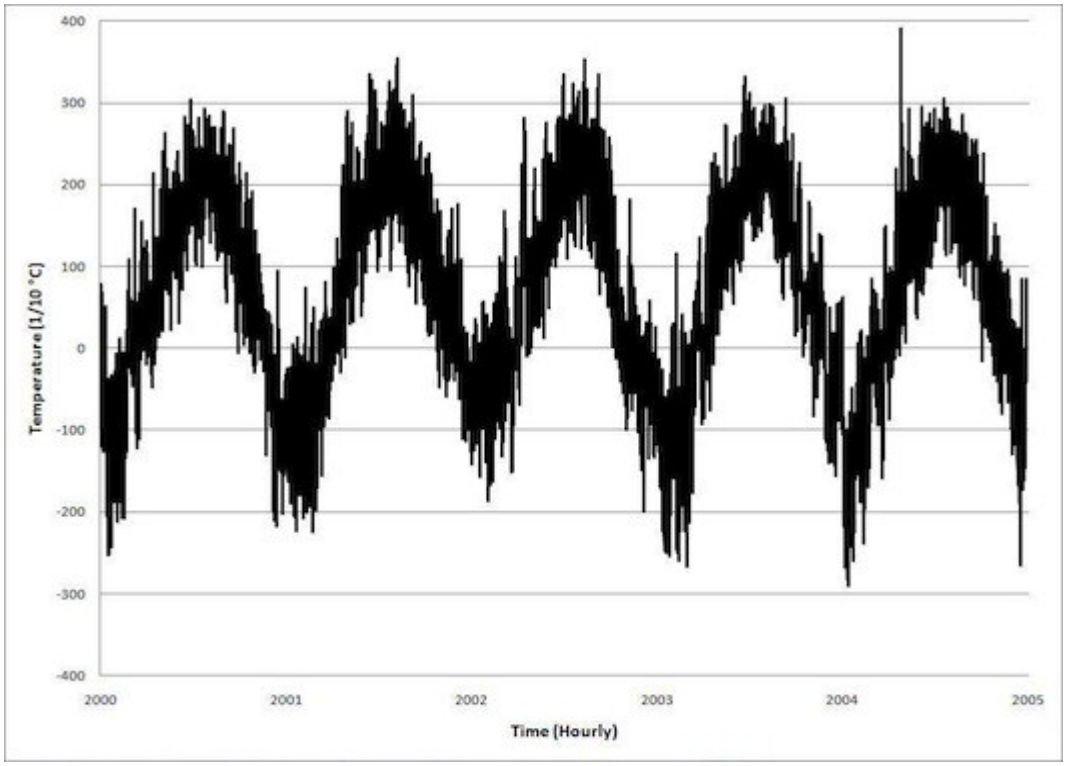

Figure 5.10: Temperature Vs. Time (2000-2005)

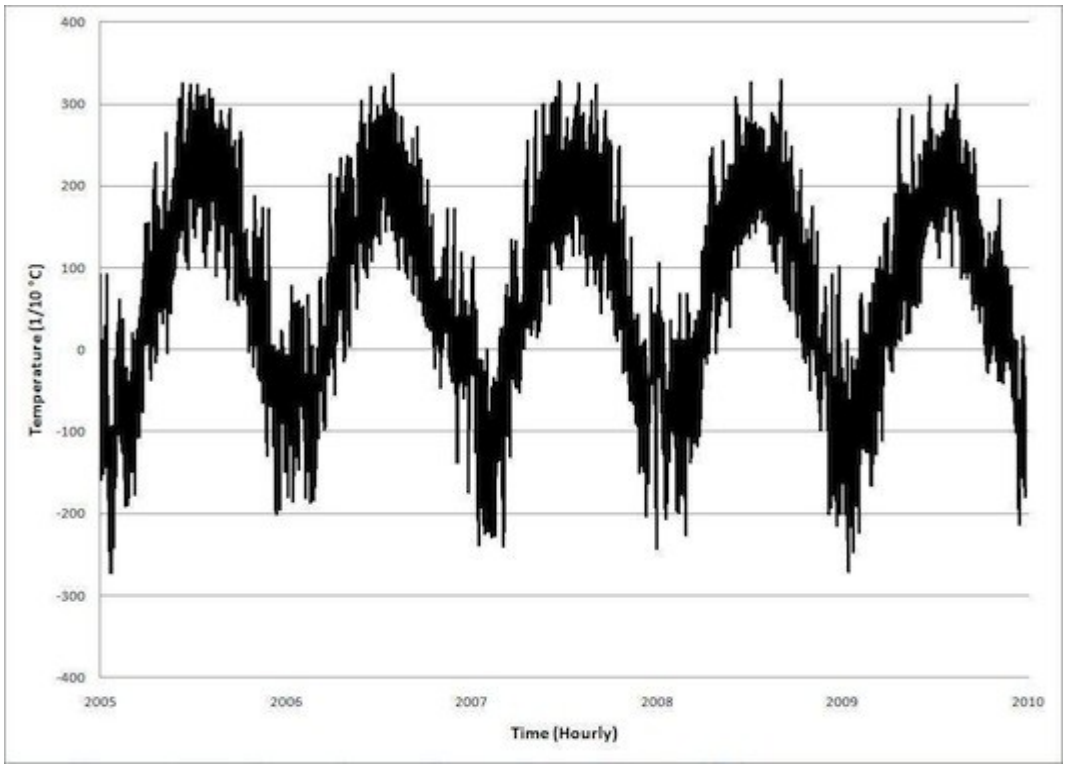

Figure 5.11: Temperature Vs. Time (2005-2010)

5.3.2 Relative Humidity Data

In this section, the hourly data provided for the relative humidity can be seen in Figures 5.12 through 5.20. The data provided from Environment Canada was in %. The TransChlor model needed the values to be in 1/10 %, which means that the data was not as precise as needed. However, the difference in performance was found to be insignificant.

Analyzing the Figures, it can be seen that the general trend is not as easily distinguishable, assuming one does exist. The range of humidity varies greatly from hour to hour and day to day and does not show any noticeable yearly pattern. The width of the band is also very large signifying great variation in hourly data. The only attribute that stands out is that there is a low relative humidity somewhere in the month of February each year.

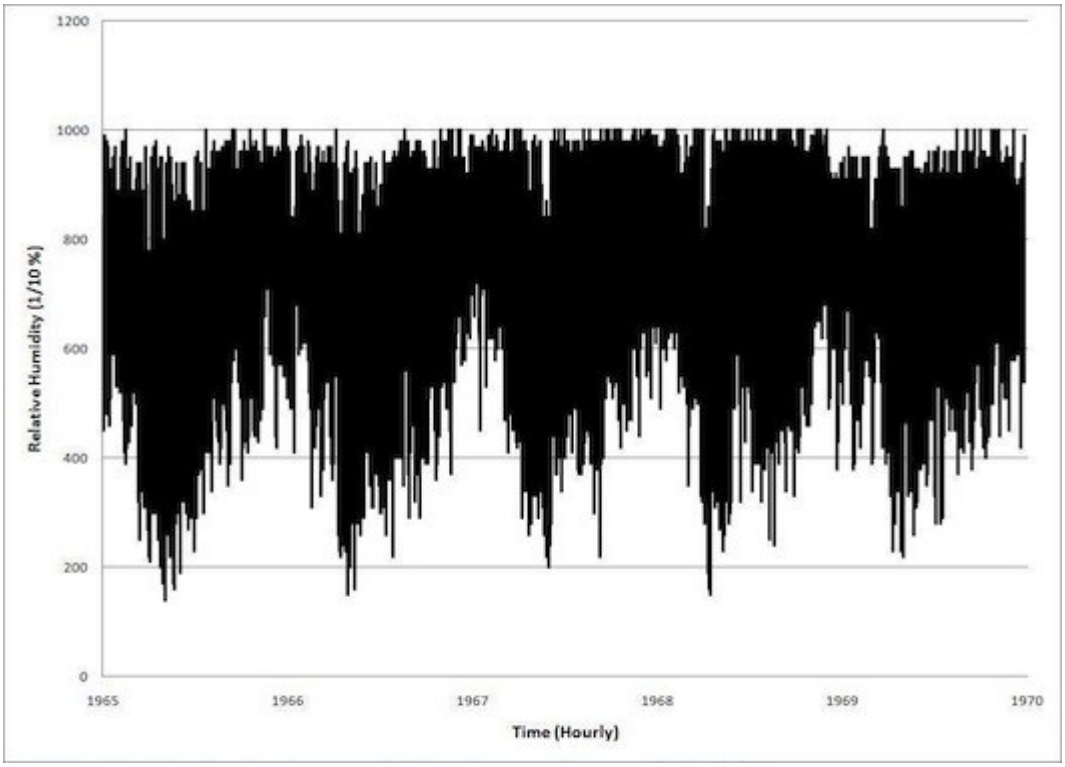

Figure 5.12: Relative Humidity Vs. Time (1965-1970)

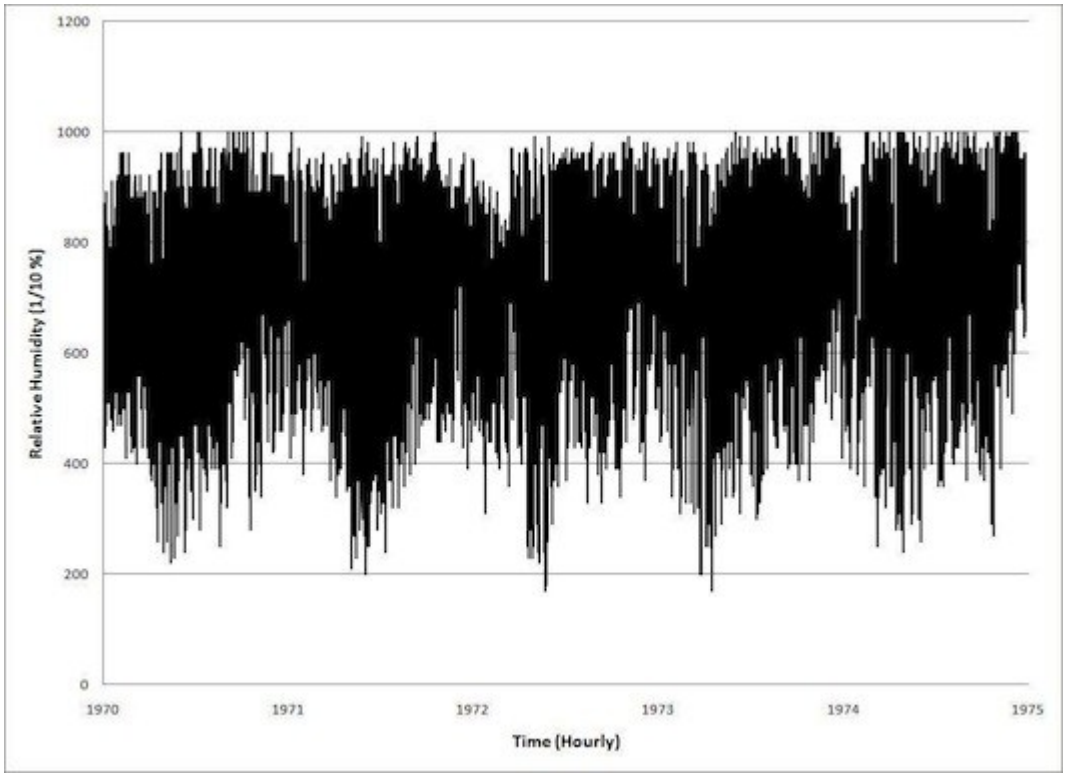

Figure 5.13: Relative Humidity Vs. Time (1970-1975)

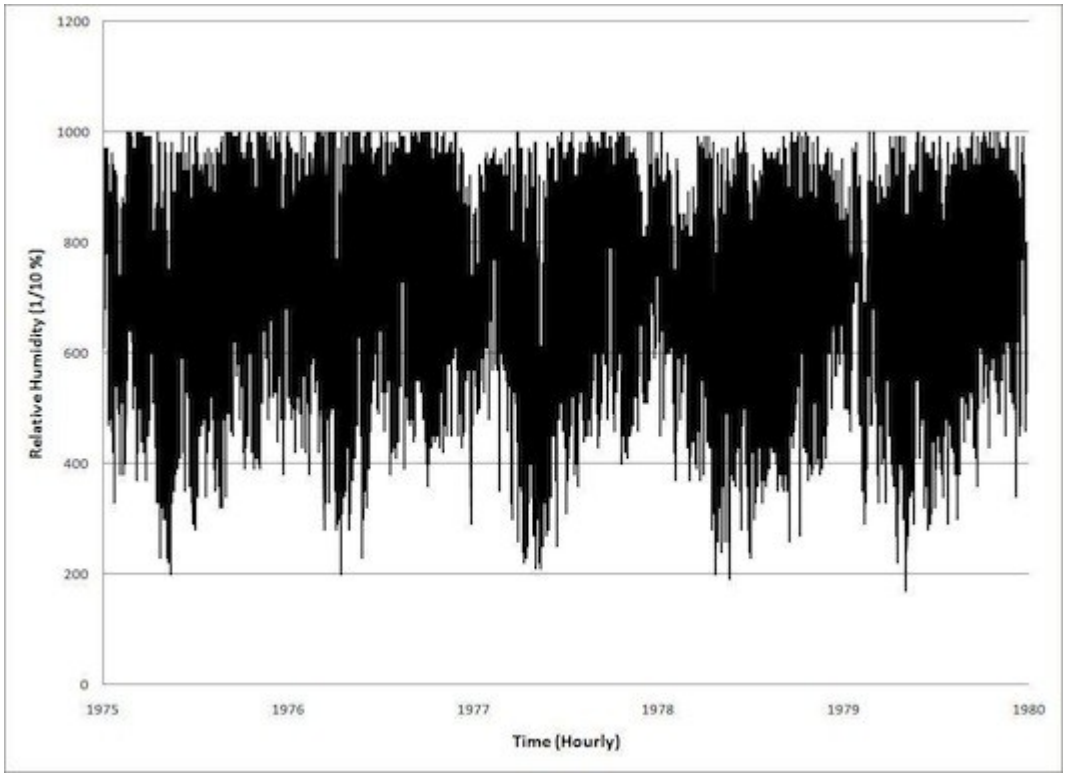

Figure 5.14: Relative Humidity Vs. Time (1975-1980)

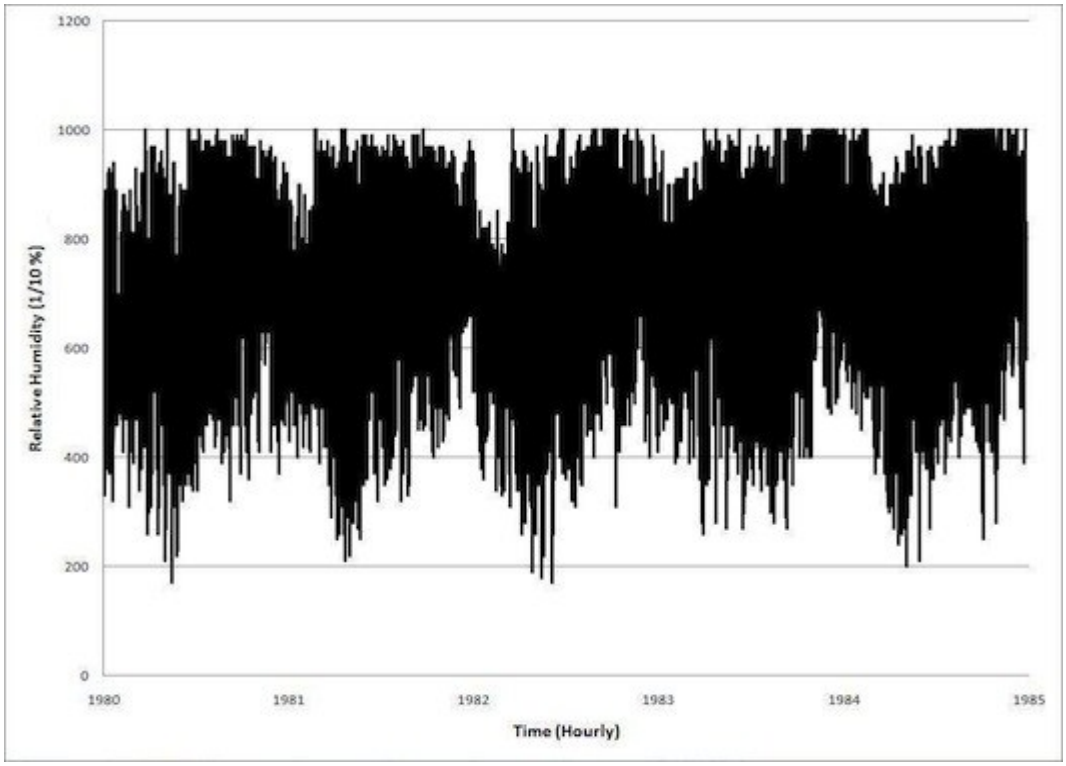

Figure 5.15: Relative Humidity Vs. Time (1980-1985)

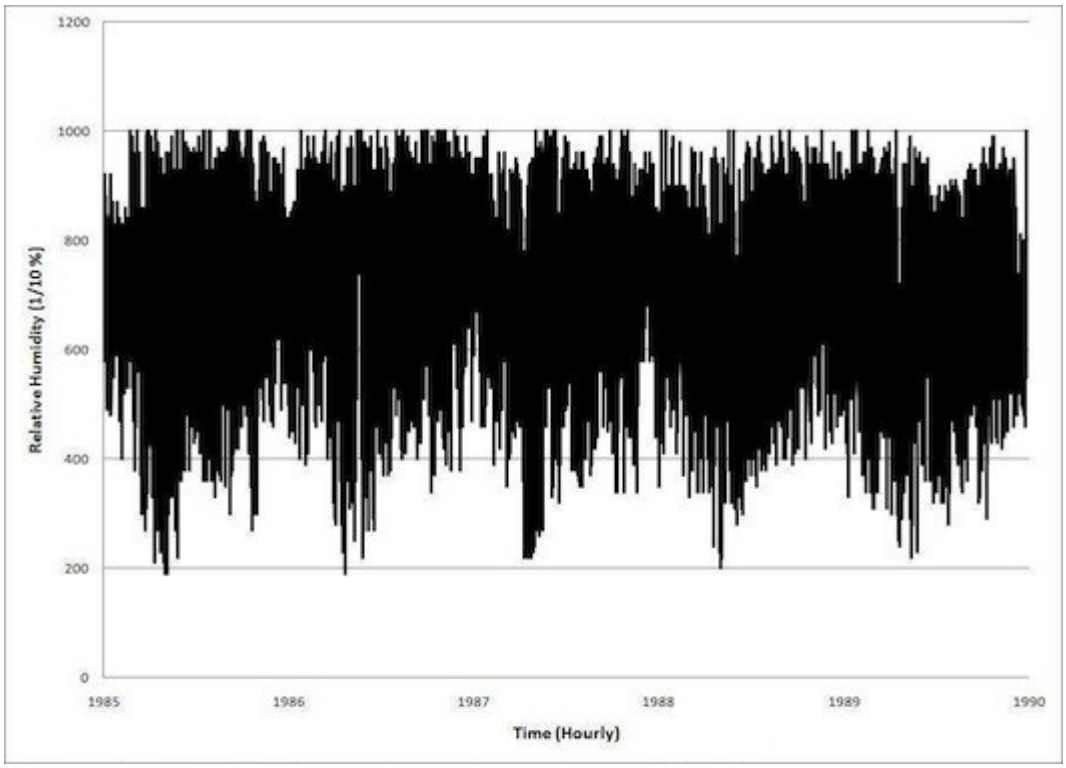

Figure 5.16: Relative Humidity Vs. Time (1985-1990)

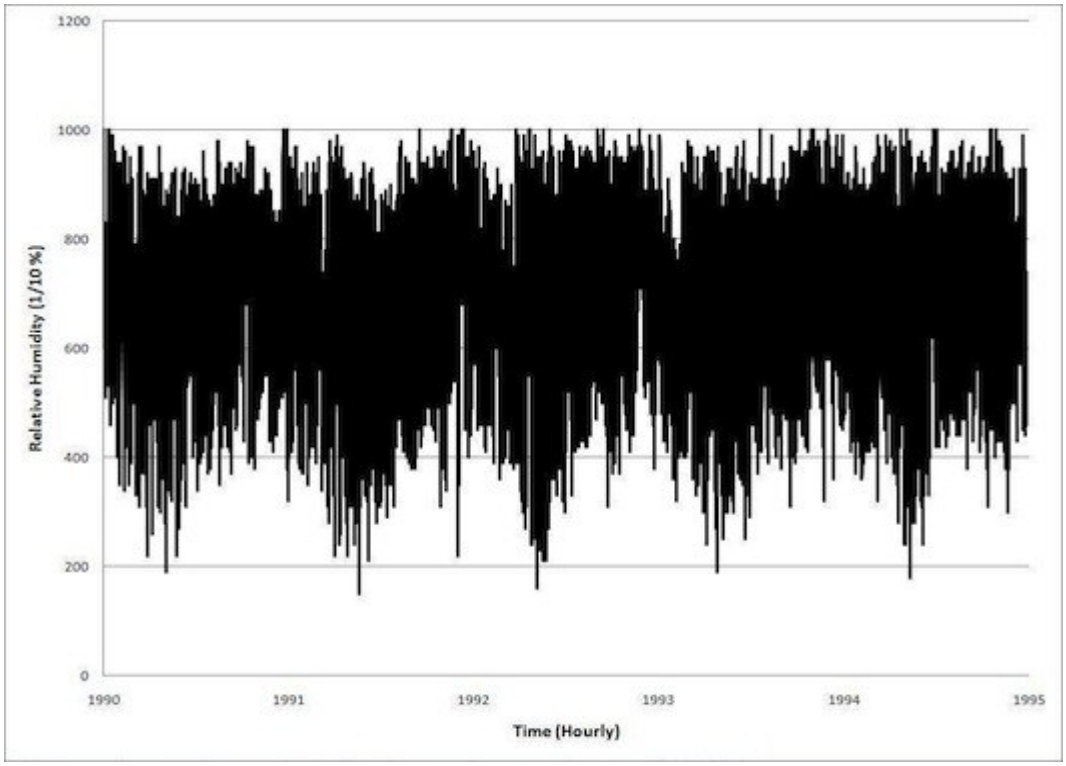

Figure 5.17: Relative Humidity Vs. Time (1990-1995)

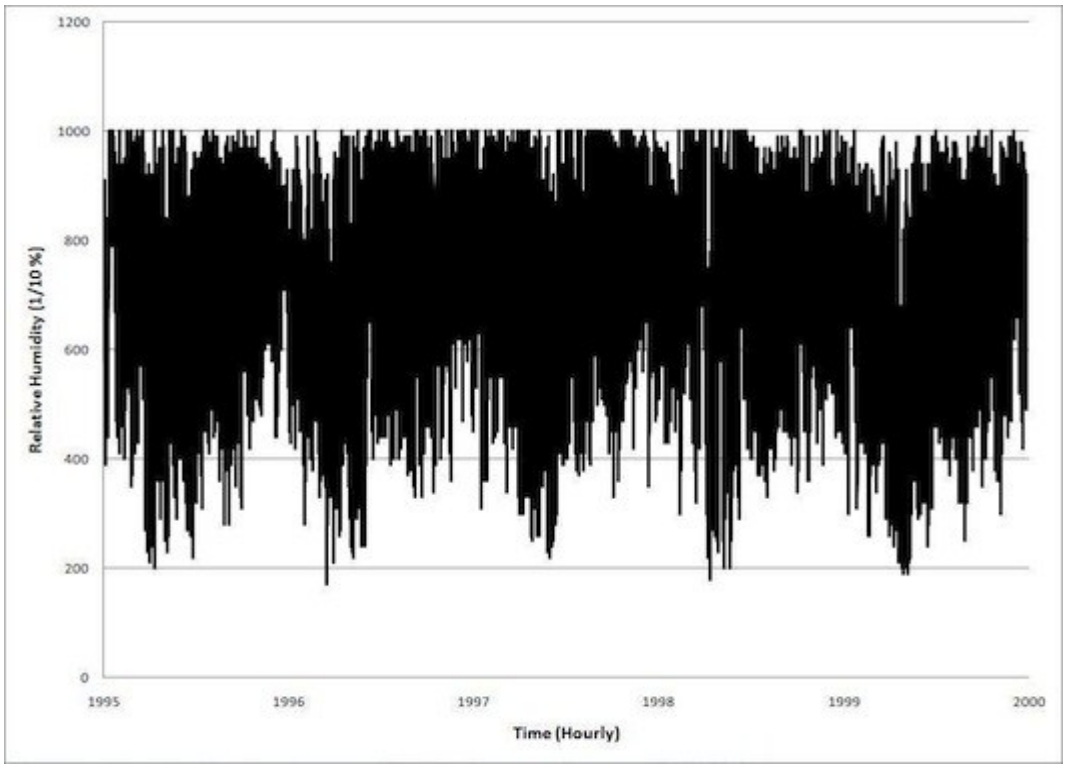

Figure 5.18: Relative Humidity Vs. Time (1995-2000)

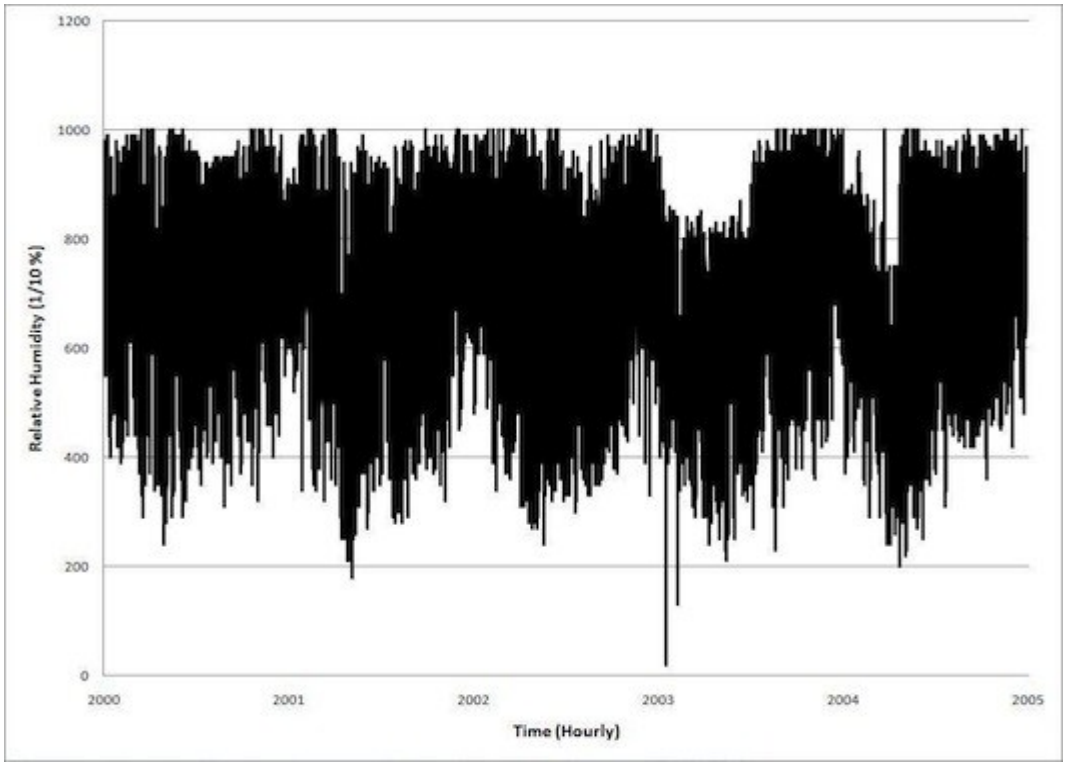

Figure 5.19: Relative Humidity Vs. Time (2000-2005)

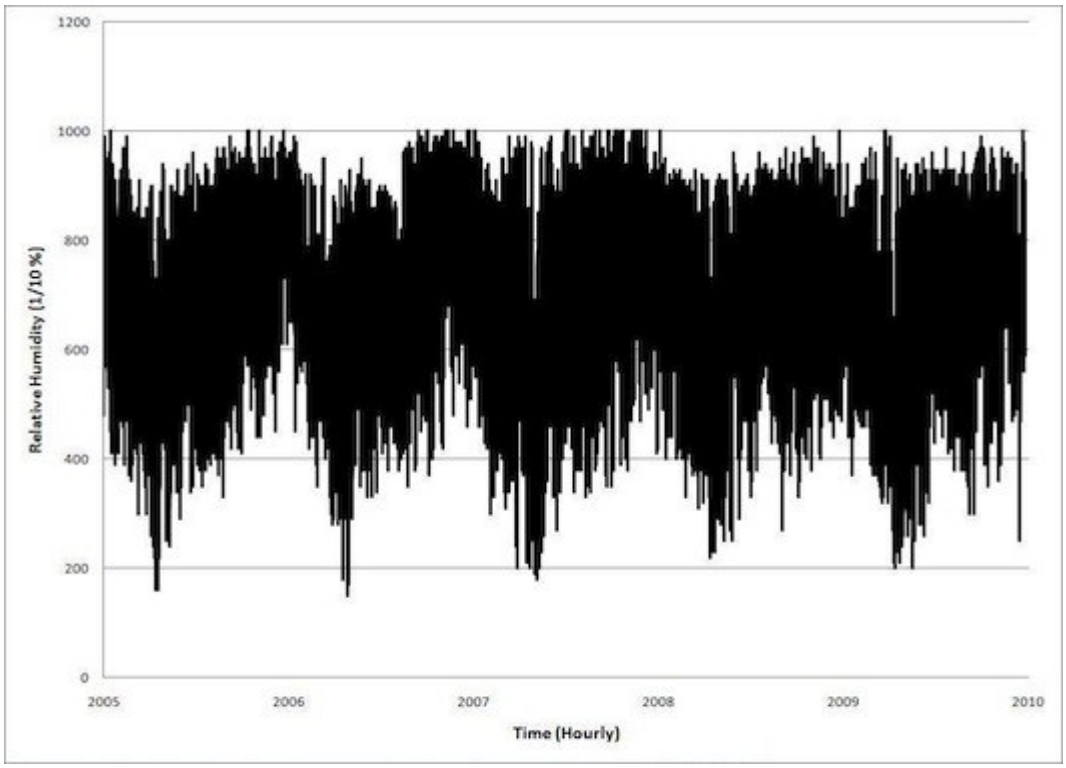

Figure 5.20: Relative Humidity Vs. Time (2005-2010)

5.3.3 Precipitation Data

In this section, the hourly data provided for precipitation can be seen in Figures 5.21 through 5.29. The data provided from Environment Canada was in 1/10mm, which is the exact format that is needed for the TransChlor model.

Precipitation is inherently variable in nature. It is difficult to predict when it will take place and how much precipitation will occur. For that reason, it can be seen that there is no general trend in the data. As a result, it is very challenging to make a precipitation data set that could be used for a future bridge project.

Shown below is the hourly precipitation provided from Environment Canada, which is shown in black, and the estimated hourly precipitation from the daily precipitation values found on the Environment Canada website, shown in red.

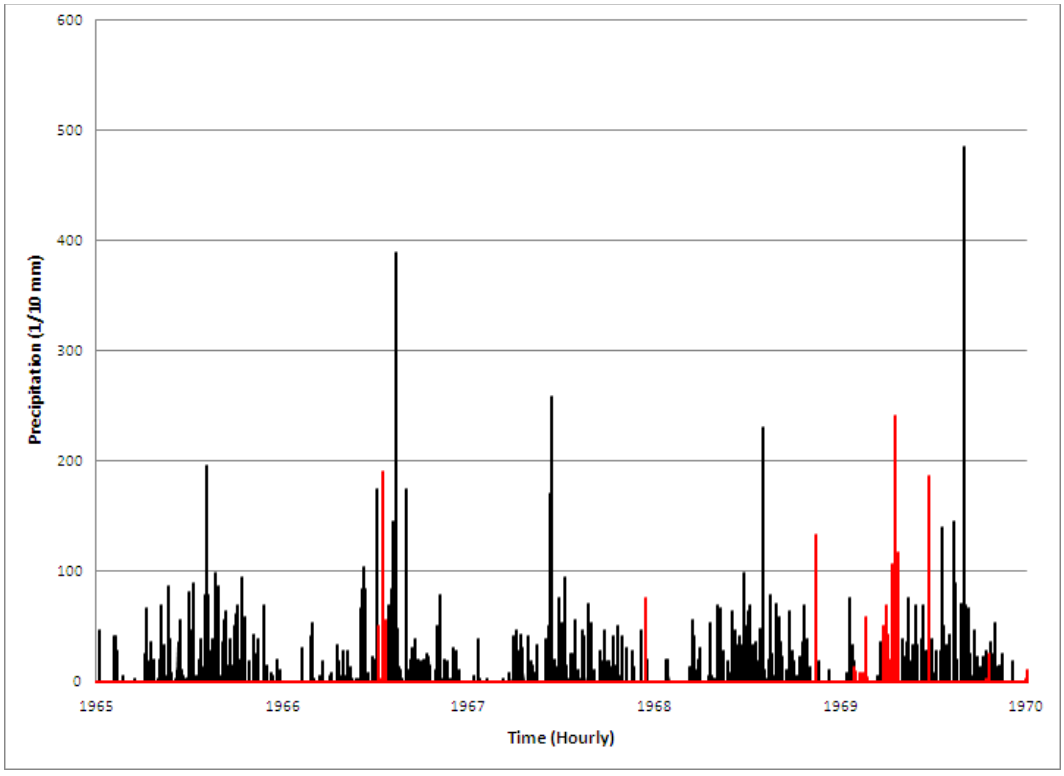

Figure 5.21: Precipitation Vs. Time (1965-1970)

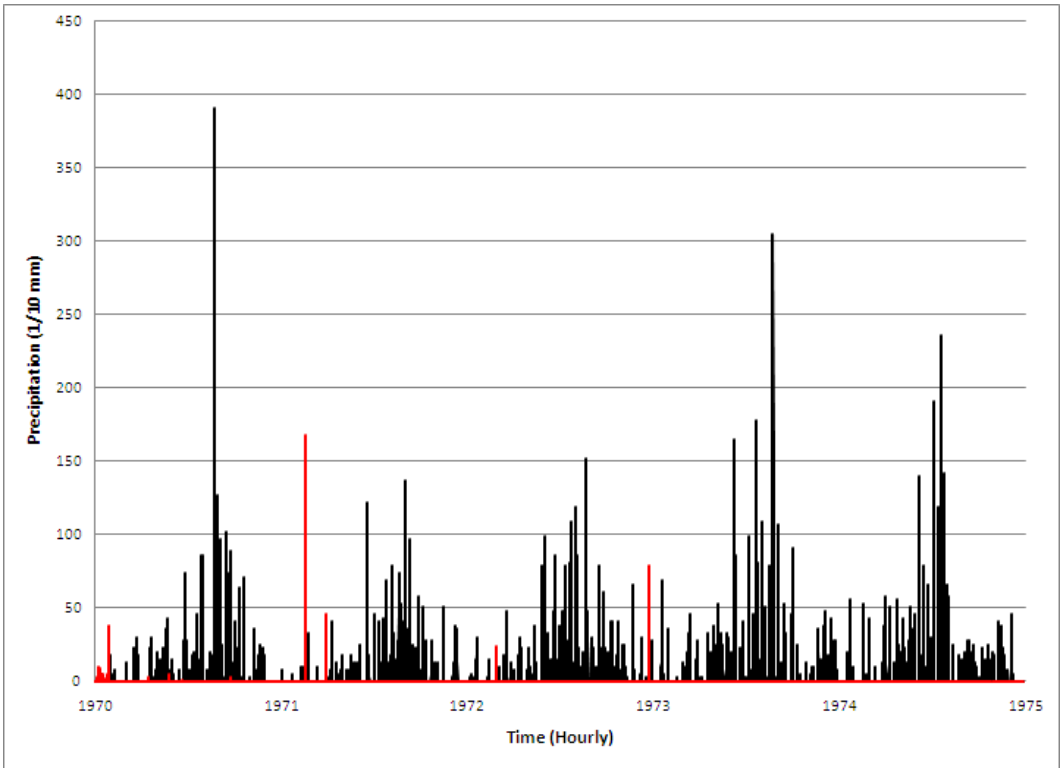

Figure 5.22: Precipitation Vs. Time (1970-1975)

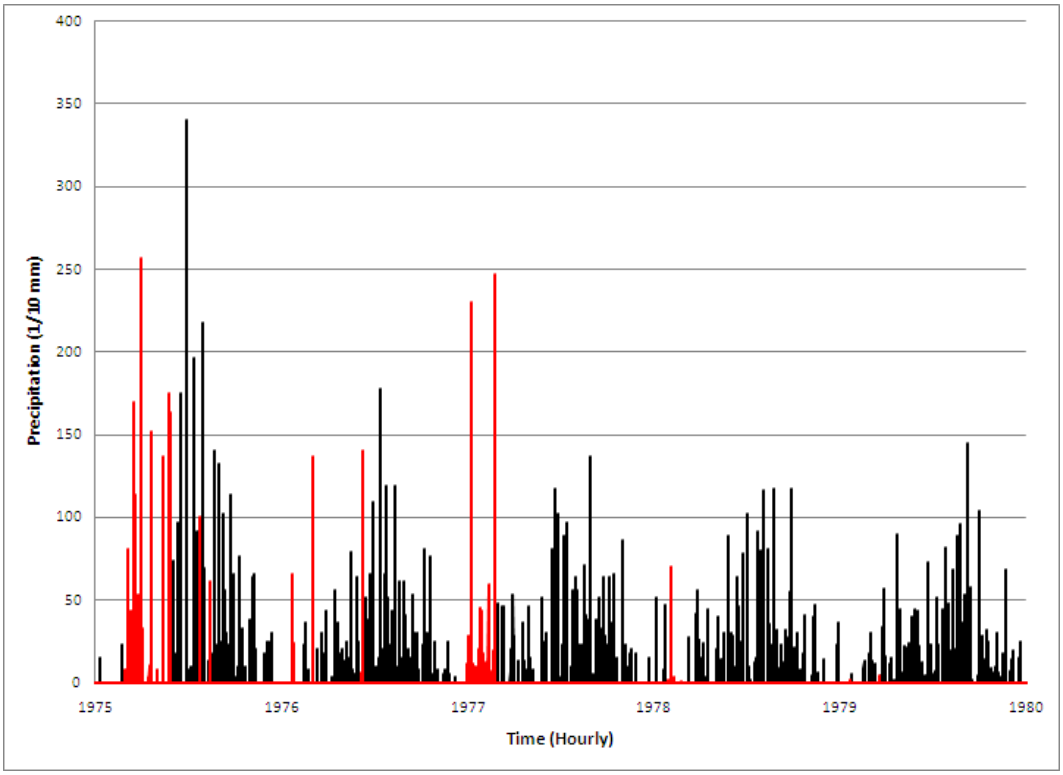

Figure 5.23: Precipitation Vs. Time (1975-1980)

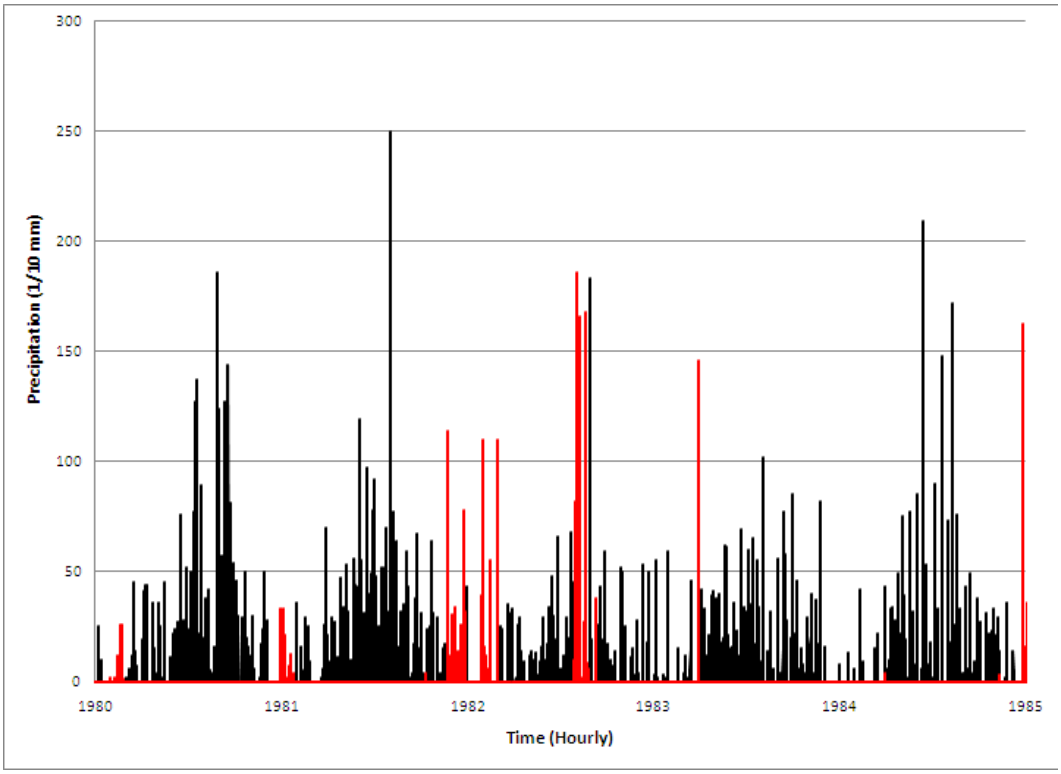

Figure 5.24:Precipitation Vs. Time (1980-1985)

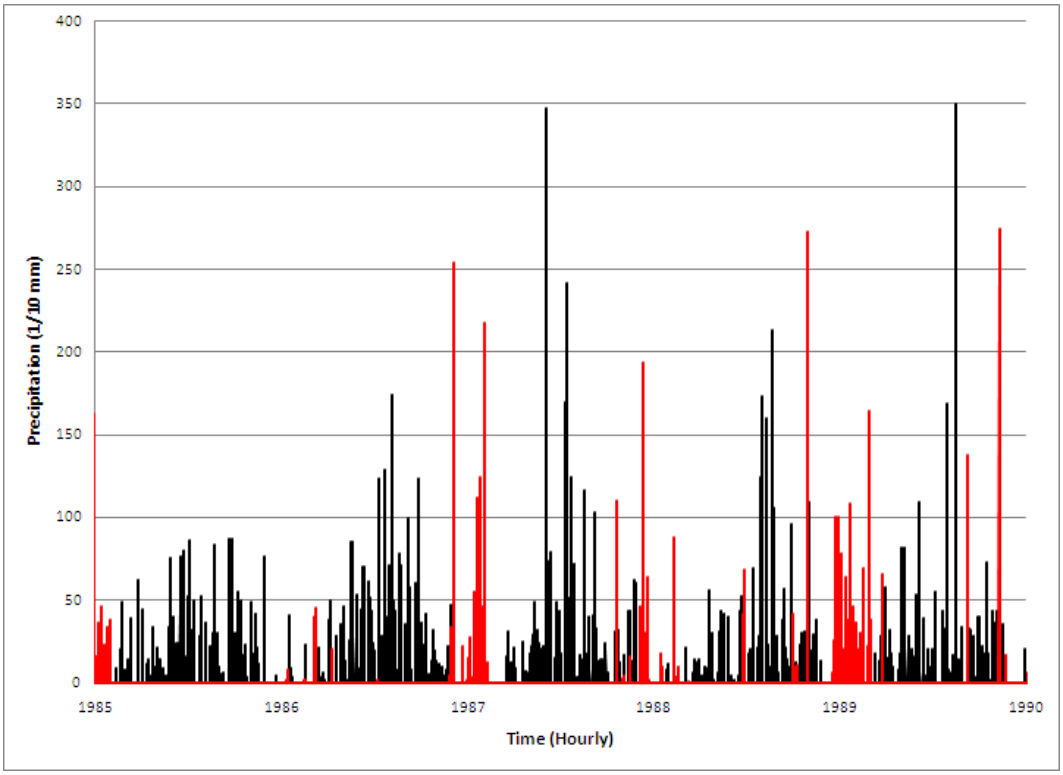

Figure 5.25: Precipitation Vs. Time (1985-1990)

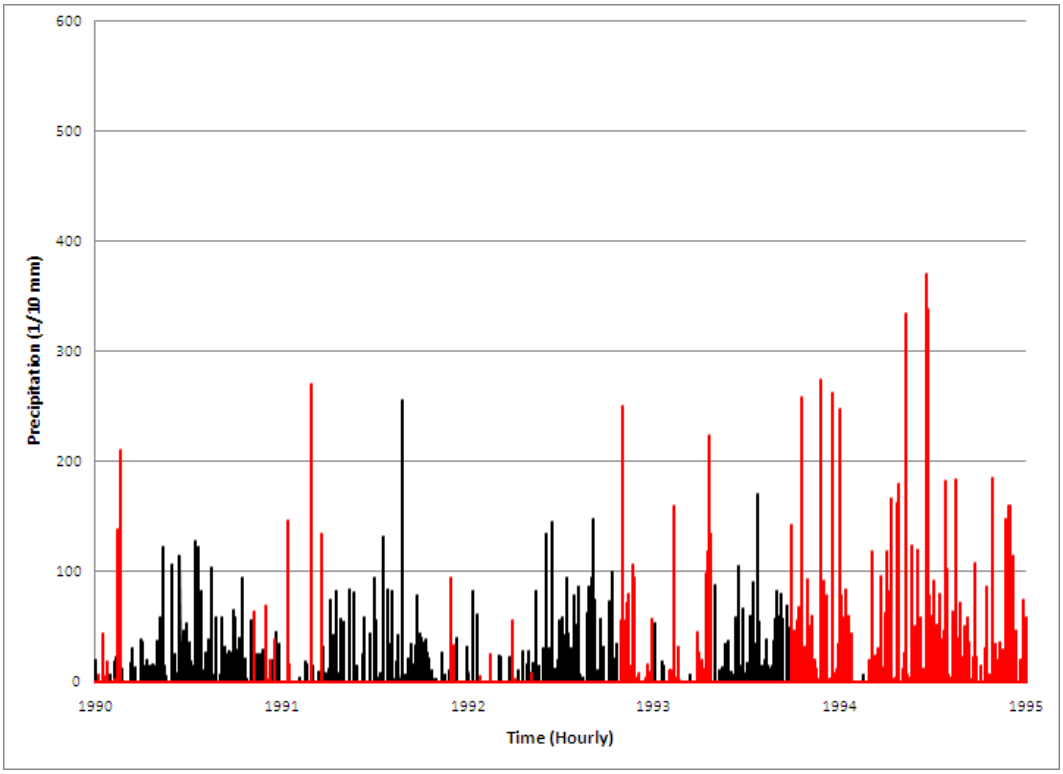

Figure 5.26: Precipitation Vs. Time (1990-1995)

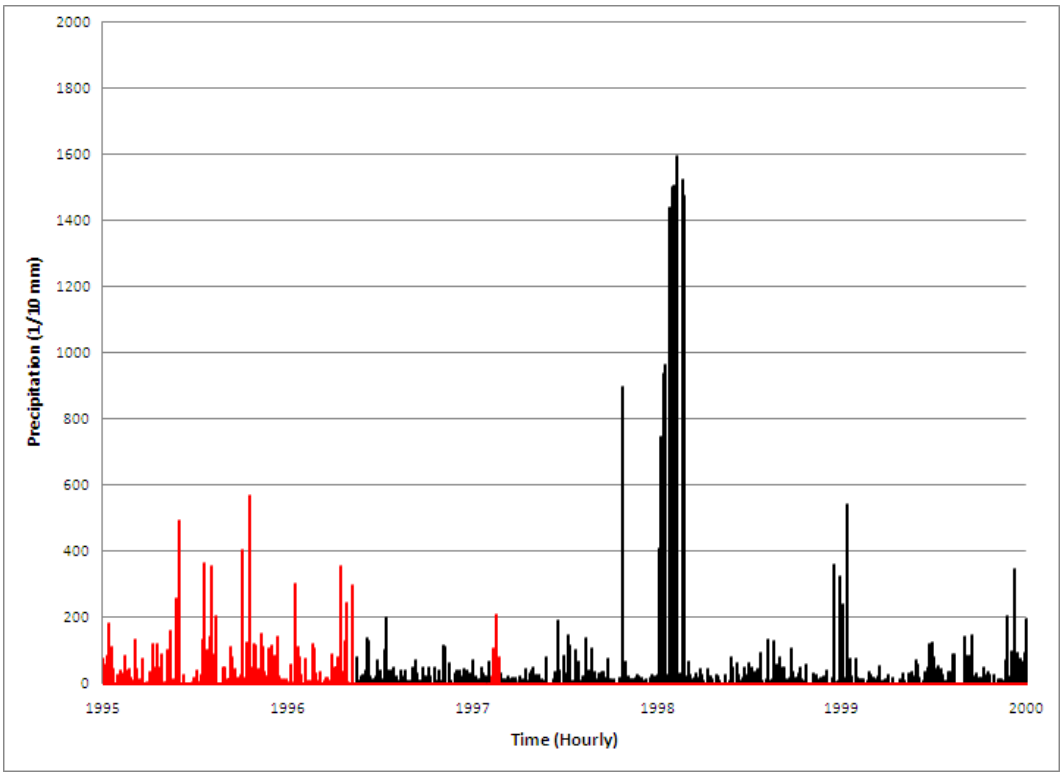

Figure 5.27: Precipitation Vs. Time (1995-2000)

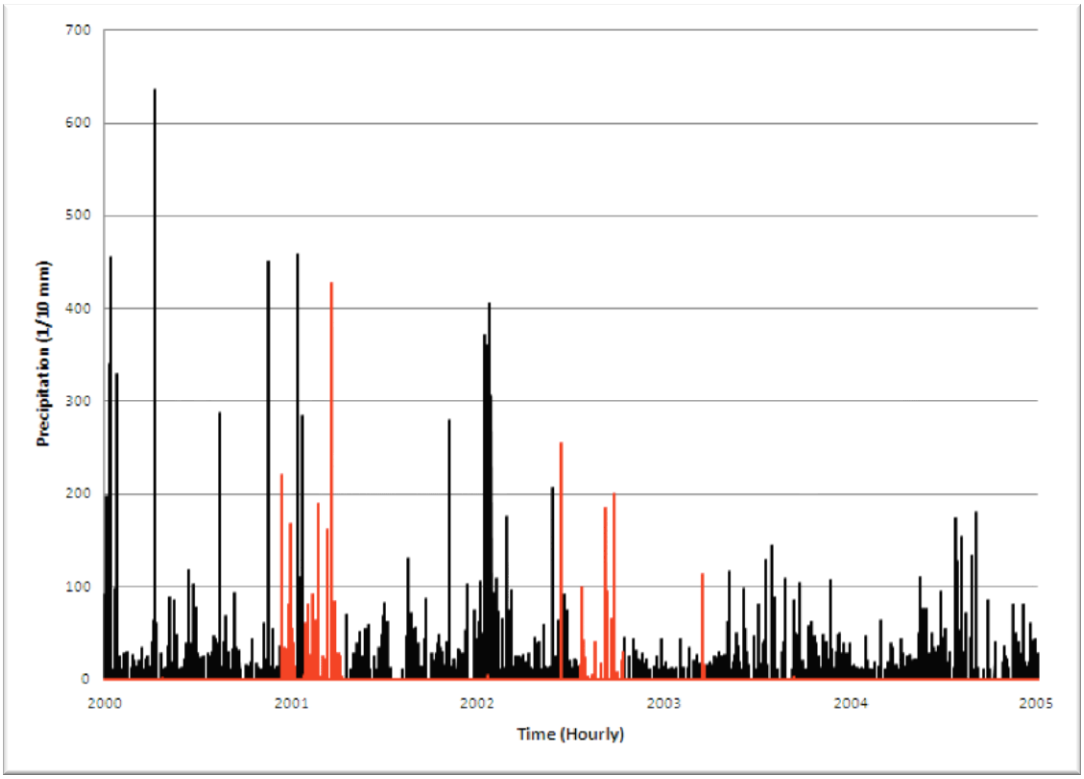

Figure 5.28: Precipitation Vs. Time (2000-2005)

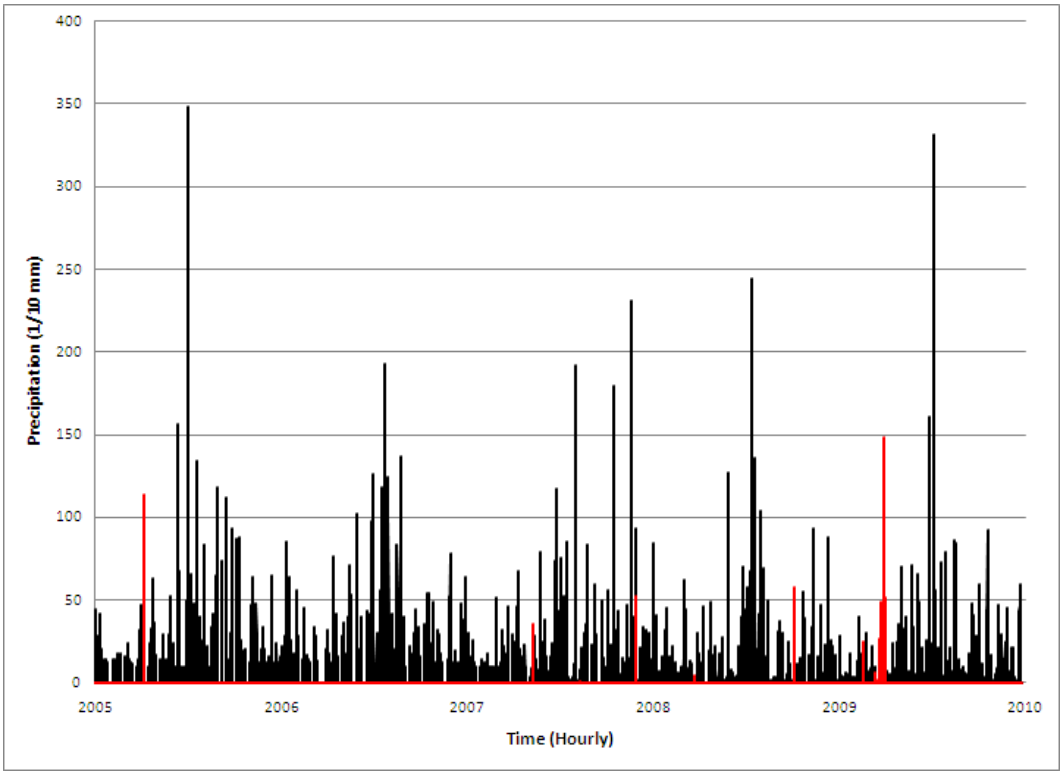

Figure 5.29: Precipitation Vs. Time (2005-2010)

5.3.4 Solar Radiation Data

In this section, the hourly data provided for the solar radiation can be seen in Figure 5.30 through 5.38. The data provided from Environment Canada was in MJ/m^2. The TransChlor model requires these values to be in Wh/m^2. A simple conversion of units was performed.

Examining the graphs, as expected there are general trends in the yearly solar radiation data. On a daily basis, the solar radiation peaks near noon and then drops to zero at night. On a seasonal basis, the length of time where solar radiation occurs during the summer is longer than during the winter. Furthermore, the peak solar radiation value is a maximum during the summer and a minimum during the winter. Therefore, using this information with past data, it is possible to create a solar radiation data set that can be used with the TransChlor model.

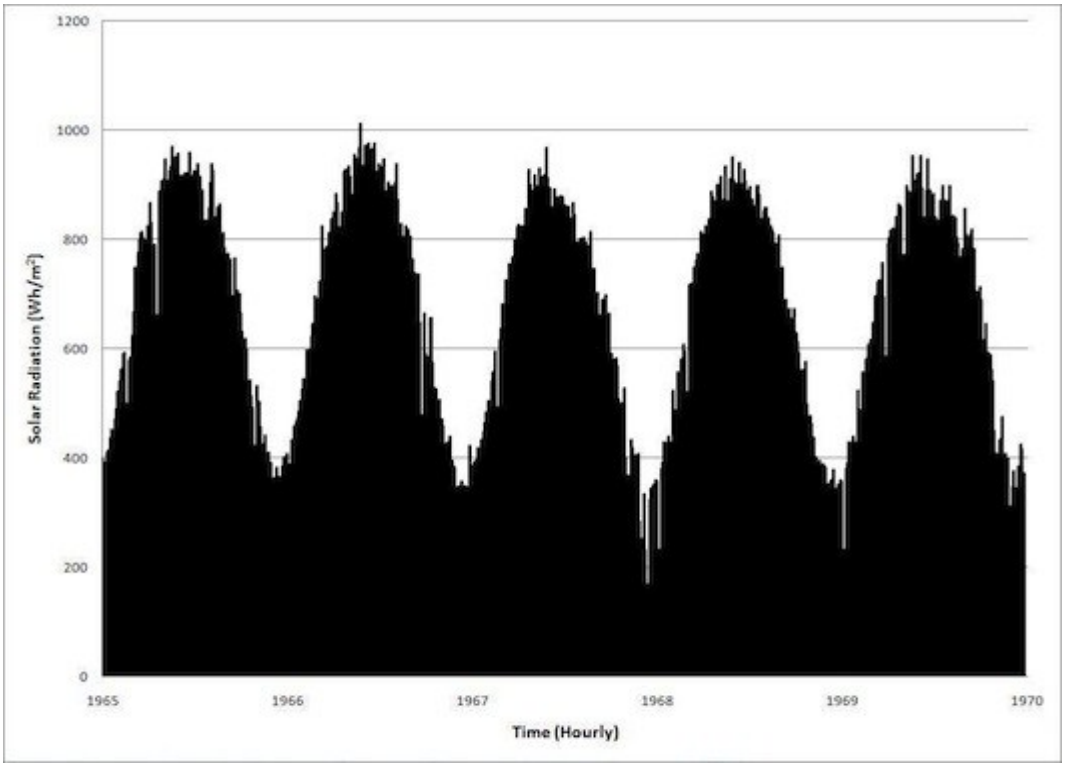

Figure 5.30: Solar Radiation Vs. Time (1965-1970)

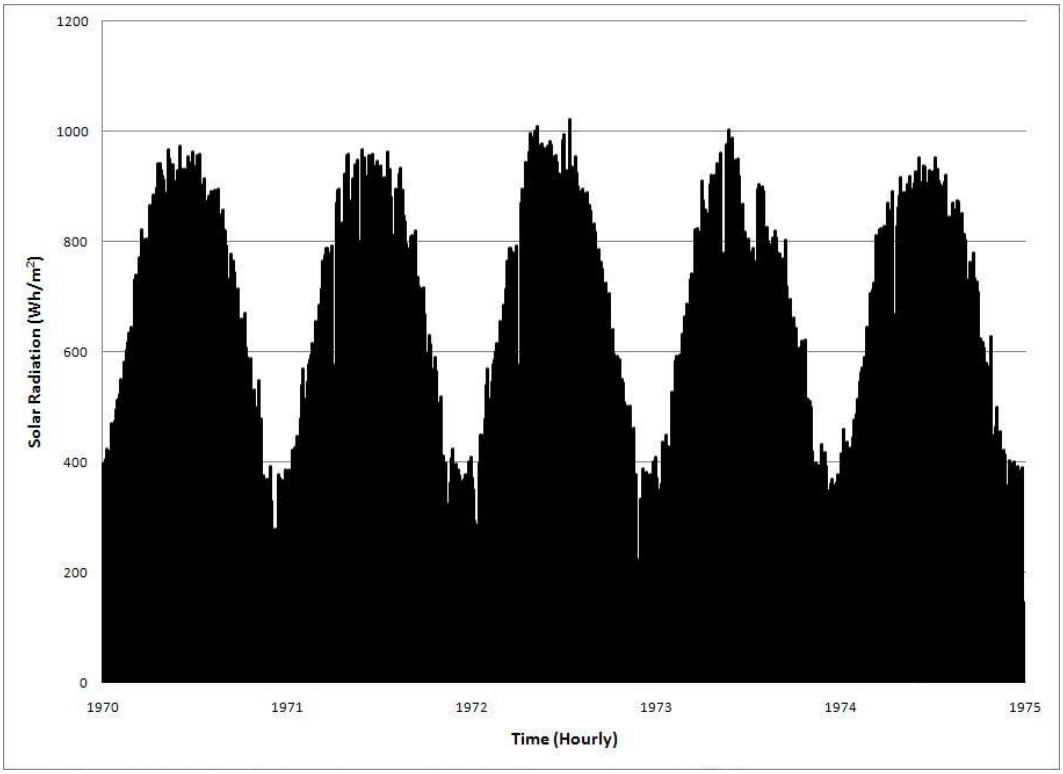

Figure 5.31: Solar Radiation Vs. Time (1970-1975)

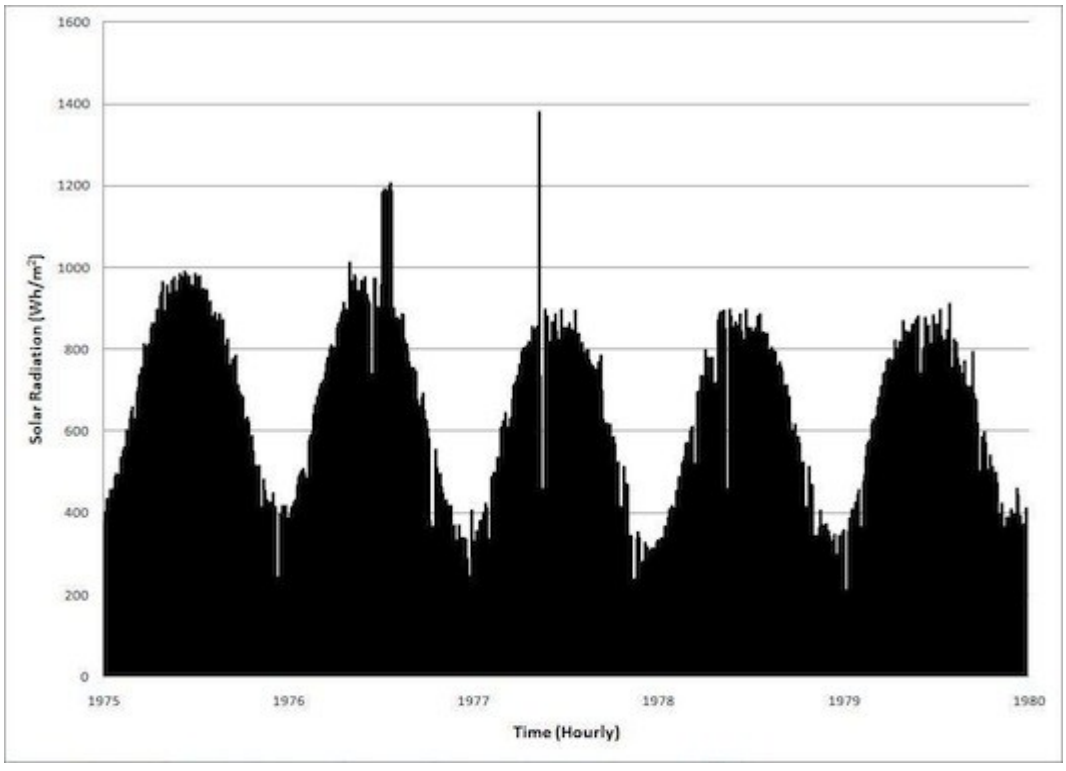

Figure 5.32: Solar Radiation Vs. Time (1975-1980)

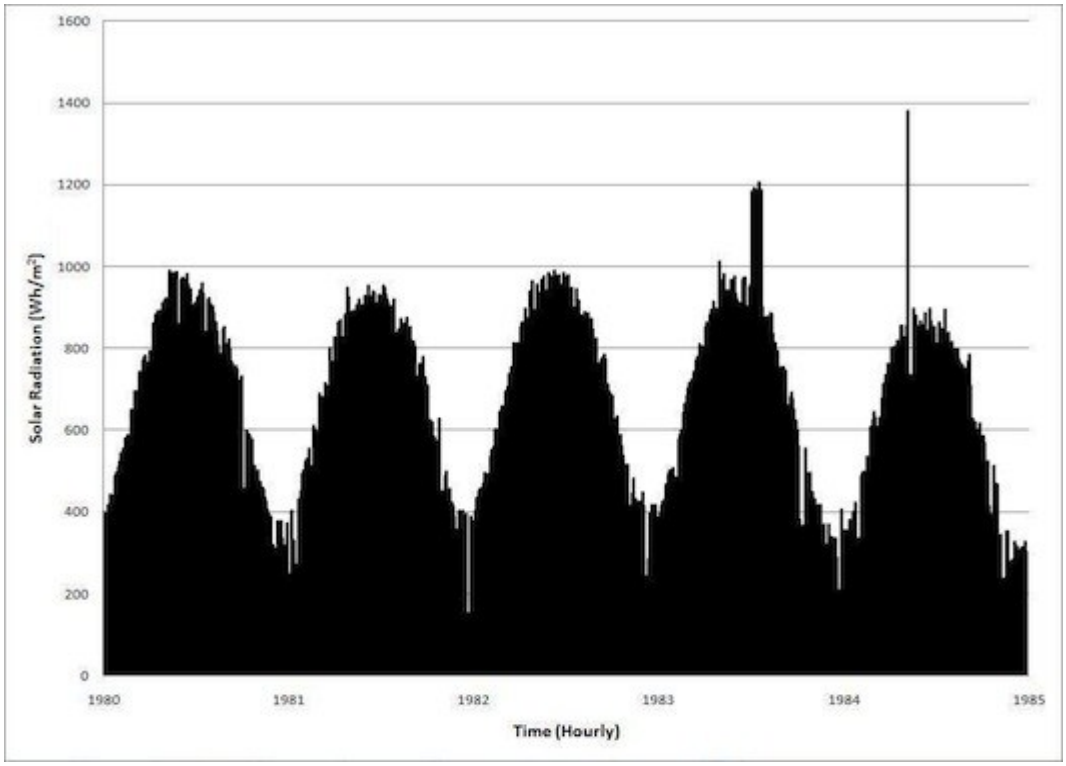

Figure 5.33: Solar Radiation Vs. Time (1980-1985)

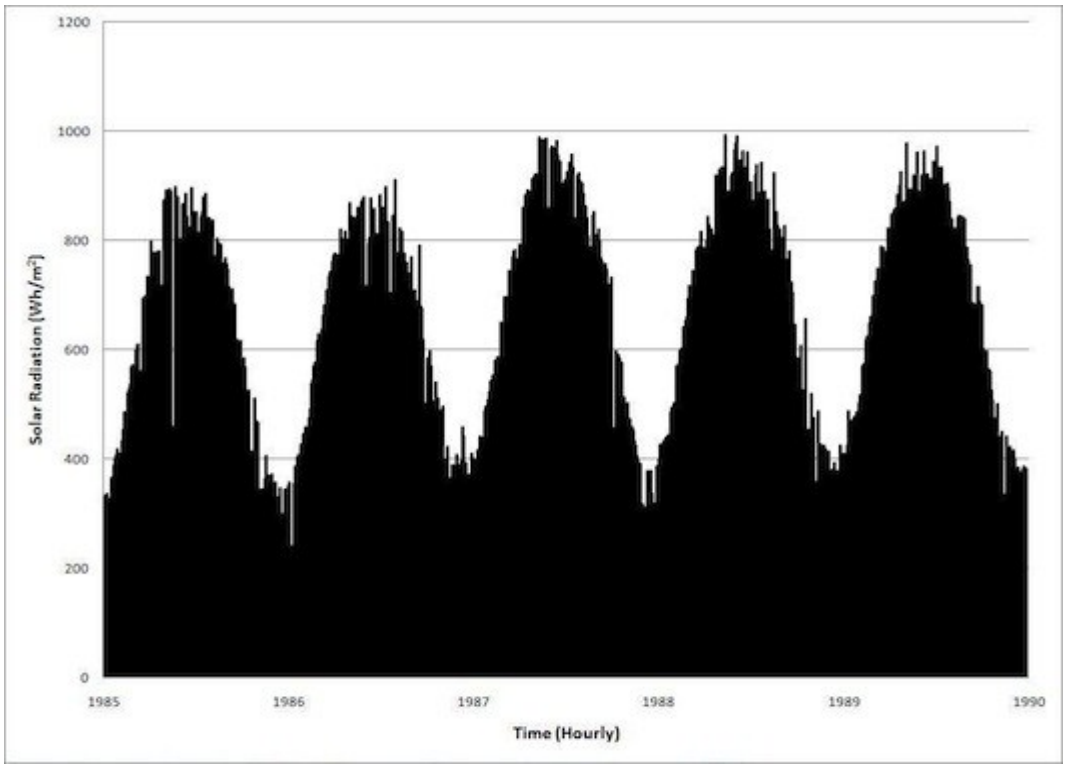

Figure 5.34: Solar Radiation Vs. Time (1985-1990)

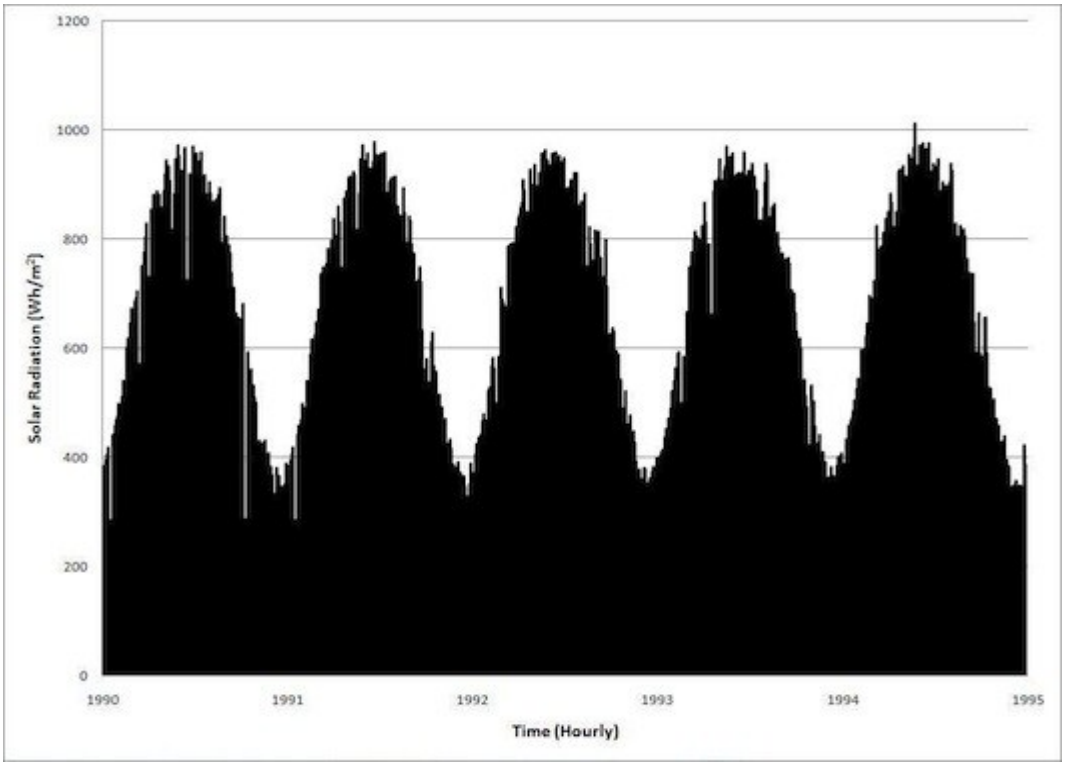

Figure 5.35: Solar Radiation Vs. Time (1990-1995)

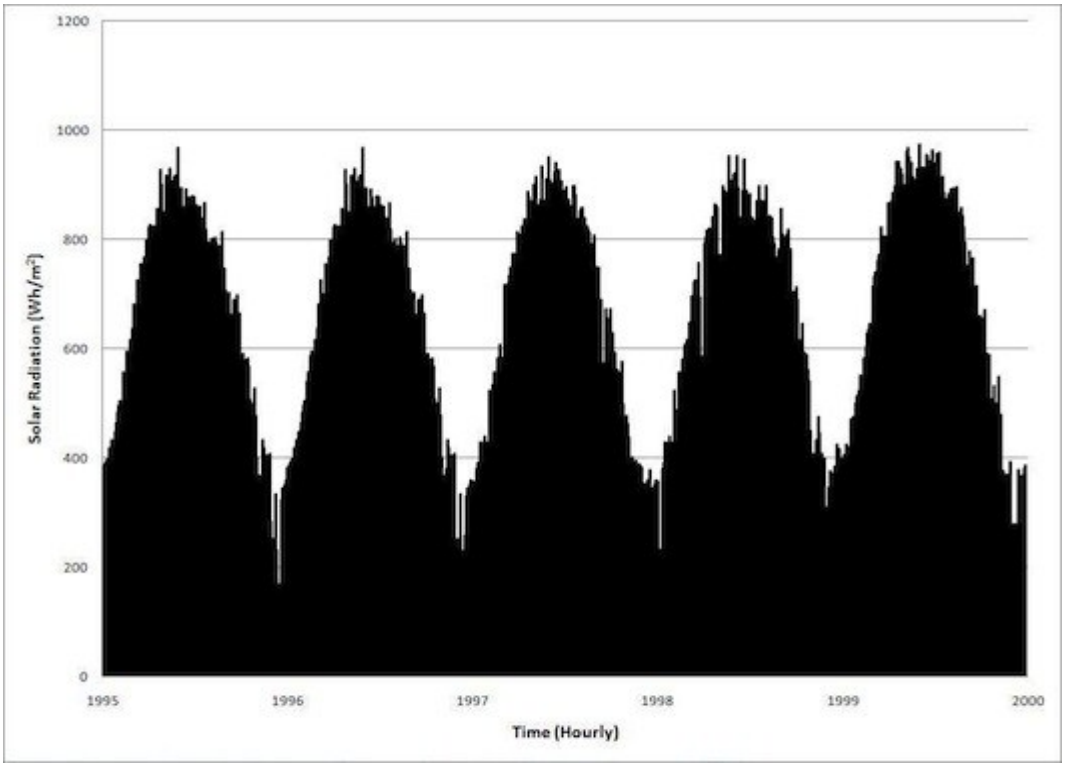

Figure 5.36: Solar Radiation Vs. Time (1995-2000)

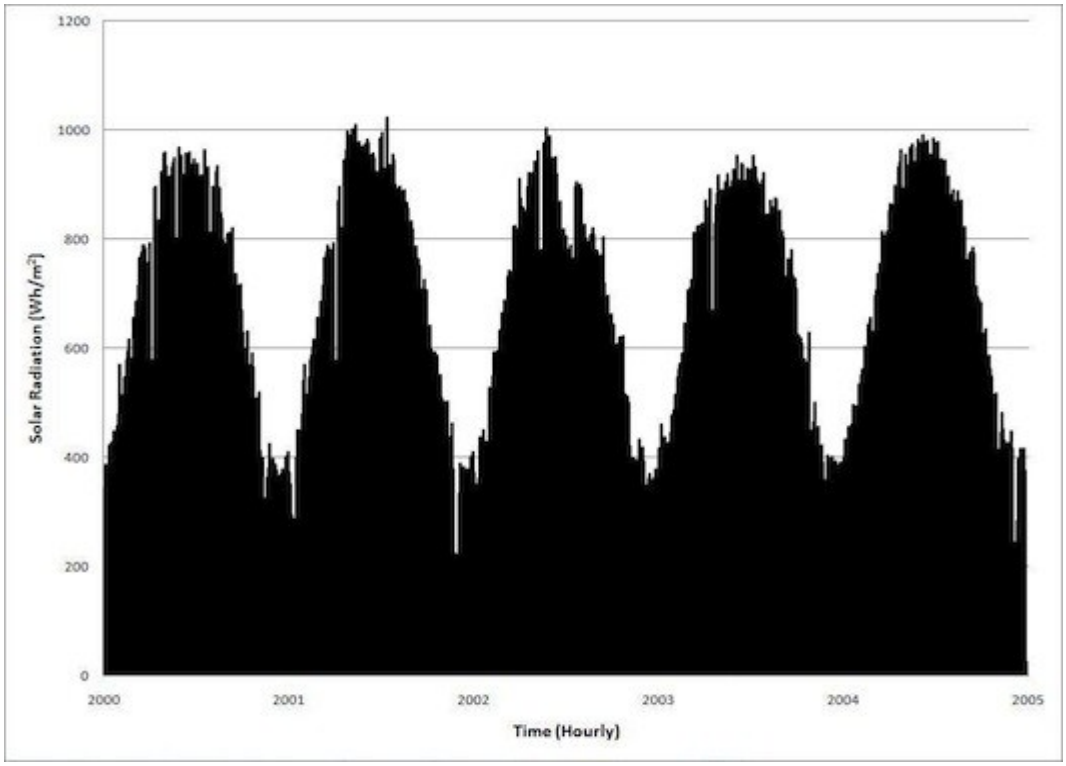

Figure 5.37: Solar Radiation Vs. Time (2000-2005)

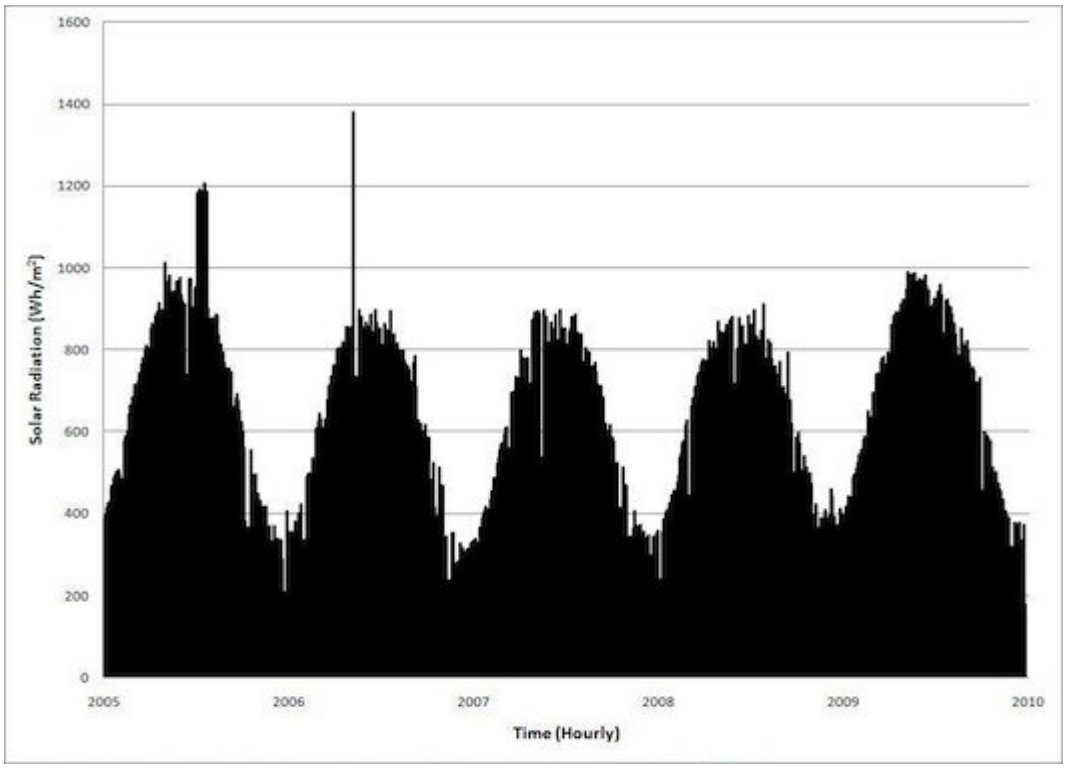

Figure 5.38: Solar Radiation Vs. Time (2005-2010)

Chapter 6

Application of TransChlor Model

6.1 General

This section focuses on the practical application of the TransChlor model. The TransChlor model combines all the information presented thus far, processes the input parameters and generates a chloride ion profile in the concrete cover. The analysis using the TransChlor model really goes above and beyond other models because it uses the chloride ion profile created, compares the profile with the type of steel and depth used, and then produces cumulative probability distribution curves for corrosion initiation with respect to time. In this chapter, the Transchlor simulation process will be discussed, as well as the preliminary and probabilistic analysis, and finally, the results will be presented.

6.2 Analysis

Analysis using the TransChlor model was divided into two sections, a preliminary analysis and a probabilistic analysis. However, before we can present the TransChlor models' analysis and display the results obtained, the input parameters will be reviewed and an explanation on how the model performs the analysis will be discussed.

6.2.1 Input Parameters

There are three categories for the input parameters in the TransChlor model. The first is the meteorological data, which includes both the climate and salt loading conditions. The second category is the concrete specifications. The last category is the simulations parameters.

The climate data is the first input file to be loaded into TransChlor. The TransChlor model checks that the file is complete without any missing data. Once this check has been completed, the parameters for salt spread of sodium chloride are entered. The three input parameters for salt spread are annual concentration of sodium chloride (g/m^2), average quantity of sodium chloride spread per intervention (g/m^2), and the time between two interventions (t).

The annual concentration of sodium chloride spread was neither readily available nor easy to obtain. There was much variability from the data found. To determine this value, a preliminary analysis with the TransChlor model using various annual concentrations was performed and is discussed in the preliminary analysis section of this chapter.

The application rate of sodium chloride per intervention was assumed to be 140 Kg/Lane-Km (City of Toronto 2004). This is the mean application rate specified by the city of Toronto for expressways and bare pavement conditions. The lower and upper bound application rates are 70 and 180 kg/Lane-km, respectively. These values are limited by the amount of salt the actual trucks can dispense. The mean value was assumed to be realistic and matches the recommended application rate provided in CEPA Priority Substance List Assessment Report.

The time between interventions was assumed to be 8 hours. In actuality, this value is not deterministic and changes with the severity and duration of the snowstorm. Interventions of 2, 4, 6, 10 or 12 hours could have been selected as well. Nevertheless, an average time of 8 hours is assumed to be the best suited since it maximizes cost effectiveness with respect to minimum safety requirements.

Once those input parameters were selected, the simulation parameters were entered into the program. The simulation was programmed to simulate 16425 days (roughly 45 years) of service life. The climatic data is entered in hourly increments. Therefore, the time step for the calculations is 3600 seconds. The thickness of the structural member is specified at 200 mm with 200 elements. Hence, a calculation was performed at every mm of depth on the member. The results were saved every 168 hours simulated (1 week). The initial parameters across the whole member were assumed to be 20°C for the thermal transport parameter, 100% saturation for the hydraulic transport parameter, and 0 kg/m^3 surface concentration for the chloride ion transport parameter.

Finally, the concrete specifications were entered. Normal Type I cement was selected. The amount of cement was determined from written reports to be 350 kg/m^3. The concrete had a w/c of 0.50 and an air content of 1.5% of mass of cement. Limestone aggregates were also specified. These specifications are representative of the type of concrete used at the time of construction. The type of concrete specified is important for the main parameters used in the simulation. These parameters are the thermal transport variable (D_T), hydraulic transport variables (D_{HR} & D_{CAP}), the ionic transport of chlorides variable (D_{Cl}), and the carbonation variable (D_{CO2}).

One of the last options is to determine if the main parameters are considered deterministic or probabilistic. If the deterministic approach is selected, the mean values determined for the main parameters are used to perform one simulation. This approach is used for the preliminary analysis since the simulation time is long. If a

probabilistic analysis is chosen, the probabilistic analysis parameters (i.e. the mean and standard deviation) are determined and the probabilistic analysis approach is performed using the Rosenblueth point estimate method. There are four variables that are included in the probabilistic approach. These are the hydraulic transport of water by diffusion (D_{HR}), the hydraulic transport of water by capillary action (D_{CAP}), the ionic transport of chlorides (D_{Cl}), and the carbonation (D_{CO2}). The number of simulations performed using the two-point Rosenblueth method is equal to 2^n, where n equals the number of variables involved. For the probabilistic analysis, all the parameters except for carbonation were selected. Therefore, 8 simulations were performed.

Once all the parameters are entered, the exposure conditions are then selected. The three exposure conditions used in this model are mist, splash and direct exposure. There are other exposure conditions that can be selected in the TransChlor model. These include inside the caisson with or without exposure to chlorides, as well as mechanical or automated spreading of salt. The exposure condition was also selected to be on one side of the member only. This is to allow simulation of chloride ingress on one side of the concrete element only. Exposure on two sides of an element is possible, with the added feature of selecting two different exposure conditions on each side.

After the input files were completed, the simulations were launched and chloride ion profiles were obtained. The simulation time varies as a function of exposure conditions and the total annual amount of salt used. For the most severe conditions, the simulation took approximately 60 hours to complete.

6.2.2 TransChlor Analytical Procedure

The TransChlor model uses a 7 steps procedure illustrated in Figures 6.1 and 6.2.

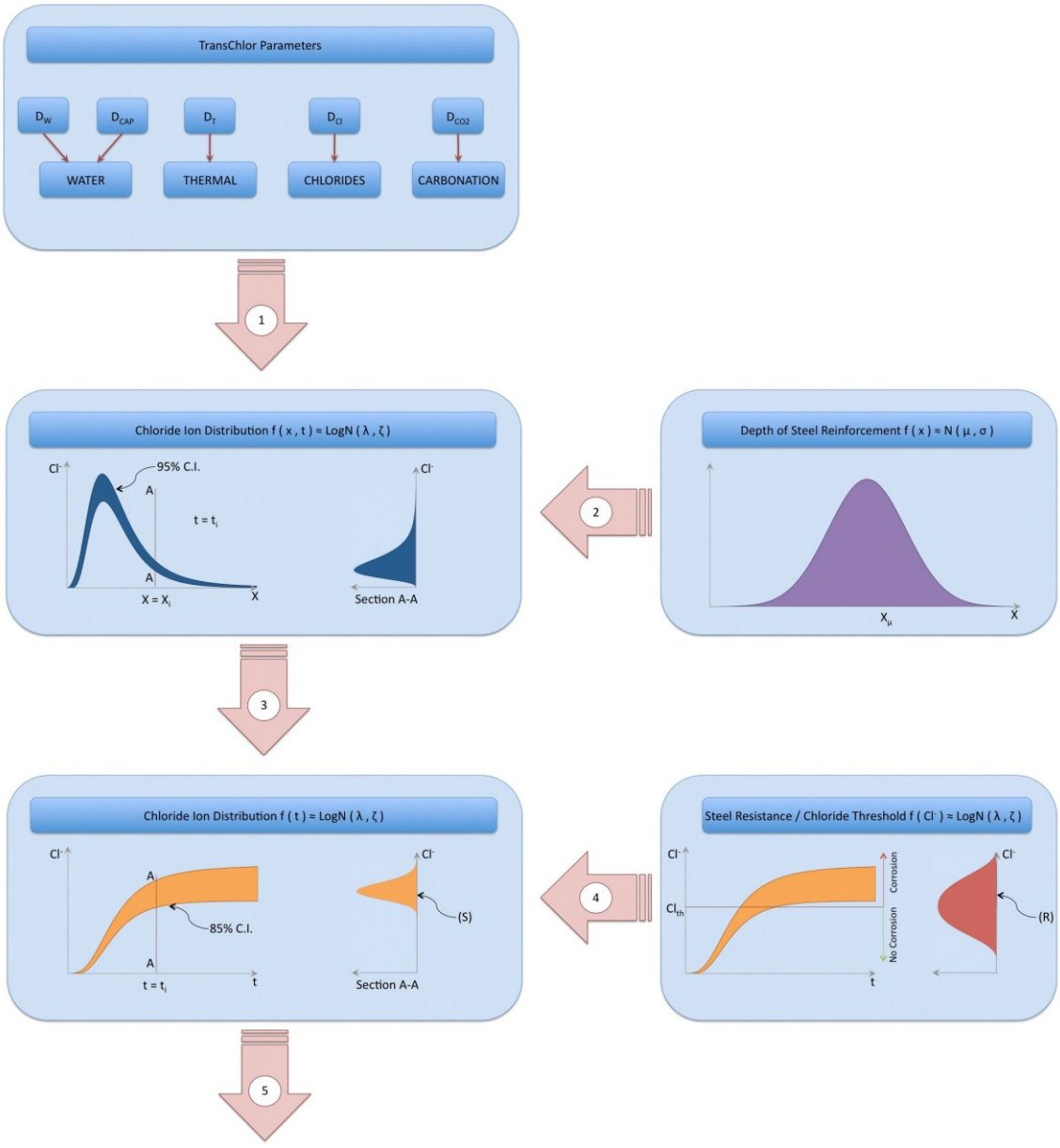

Figure 6.1: Schematic of TransChlor Analytical Procedure

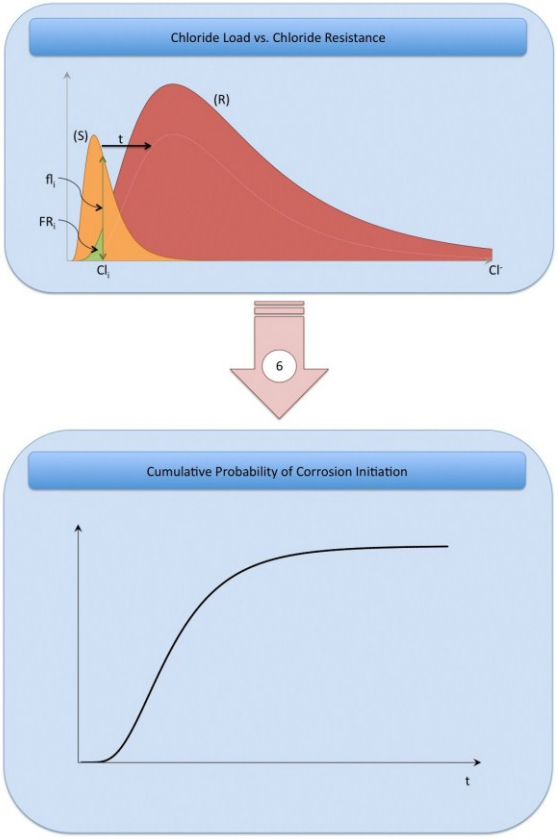

Figure 6.2: (Continued) Schematic of TransChlor Analytical Procedure

The starting point for the TransChlor analytical process is to specify the initial parameters. As was described earlier, the initial parameters are entered into the model and five transport variables are produced. Those five variables are the thermal transport variable (D_T), the hydraulic transport variable (D_{HR} & D_{CAP}), the ionic transport of chlorides variable (D_{Cl}), and the carbonation variable (D_{CO2}) (Figure 6.1).

There are relationships between these five variables. The thermal properties, (D_T), influence both the hydraulic transport properties, (D_{HR} & D_{CAP}), as well as the ionic transport of chlorides (D_{Cl}). The hydraulic transport properties, (D_{HR} & D_{CAP}), influence both the ionic transport of chlorides, (D_{Cl}), and carbonation, (D_{CO2}). These relationships and correlations are incorporated directly in the TransChlor software (Conciatori, Laferrière et al. 2010).

These parameters are used to run the first TransChlor simulation to produce a chloride ion distribution as a function of depth and time (step 1).

For the preliminary analysis, deterministic values for the main parameters are used and only one simulation is performed. As a result, only one chloride ion profile is created. Graphs displaying chloride profiles with respect to depth and time can be produced. This feature was used and results are shown in the preliminary analysis section.

For the probabilistic approach, mean and standard deviations for the main parameters are required and simulations are performed using the Rosenblueth point estimate method. This approach produces distributions of chloride ion profiles that follow a lognormal distribution with respect to depth and time. This is shown in the second diagram. The band shown in the chloride ion distribution profile represents the 95% confidence interval of this section.

The next step, shown by the second red arrow, is the comparison of reinforcing steel depth with the chloride ion distribution profile. The depth of reinforcing steel is shown in the third diagram and has a normal distribution (Tikalsky, Pustka et al. 2005). In the probabilistic analysis using the TransChlor model, a deterministic value for the depth of the reinforcing steel can be used instead of a normal distribution.

At each time step, a weighted average using the depth of reinforcing steel distribution and the chloride ion distribution was performed. This produced a chloride ion distribution as a function of time and is shown in the fourth diagram. The third red arrow indicates the weighted average performed.

Also shown in the fourth diagram is a section (A-A) at a specific point in time. This curve has a lognormal distribution. The band shown in the chloride ion distribution

profile represents the 85% confidence interval of this section. This section can also indicate the chloride loading at that particular point in time and has been denoted (S).

The fifth diagram shows the chloride ion threshold with respect to the chloride ion distribution profile, which is shown in the fourth diagram. In the previous analysis, the chloride ion threshold was taken as a deterministic value. Hence, no corrosion was assumed to occur if the chloride ion distribution profile was found below the chloride ion threshold. Inversely, corrosion was assumed to occur if the chloride ion distribution profile was found to be above the chloride ion threshold. However, it has been recognized that the chloride ion threshold is not a deterministic value and is assumed to follow a lognormal distribution. This variability is due to the variability of steel properties. The lognormal distribution of the chloride threshold is related to the resistance of the steel to chlorides and has been denoted (R).

The next step, shown by the fifth red arrow, is to compare the chloride loading at each point in time (S) with the resistance of the steel to chlorides (R). This is shown in the sixth diagram. In the sixth diagram, the chloride loading is depicted by the orange curve at a particular point in time. The chloride loading progresses with time and this evolution is marked by the dotted curve. The resistance of the steel is shown as the red curve and stays constant with time. At each time step, the convolution product between the chloride loading and the steel resistance to the chloride ion concentration provides the corrosion initiation probability (Conciatori, Brühwiler et al. 2009a). The corrosion initiation probability is shown in equation 6.1:

$$P_f = \sum_{Cl_i=0}^{\infty} fl_i \cdot FR_i \qquad [6.1]$$

where:

Cl_i = Chloride ion concentration variable

fl_i = Probability density function of chloride ion concentration (Green line)

FR_i = Probability of non-exceedance of the resistance given a Cl_i value (Green Area)

After the calculation of the corrosion initiation probability at each time step, the cumulative probability density function for the corrosion initiation is obtained as a function of time. The sixth arrow illustrates this last step and the cumulative density function is shown in the last diagram.

6.2.3 Preliminary Analysis

The purpose of the preliminary analysis is to determine the annual average amount of salt spread on Montreal elevated highways. It is important that determine this value accurately so that the TransChlor predictions reflect the actual conditions in the structural elements.

For this analysis, the following approach was used in the simulations. Chloride ion profiles were obtained using different input parameters and compared with chloride ion concentrations obtained from samples taken from the bridge, (Chapter 5). The optimal annual salt spread amount was determined by comparing the chloride ions profiles obtained by simulation and from the field survey and used for the probabilistic analysis.

Chloride profiles for all three exposure conditions are shown in Figures 6.1 to 6.11 for depths of 25 mm and 50 mm at the time of sampling (between October 6 and October 16, 2009). In each profile, 3 different annual concentrations were used in the simulations. The annual salt concentrations used for simulations were 5, 10 and 20 tonnes per 2-lane km. A value of 30 tons per 2-lane km had been suggested for

Montreal (Jefremczuk 2005); however, this amount is unrealistic in the TransChlor model since the calculated limiting temperature (see section 4.5) would be 7°C, which is larger than the maximum allowable temperature of 5°C. The three graphs for mist, direct and splash exposures are shown in Figures 6.3 to 6.5, Figures 6.6 to 6.8, and Figures 6.9 to 6.11, respectfully.

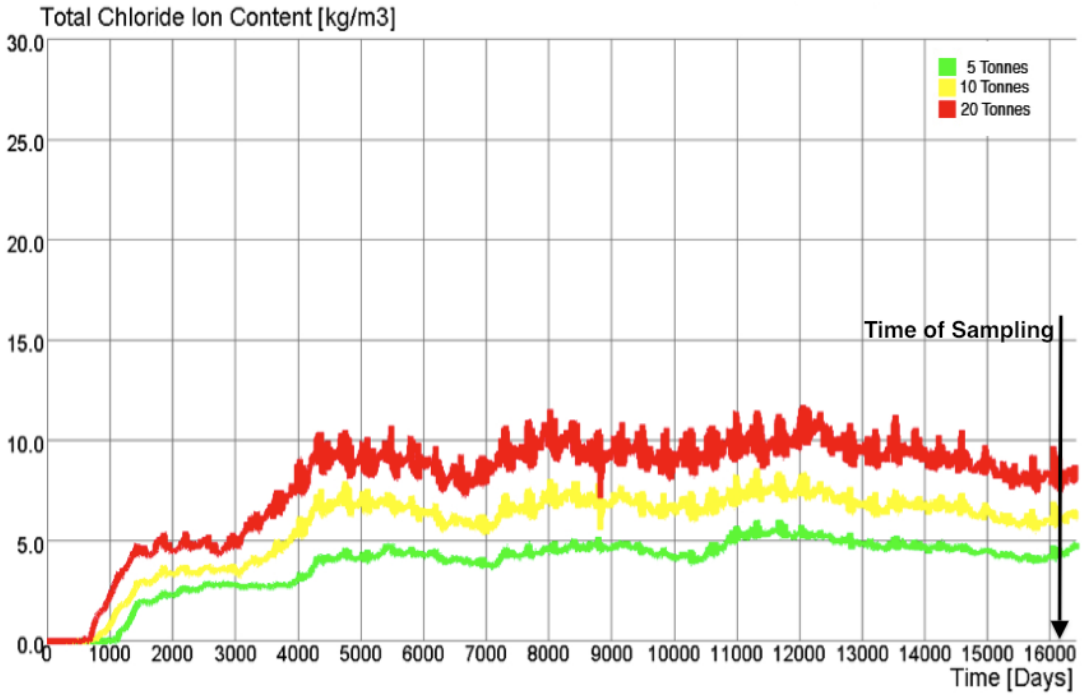

Figure 6.3: Total Chloride Ion Distribution at 25 mm for Mist Exposure using Simple Analysis

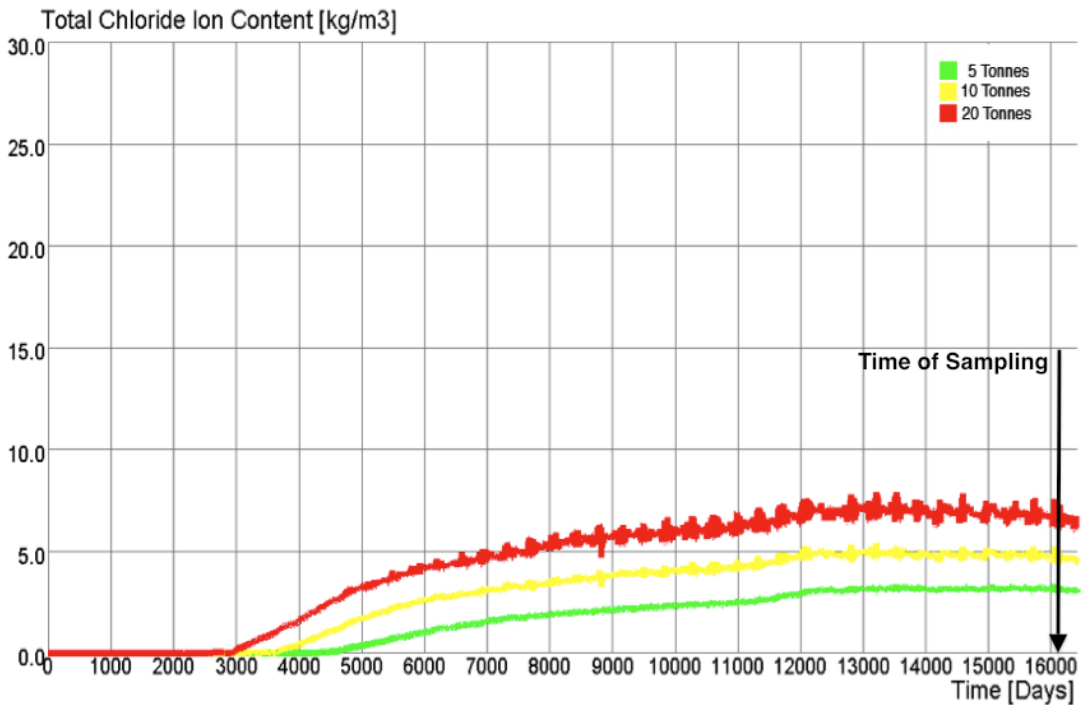

Figure 6.4: Total Chloride Ion Distribution at 50 mm for Mist Exposure using Simple Analysis

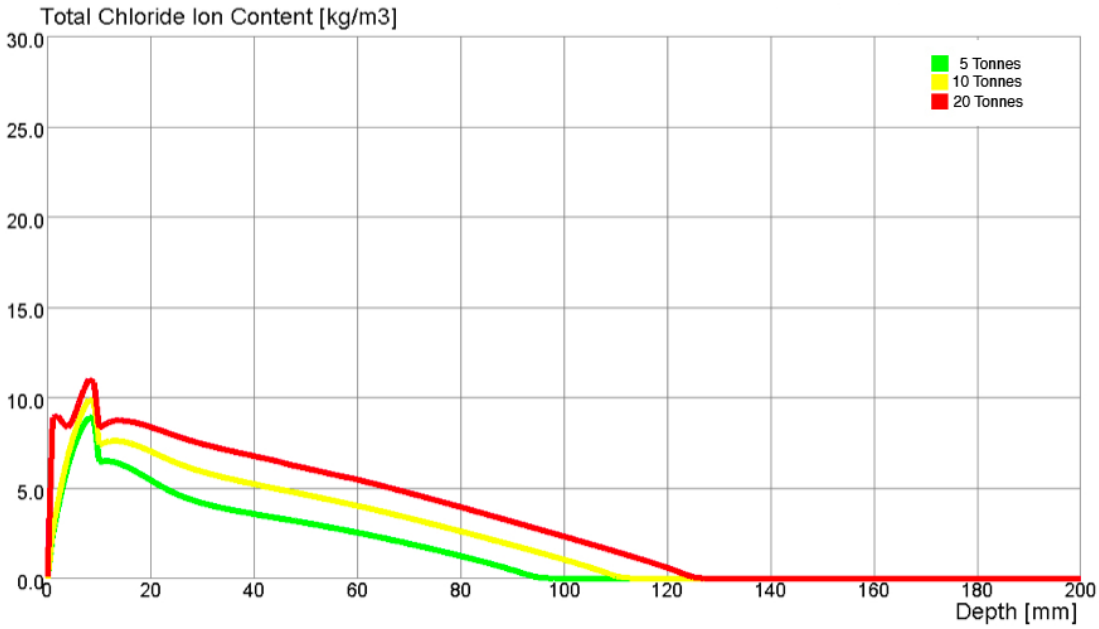

Figure 6.5: Total Chloride Ion Distribution at Time of Sampling for Mist Exposure using Simple Analysis

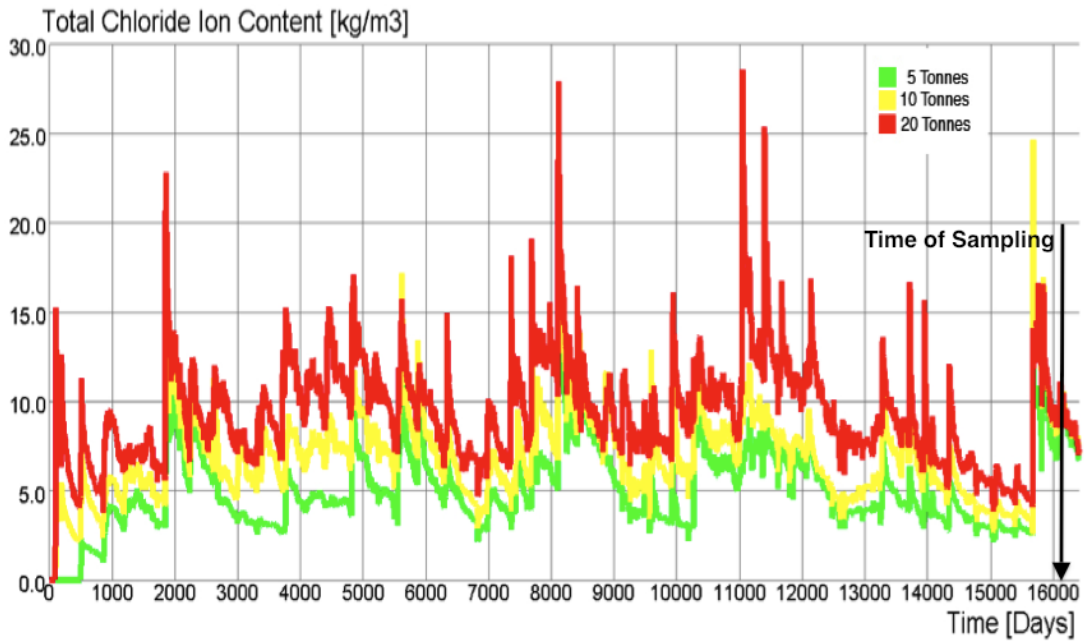

Figure 6.6: Total Chloride Ion Distribution at 25 mm for Direct Exposure using Simple Analysis

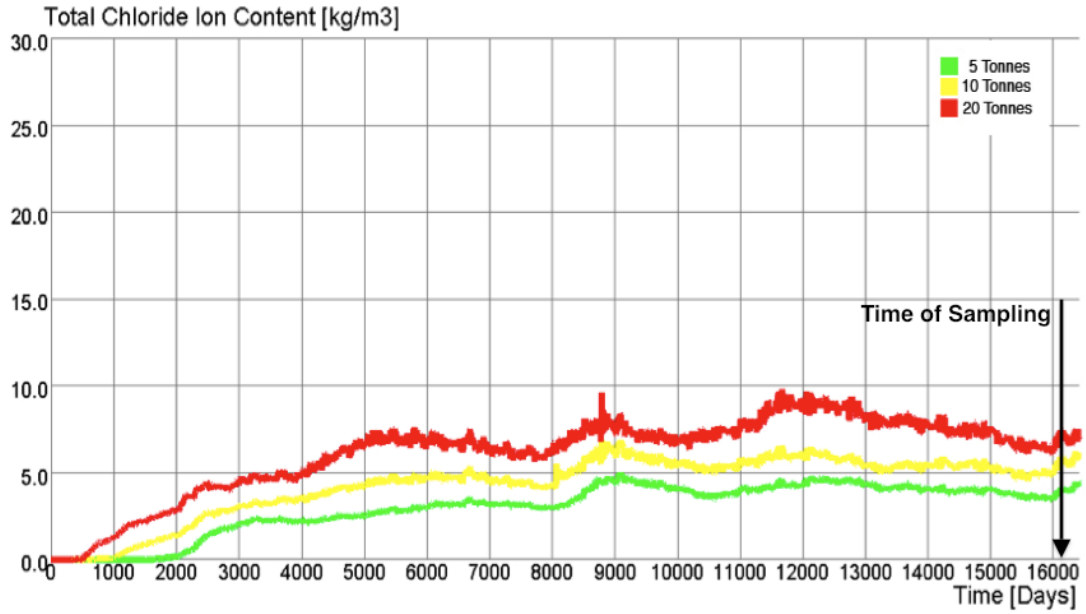

Figure 6.7: Total Chloride Ion Distribution at 50 mm for Direct Exposure using Simple Analysis

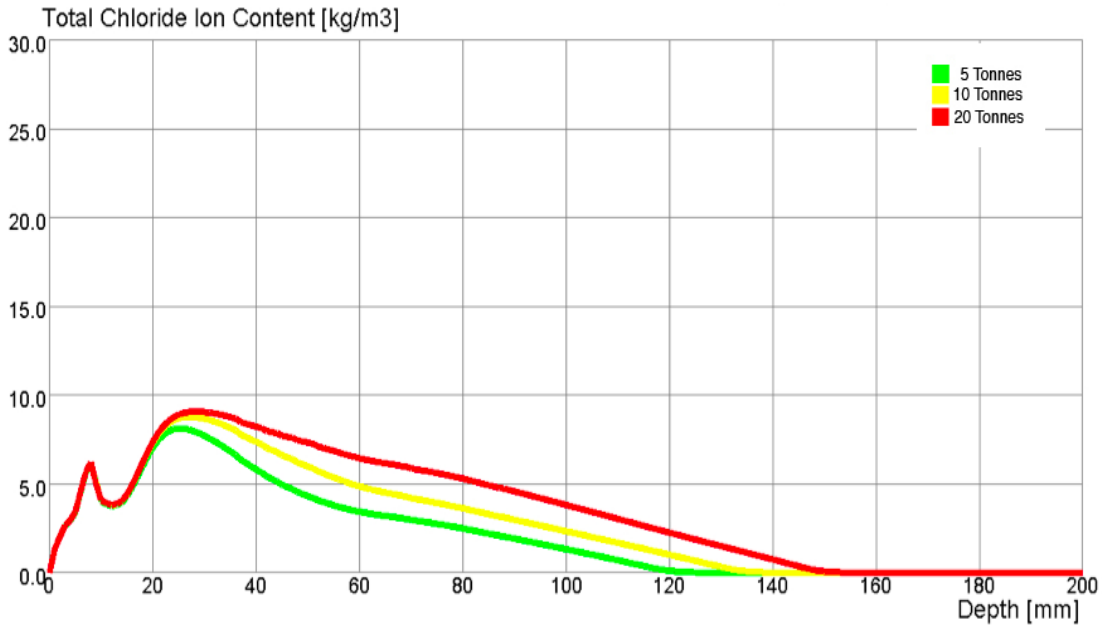

Figure 6.8: Total Chloride Ion Distribution at Time of Sampling for Direct Exposure using Simple Analysis

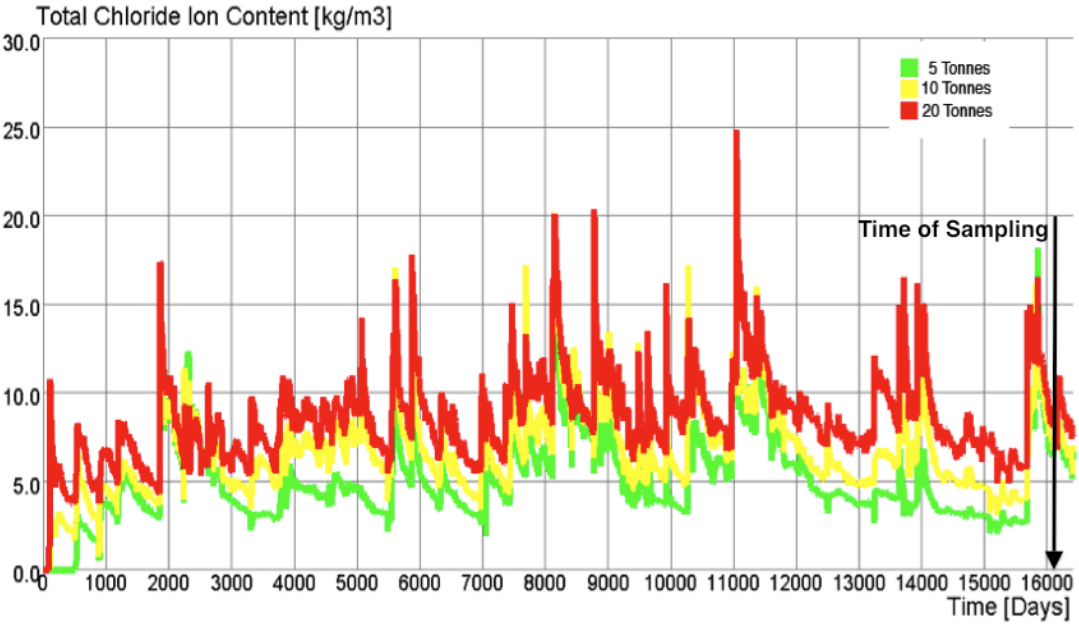

Figure 6.9: Total Chloride Ion Distribution at 25 mm for Splash Exposure using Simple Analysis

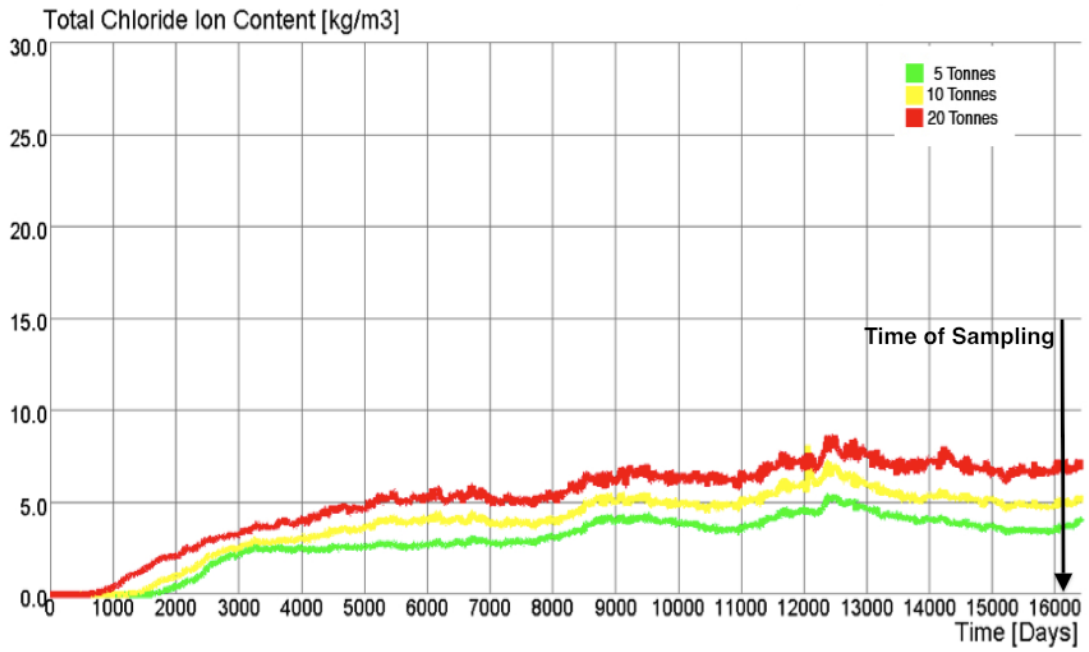

Figure 6.10: Total Chloride Ion Distribution at 50 mm for Splash Exposure using Simple Analysis

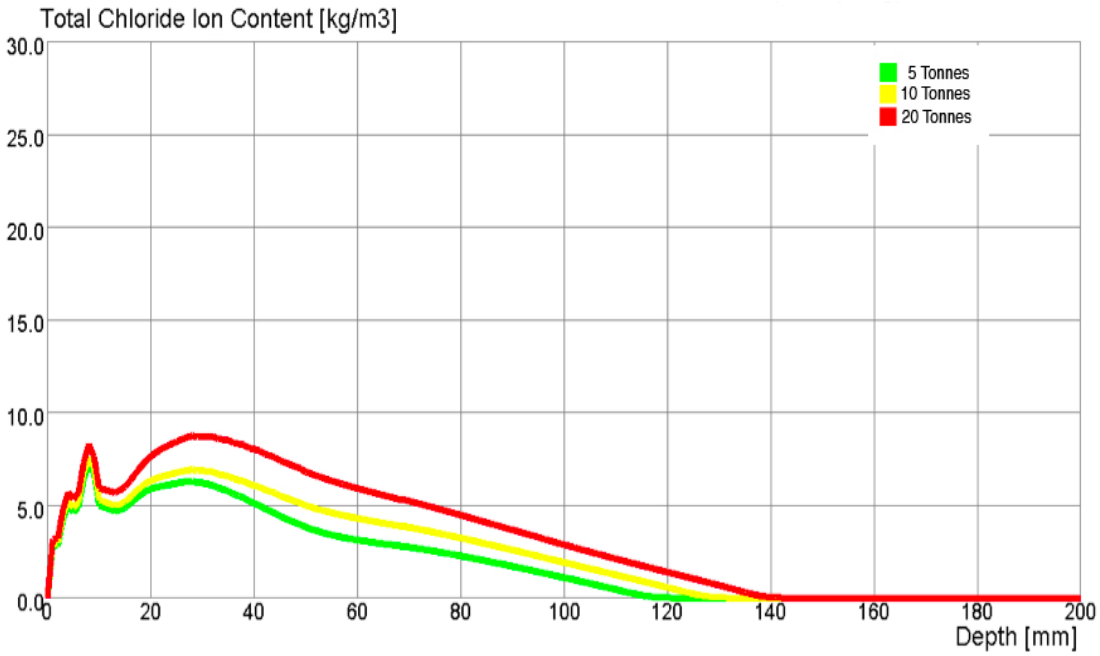

Figure 6.11: Total Chloride Ion Distribution at Time of Sampling for Splash Exposure using Simple Analysis

Analyzing the chloride ion profiles for each exposure condition, it was found that the simulations for mist exposure did not accurately represent the data provided. The high humidity caused the mist exposure to be excessively large, and almost as severe as the direct and splash exposure conditions. However, this is contradictory to the data samples provided, which showed low chloride ion concentration in zones assumed to be more susceptible to mist exposure.

It is hypothesized that the effect of wind, which is not directly considered in the model, led to this discrepancy. Wind transports chloride ions in the mist away from the structure and a large proportion of airborne ion chlorides never come into contact with the concrete structure (Figure 6.12). For this reason, simulation results for mist exposure were not used to calibrate the annual chloride ion concentration.

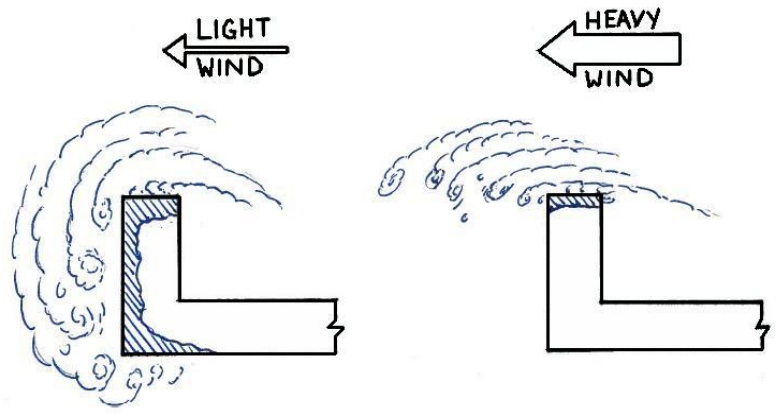

Figure 6.12: Effect of Wind on Mist Exposure

Annual salt concentrations used in the probabilistic analysis were determined by comparing simulations results for mist, direct and splash exposure at the time of sampling with data from the core samples (Figures 5.1 and 5.2). The graphs are shown in Figures 6.13, 6.14, and 6.15. The simulations for splash and direct exposure show that the concentration for chloride ions varies greatly during the winter season; however, this level of variability is not present in the summer season when the concrete samples were obtained. The simulations for mist exposure do not correspond well with the samples obtained. Therefore, the simulations for mist exposure were not used to calibrate the model.

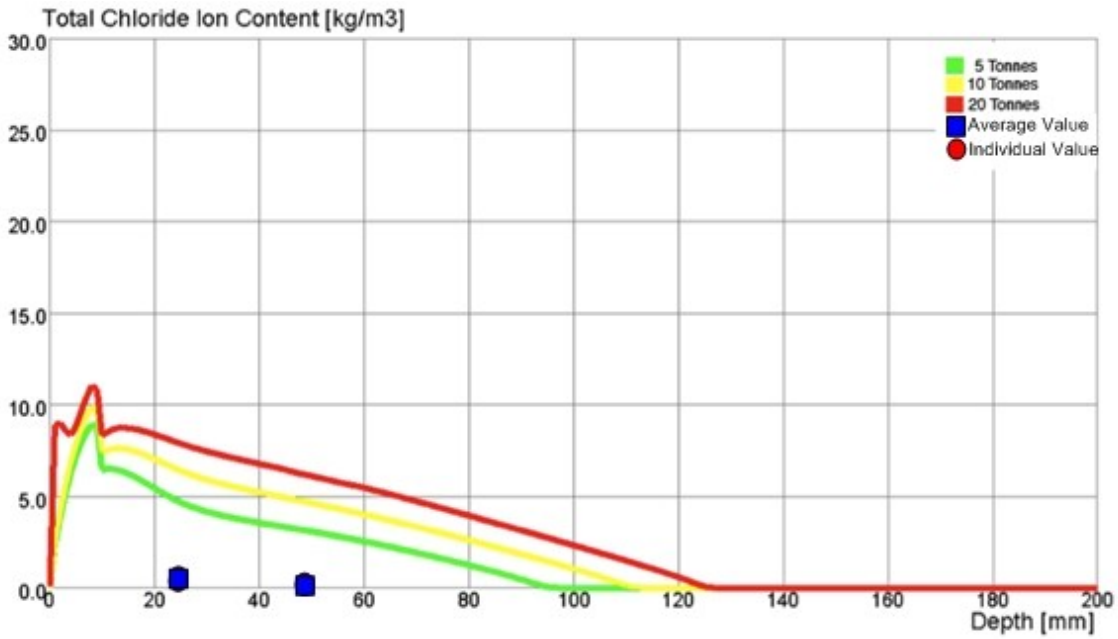

Figure 6.13: Comparison of Sample Data with Chloride Ion Distribution Curves for Mist Exposure using Simple Analysis

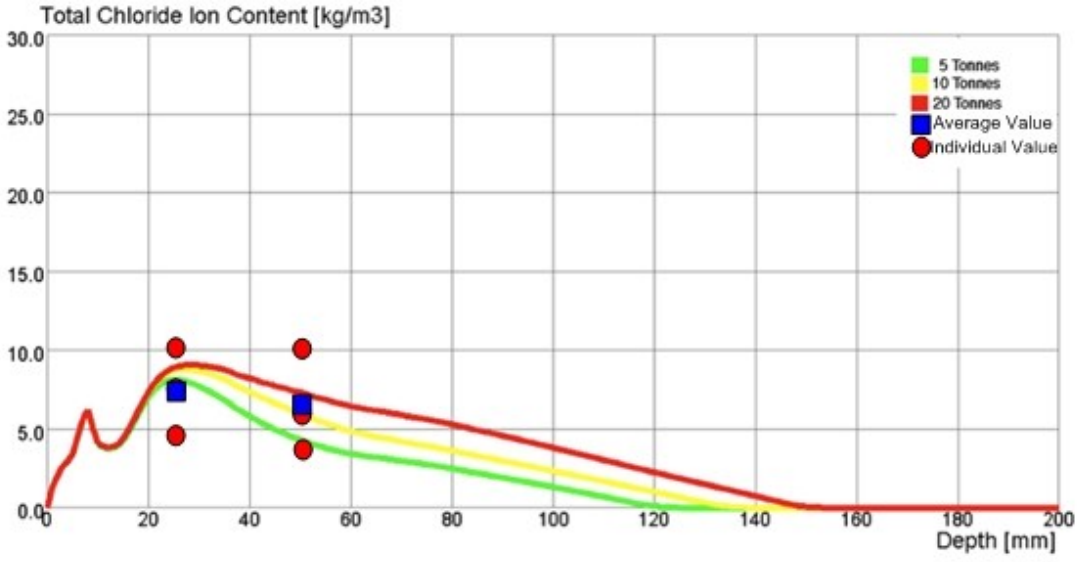

Figure 6.14: Comparison of Sample Data with Chloride Ion Distribution Curves for Direct Exposure using Simple Analysis

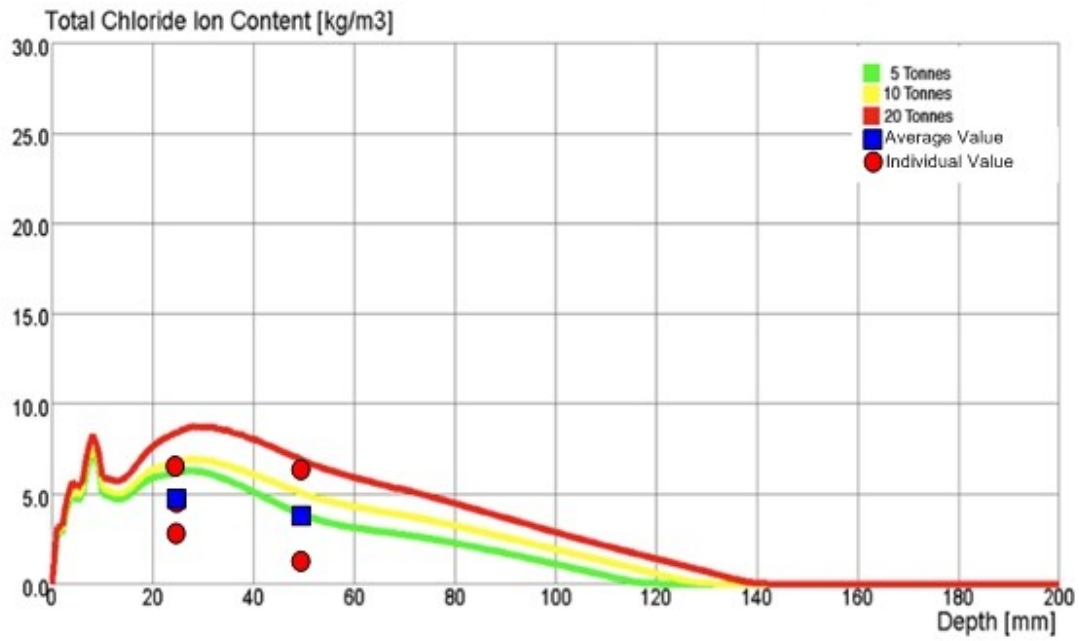

Figure 6.15: Comparison of Sample Data with Chloride Ion Distribution Curves for Splash Exposure using Simple Analysis

The blue square in the graphs represents the average value of the samples for a given exposure condition for both 25 and 50 mm depth, while the red dots indicate the values observed for individual samples. For mist exposure, the average total chloride ion content is 0.3 and 0.2 kg/m^3 for 25 mm and 50 mm depth, respectively. For direct exposure, the average total chloride ion content is 7.6 and 6.7 kg/m^3 for 25 mm and 50 mm depth, respectively. For splash exposure, the average total chloride ion content was 4.9 and 4.1 kg/m^3 for 25 and 50 mm depth, respectively. The mean error (ME) and mean square error (MSE) between the predicted and observed values for both exposures is shown in Table 6.1.

Table 6.1: ME and MSE for Direct and Splash Exposure

Direct Exposure				
Depth (mm)	25		50	
Annual Concentration (Tons)	ME	MSE	ME	MSE
5	0.211	4.887	-2.357	12.614
10	0.771	5.437	-0.698	7.546
20	0.790	5.466	0.646	7.477
Splash Exposure				
Depth (mm)	25		50	
Annual Concentration (Tons)	ME	MSE	ME	MSE
5	1.308	3.921	-0.145	6.284
10	1.875	5.727	1.085	4.960
20	3.364	13.526	3.018	15.369

It was determined that the best-fit value for the annual concentration was 15 tons per 2-lane km. This value is a reasonable assumption since other sources have suggested that almost 20 to 30 percent of deicing salts applied can be blown off the road by wind, bounced off by momentum or pushed off by cars and snow removal trucks (U.S. Roads 1997).

After the preliminary analysis was completed and the estimated annual concentration was determined, a probabilistic analysis with the TransChlor was performed.

6.2.4 Probabilistic Analysis

The purpose of the probabilistic analysis is to create cumulative distribution curves with respect to corrosion initiation. The method used to obtain these curves was described in section 6.2.2.

The annual chloride ion concentration was determined in the previous section to be 15 tons per 2-lane km and was used for the probabilistic analysis. All other parameters were left unchanged except for the fact that the mean and standard deviation were determined for the parameters involving the transport properties. The mean and standard deviation for carbonation was not considered as a probabilistic parameter since the depth of carbonation for all exposures conditions did not reach a significant level (Figure 6.16). It can be seen that the depth of carbonation after 45 years does not reach 10 mm in depth. Thus, only a deterministic value for carbonation was used.

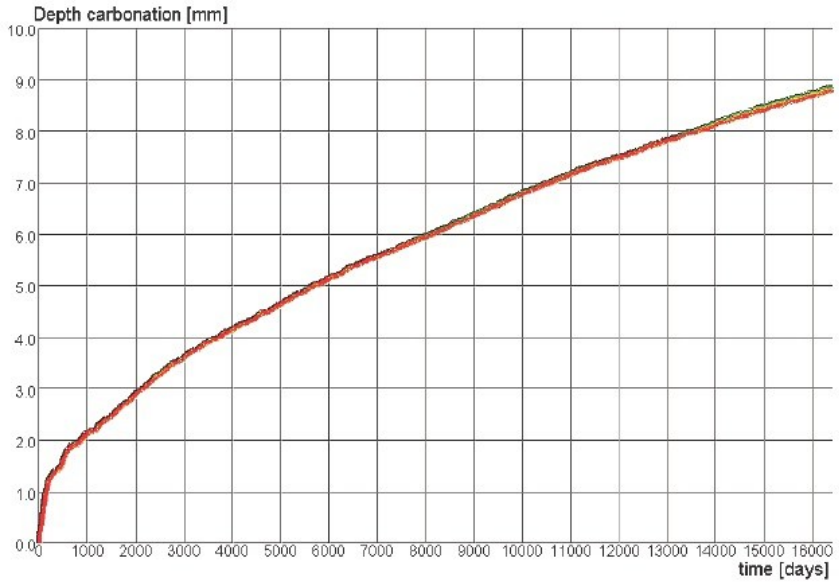

Figure 6.16: Depth of Carbonation with Time

A Rosenblueth two-point estimate method was used in the simulation. The Rosenblueth method is used to solve numerical models that involve random inputs. The concept of the Rosenblueth method is to approximate the continuous distribution with a discrete distribution with a finite amount of distinct values with positive probability, in our case three variables with two points. The approximation is performed such that the moments of the discrete distribution and the continuous distribution are the same. Conciatori (2009a) compares the approximation process to a simple beam analysis. All the different permutations of the various inputs are then used in the model and the corresponding solutions determined. Lastly, the discrete results produced are combined so that a continuous distribution can be derived from them. This approach has been compared with the computationally intensive Monte Carlo simulation and preliminary studies have shown promising results (Rosenblueth 1975; Conciatori, Brühwiler et al. 2009a).

The Rosenblueth two-point estimate method uses two values to represent the distribution. In our simulations, the lower value is represented by X_1 and the upper value by X_2. Since there are three (3) variables, each with two (2) possible values, eight (2^3) simulations are performed while using the Rosenblueth method in the TransChlor model.

The formulas used to determine the distinct values (x_1, x_2) and the associated probabilities (F_1, F_2) are shown as follows (Rosenblueth 1975; Conciatori, Brühwiler et al. 2009a):

$$F_2 = \frac{1}{2} \cdot \left[1 - \frac{\beta}{|\beta|} \cdot \sqrt{1 - \frac{1}{1 + (\beta/2)^2}} \right] \qquad [6.2]$$

$$F_1 = 1 - F_2 \qquad [6.3]$$

$$x_2 = \mu_x + \sigma_x \cdot \sqrt{\frac{F_1}{F_2}} \qquad [6.4]$$

$$x_1 = \mu_x - \sigma_x \cdot \sqrt{\frac{F_2}{F_1}} \qquad [6.5]$$

The distinct values (x_1, x_2) and the associated probabilities (F_1, F_2) for a normal and lognormal distribution are shown in Table 6.2 (Conciatori, Brühwiler et al. 2009a):

Table 6.2: Distinct Values and Associated Probabilities for Normal and Log-normal Distribution

	Points		*Associated probabilities*	
Distribution	x_1	x_2	F_1	F_2
Normal N (μ, σ)	$\mu + \sigma$	$\mu - \sigma$	0.5	0.5
Log-normal LN (λ, ζ)	$e^{\lambda - \frac{\zeta}{2}}$	$e^{\lambda + \frac{\zeta}{2}}$	$\frac{\alpha_p}{\alpha_p + \alpha_m}$	$\frac{\alpha_m}{\alpha_p + \alpha_m}$

$$\alpha_m = e^{\lambda} \cdot (1 - e^{-\frac{\zeta}{2}}), \quad \alpha_p = e^{\lambda} \cdot (e^{\frac{\zeta}{2}} - 1)$$

For the probabilistic analysis, lognormal distributions were used for the three parameters (D_{HR}, D_{CAP}, and D_{Cl}). The average value used in the preliminary analysis and the distinct values with their associated probabilities for the probabilistic analysis are shown in Table 6.3:

Parameter Coefficient (mm^2/s)	μ	C.O.V.	x_1	x_2	F_1	F_2
D_{HR}	1.3x10-4	30%	9.28x10-5	1.67x10-4	0.573	0.427
D_{CAP}	6.5x10-4	30%	4.64x10-4	8.34x10-4	0.573	0.427
D_{Cl}	4.9x10-6	40%	3.09x10-6	6.68x10-6	0.595	0.405

Table 6.3: Average Values, Distinct Values, and Associated Probabilities used in the Preliminary and Probabilistic Analysis

Once all the simulations were finished for each of the exposure conditions, chloride ion profiles were created and compared with the chloride ion samples again. This

was to confirm if the annual chloride ion concentration was properly selected. The two graphs for direct and splash exposure are shown in Figure 6.17 and Figure 6.18, respectively. The curves represent the 8 simulations permutations for the Rosenblueth method. The values in red show the chloride ion concentrations from the samples taken from the bridge and indicate that the observed values are within the range of simulated values at a depth of 25 mm and in the lower range of predicted values at a depth of 50 mm.

The chloride ion profiles for all three exposure conditions are also shown below at 25 mm and 50 mm depth as well as at the time of sampling. The mean and standard deviation at the time of sampling has also been shown. They were determined by taking a weighted mean and standard deviation from the associated probabilities of each variable (Conciatori, Brühwiler et al. 2009a). The number in the legend represents which point was used in the Rosenblueth method, either X_1 (1) or X_2 (2). The first value represents the hydraulic transport of water by diffusion (D_{HR}), the second the hydraulic transport of water by capillary action (D_{CAP}), the third the ionic transport of chlorides (D_{Cl}), and the fourth the depth of carbonation (D_{CO2}). As was mentioned, carbonation was not taken into account and therefore, is represented by a zero (0). As an example, the curve (1210) would denote the lower value X_1 for D_{HR}, the higher value X_2 for D_{CAP}, the lower value X_1 for D_{Cl}, and no value for D_{CO2}. The four graphs for mist, direct and splash are shown in Figures 6.19 to 6.22, Figures 6.23 to 6.26, and Figures 6.27 to 6.30, respectfully.

For each exposure condition, cumulative probability distribution curves with respect to corrosion initiation were produced and are shown in Figures 6.31 to 6.33. The methodology used to produce these curves was described in section 6.2.2. Deterministic values for the depths of steel reinforcement were used. Therefore, the normal distribution for the depth of steel was not taken into account. The various depths used can be seen in the legend of each graph.

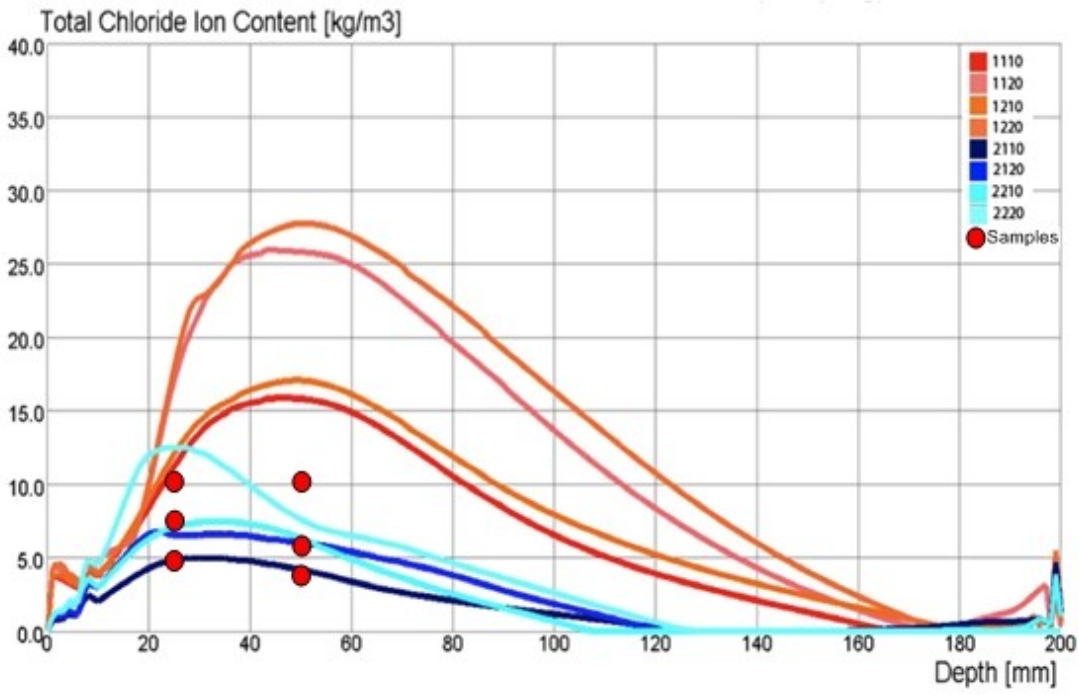

Figure 6.17: Comparison of Sample Data with Chloride Ion Distribution Curves for Direct Exposure using Probabilistic Analysis

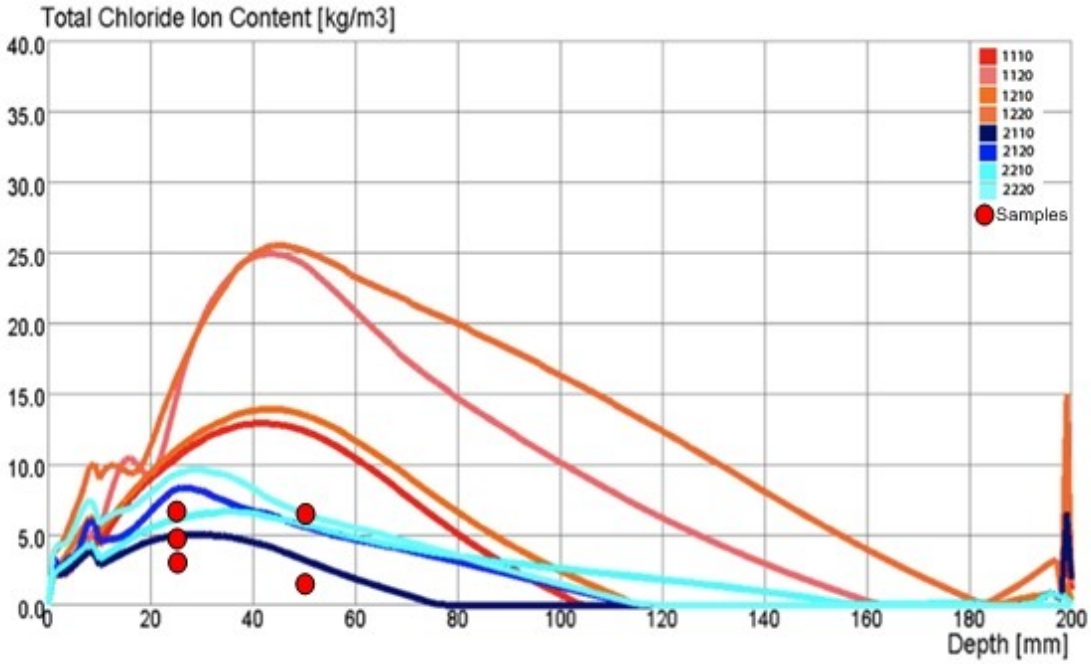

Figure 6.18: Comparison of Sample with Chloride Ion Distribution Curves for Splash Exposure using Probabilistic Analysis

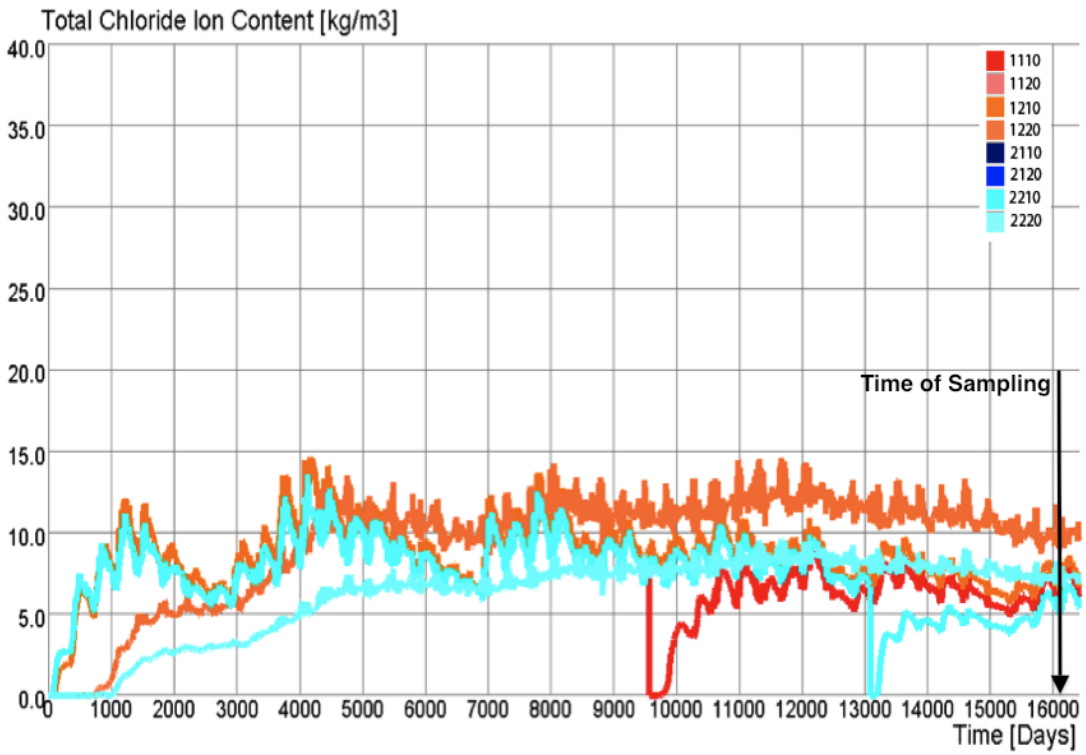

Figure 6.19: Total Chloride Ion Distribution at 25 mm for Mist Exposure using Probabilistic Analysis

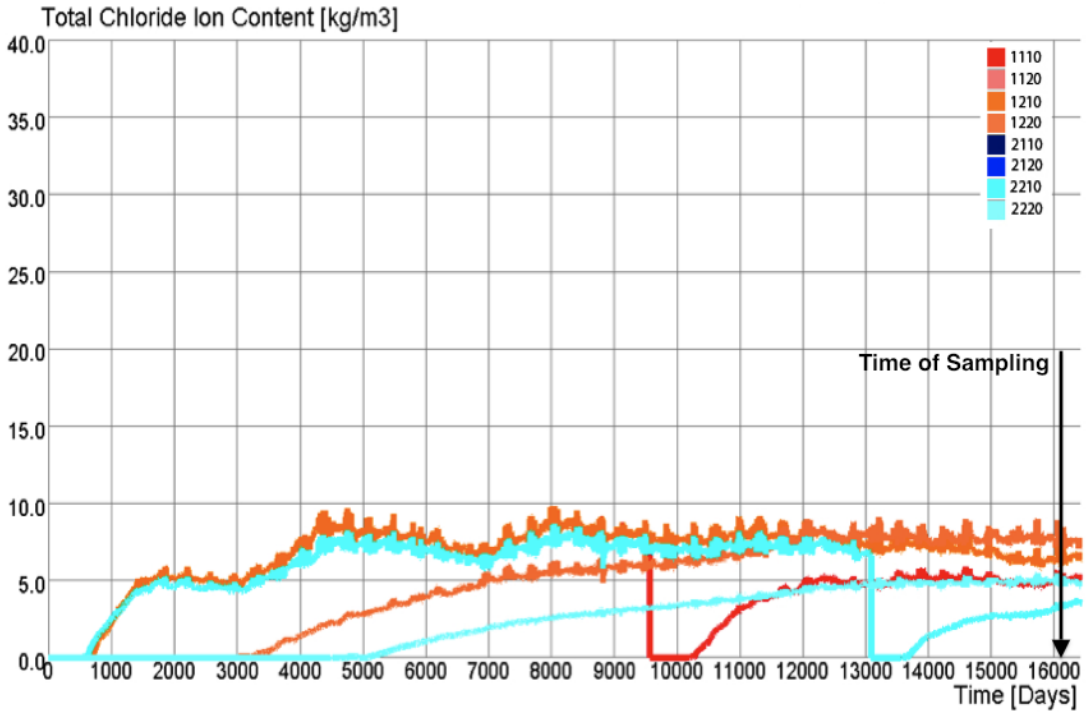

Figure 6.20: Total Chloride Ion Distribution at 50 mm for Mist Exposure using Probabilistic Analysis

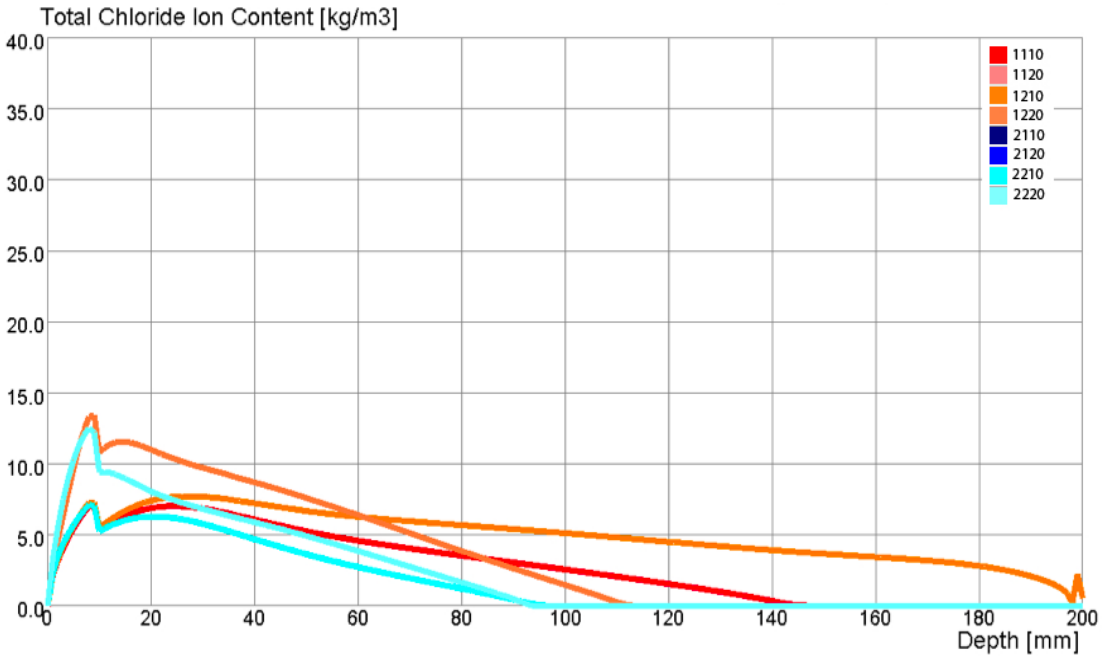

Figure 6.21: Total Chloride Ion Distribution at Time of Sampling for Mist Exposure using Probabilistic Analysis

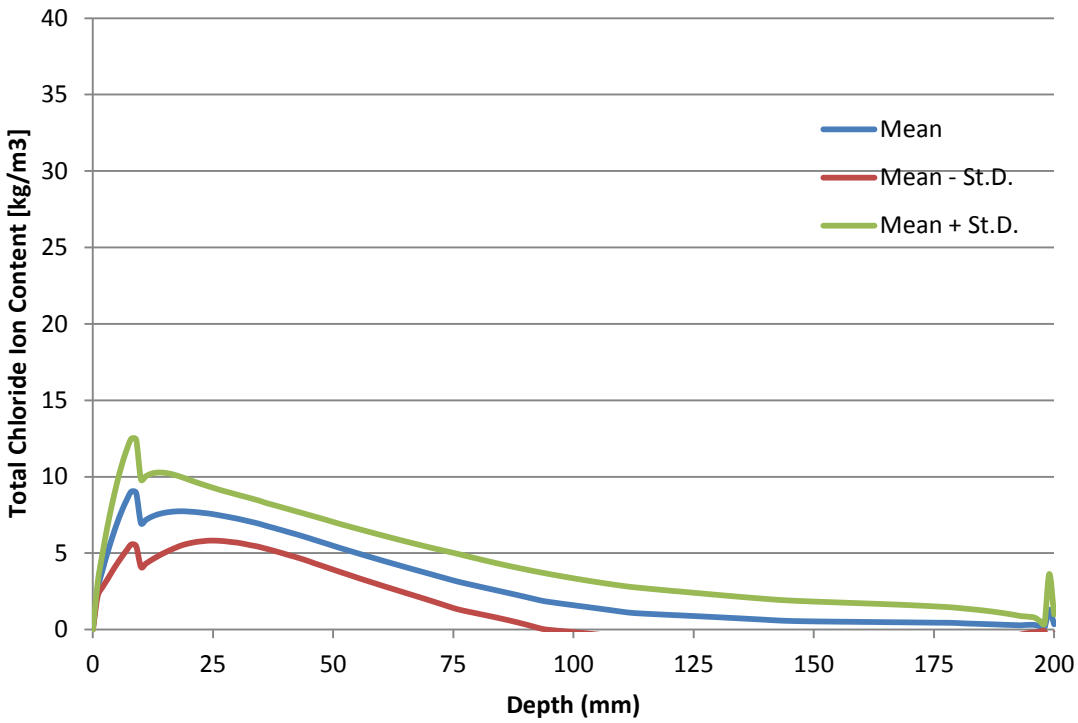

Figure 6.22: Mean and Standard Deviation at Time of Sampling for Mist Exposure

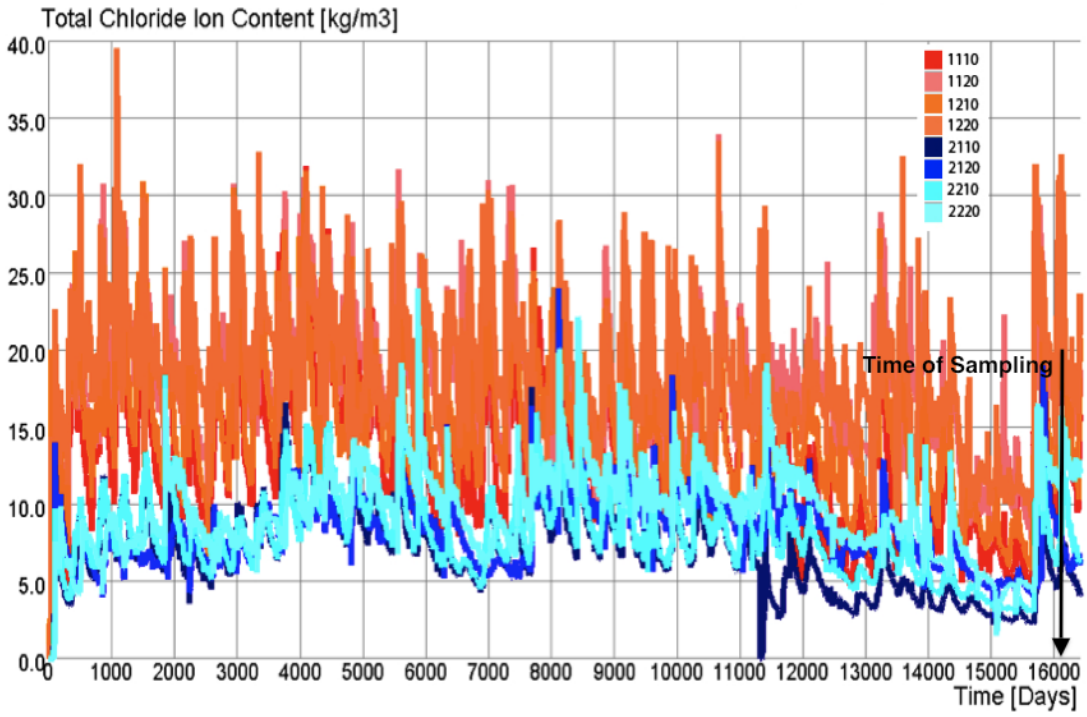

Figure 6.23: Total Chloride Ion Distribution at 25 mm for Direct Exposure using Probabilistic Analysis

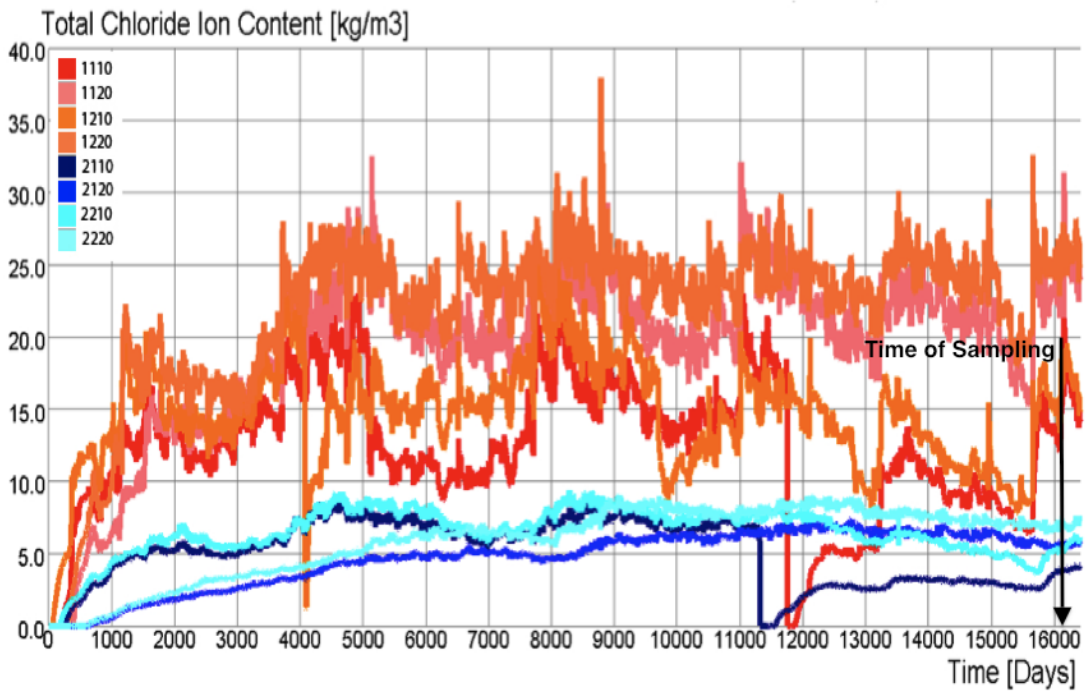

Figure 6.24: Total Chloride Ion Distribution at 50 mm for Direct Exposure using Probabilistic Analysis

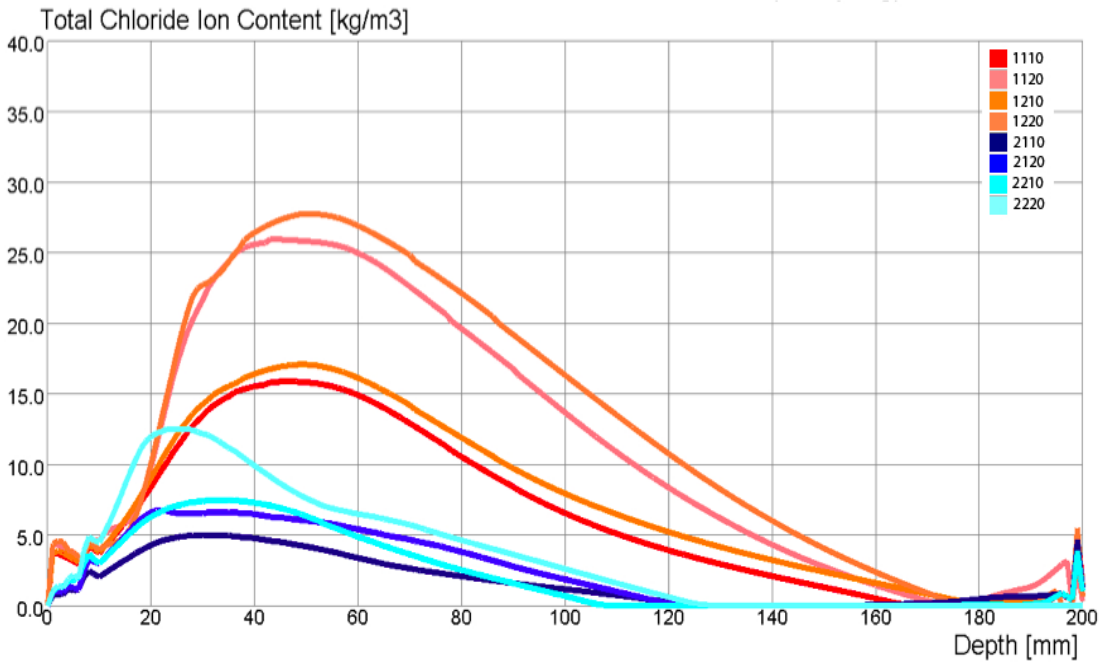

Figure 6.25: Total Chloride Ion Distribution at Time of Sampling for Direct Exposure using Probabilistic Analysis

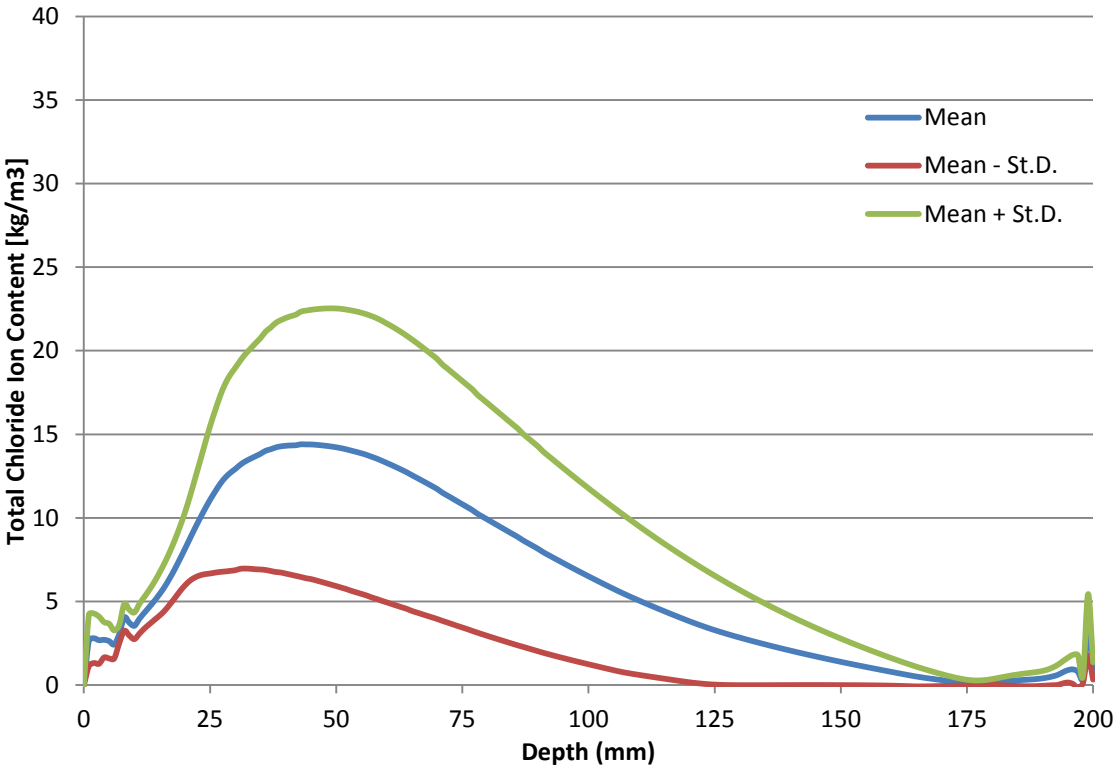

Figure 6.26: Mean and Standard Deviation at Time of Sampling for Direct Exposure

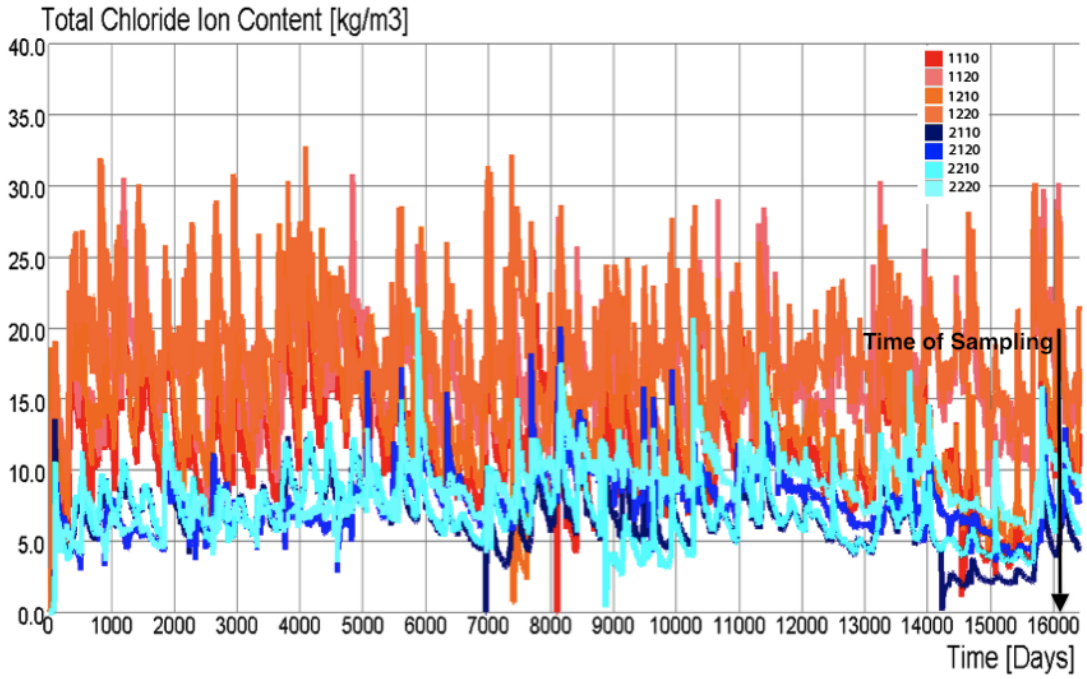

Figure 6.27: Total Chloride Ion Distribution at 25 mm for Splash Exposure using Probabilistic Analysis

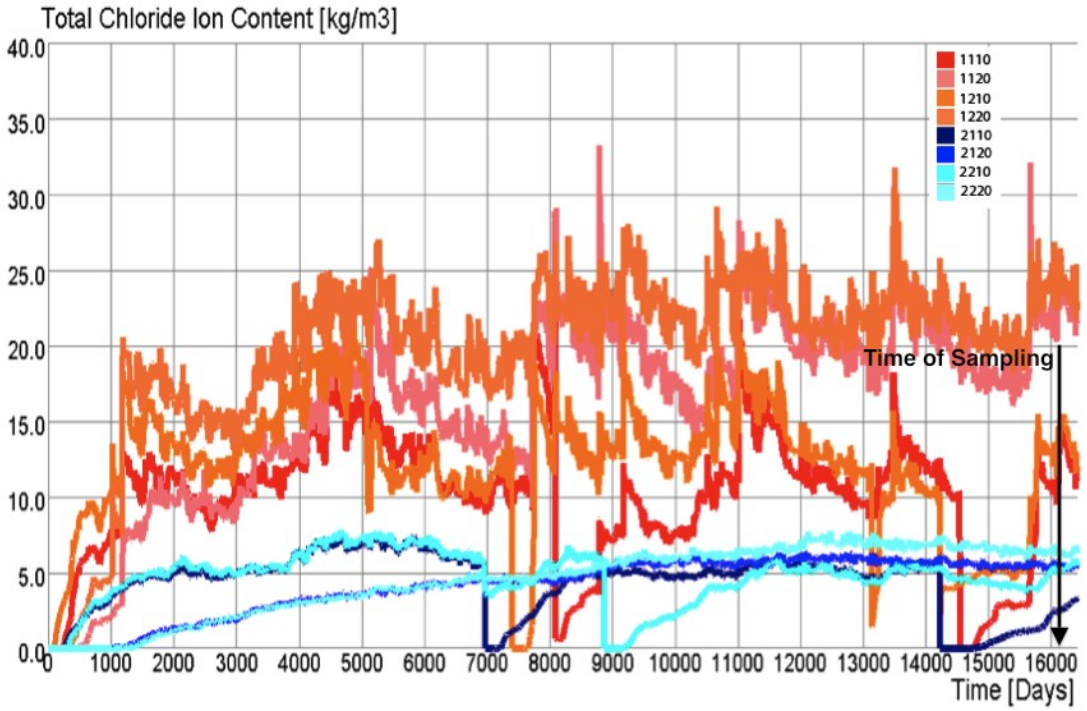

Figure 6.28: Total Chloride Ion Distribution at 50 mm for Splash Exposure using Probabilistic Analysis

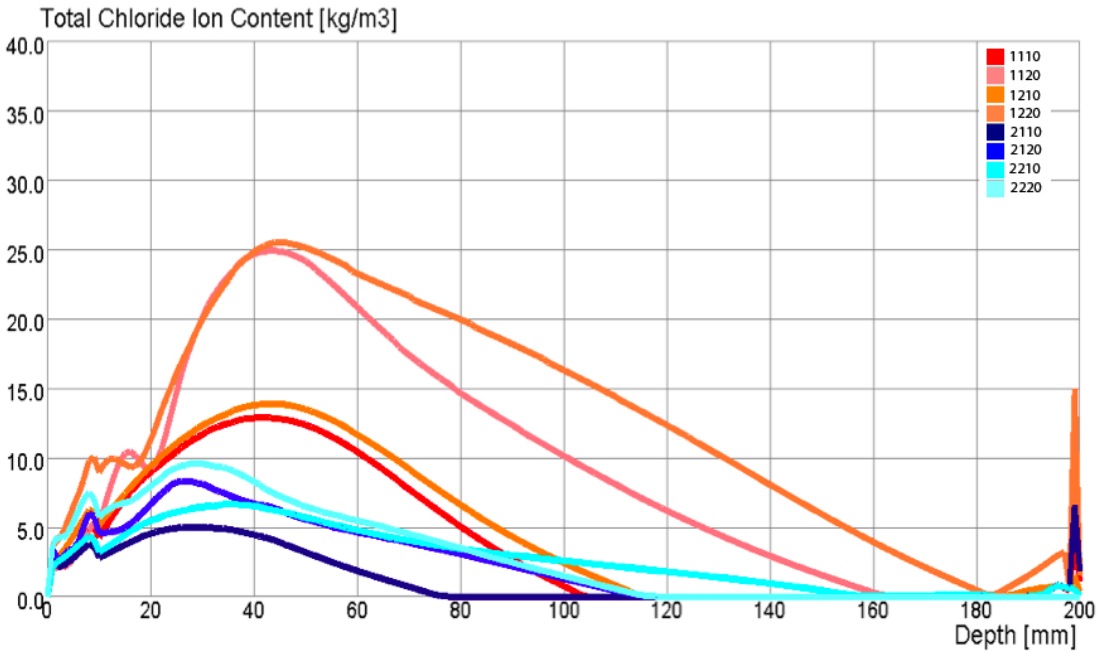

Figure 6.29: Total Chloride Ion Distribution at Time of Sampling for Splash Exposure using Probabilistic Analysis

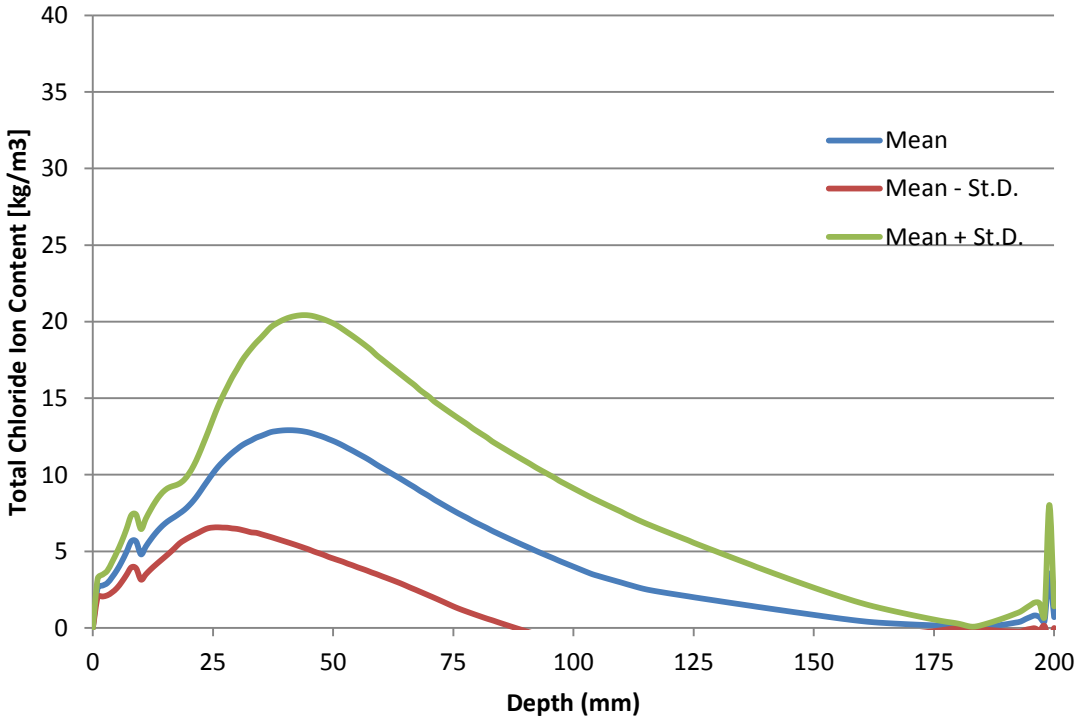

Figure 6.30: Mean and Standard Deviation at Time of Sampling for Splash Exposure

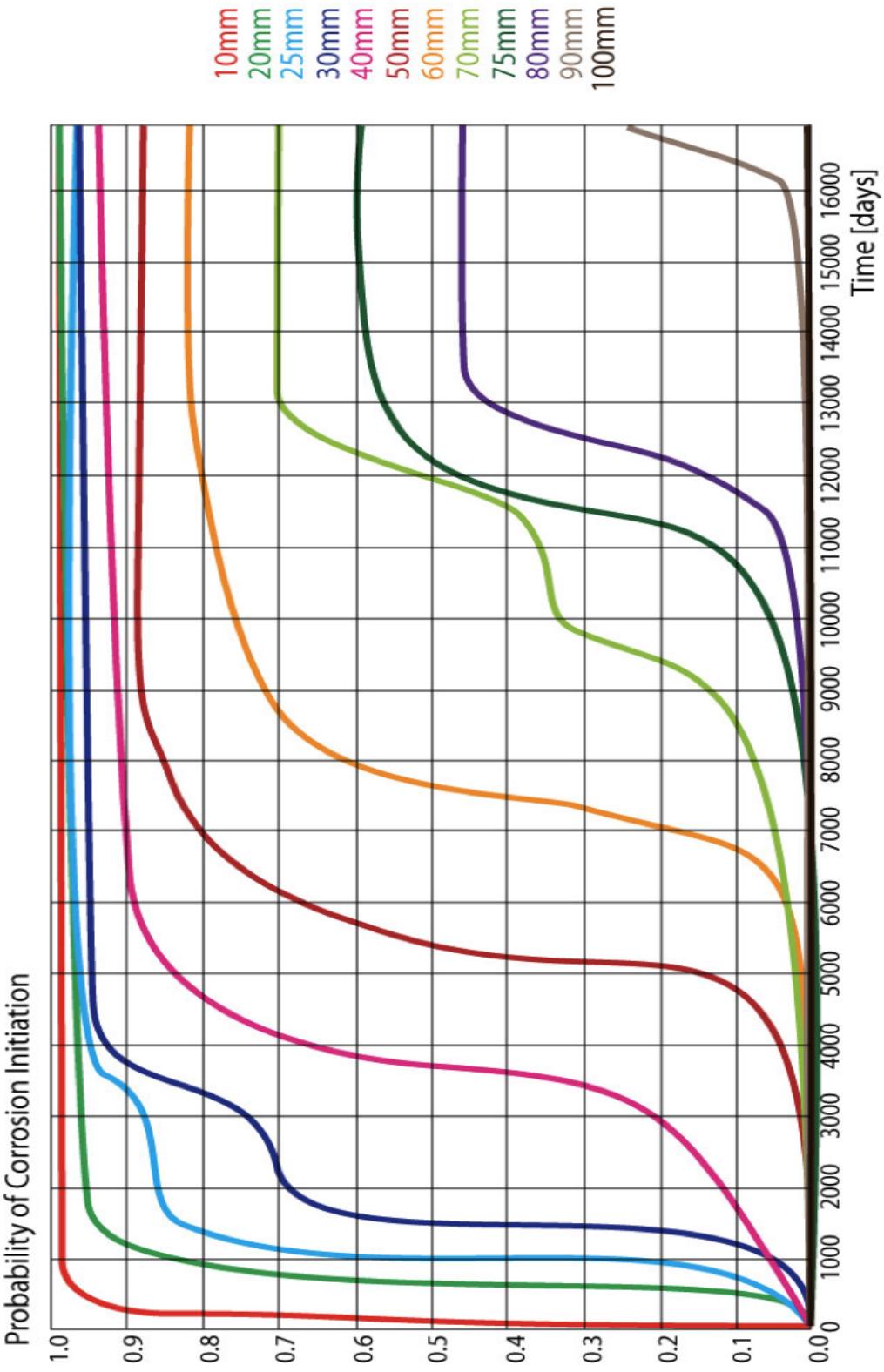

Figure 6.31: Probability of Corrosion Initiation Distributions under Mist Exposure for Various Depths of Reinforcing Steel

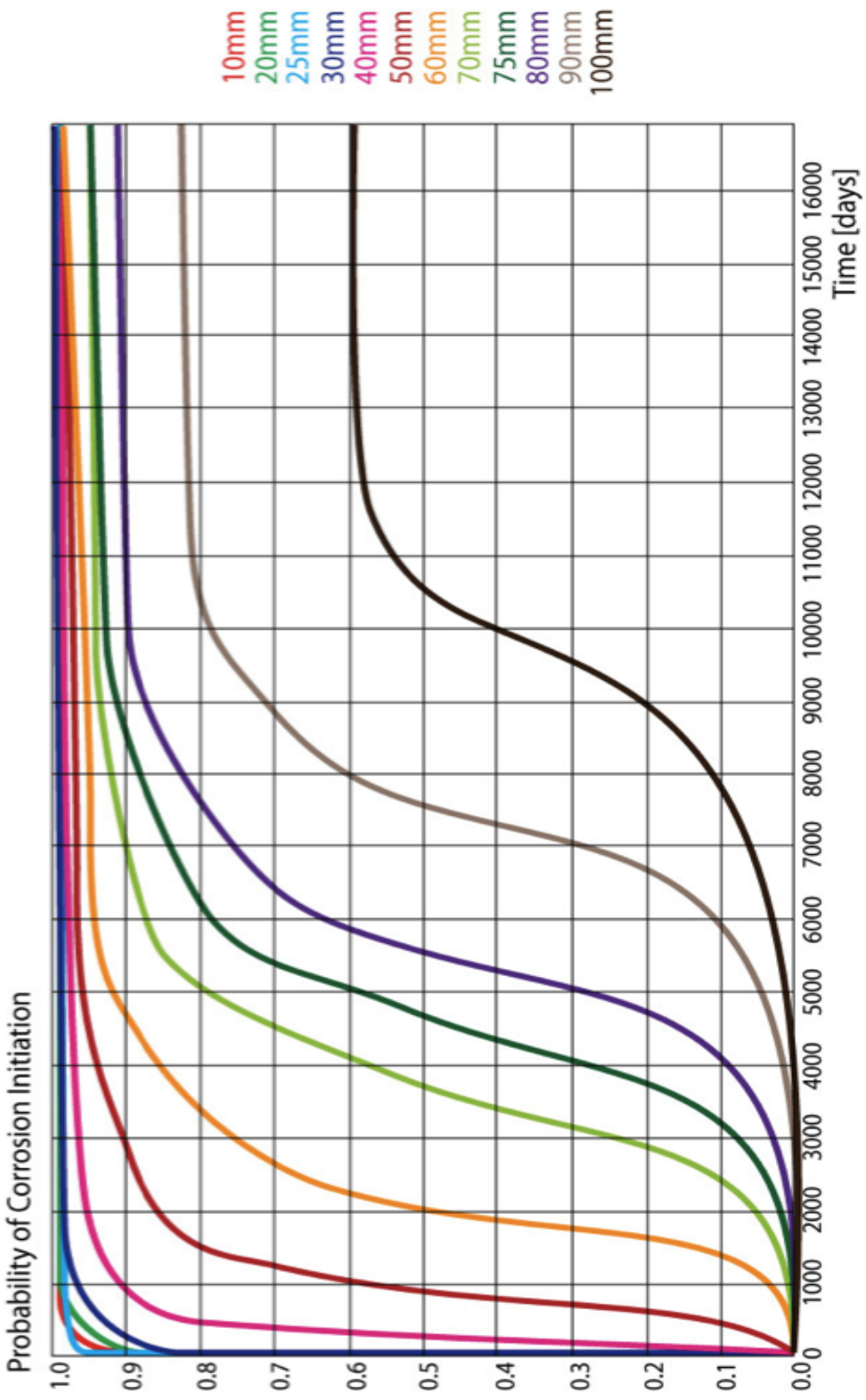

Figure 6.32: Probability of Corrosion Initiation Distributions under Direct Exposure for Various Depths of Reinforcing Steel

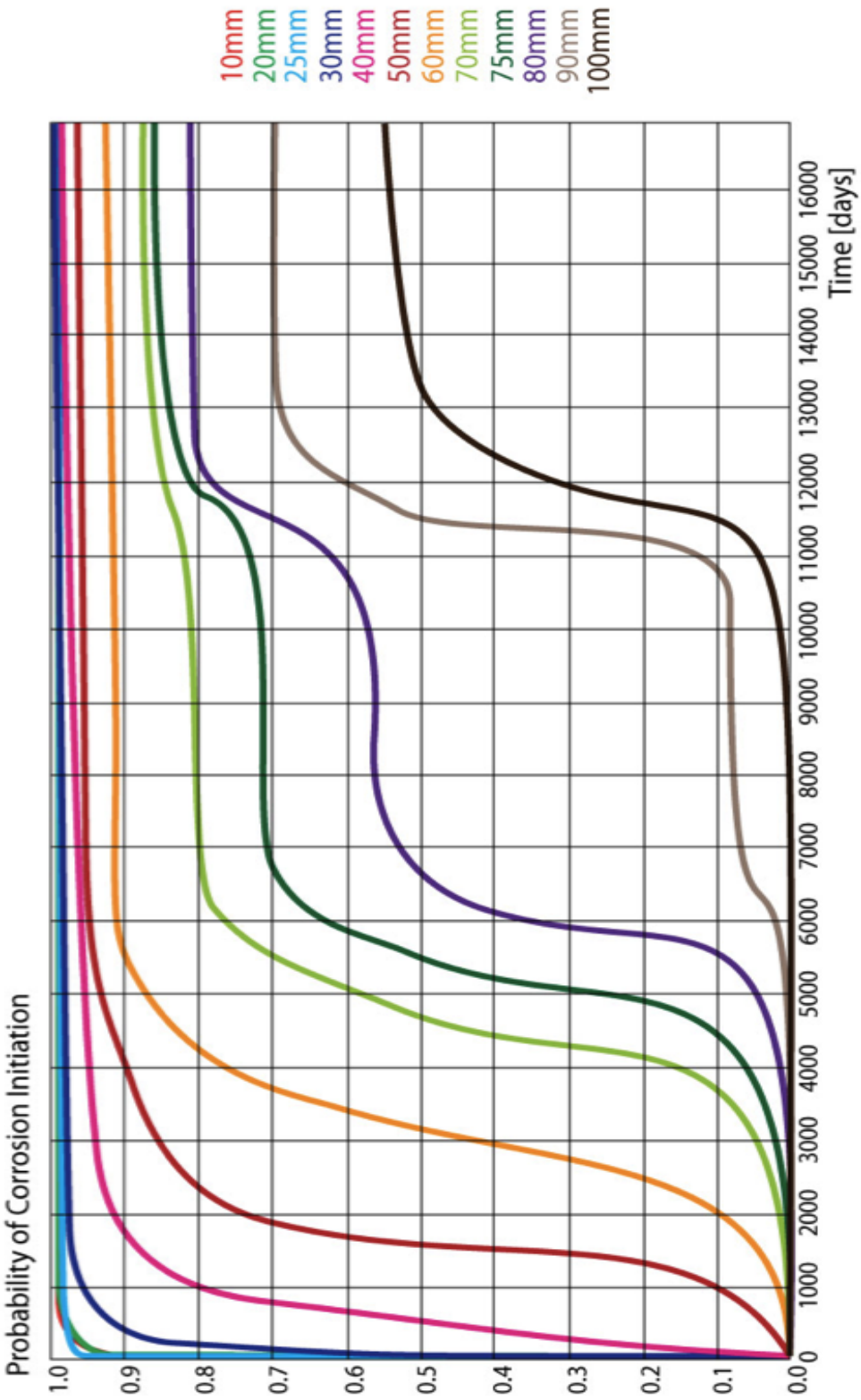

Figure 6.33: Probability of Corrosion Initiation Distributions under Splash Exposure for Various Depths of Reinforcing Steel

Chapter 7

Discussion

7.1 General

Many different disciplines were introduced that are necessary for the TransChlor model. It is important then to validate the work and give merit to the results. In this chapter, the input parameters, advantages and disadvantages of TransChlor, preliminary analysis, probabilistic analysis, and results are further discussed.

7.2 Input Parameters

In this section, validation of the assumptions and input parameters are discussed, as well as the climatic and salt estimation model. It is crucial that the input parameters are correct and as realistic as possible because the results are dependant on them. If the initial assumptions and parameters are not right, then the results will not be relevant and not represent the state of the structure under investigation. For instance, if a structure in the Northern Territories is being analyzed, input parameters for a structure in the Prairies will not be suitable and the results will have no significance.

There are three main types of input parameters used in the TransChlor; climatic data, concrete specification, and model parameters. Salt estimation is included in the model parameters.

There are several advantages and disadvantages of using climatic data as opposed to a general seasonal trend. When past climatic data is used, the precision of the simulation is increased since more factual climatic events are processed. The data provided from Environment Canada provides a wide range of data, including hourly temperature, relative humidity, wind, precipitation, etc. The TransChlor model uses this data to simulate salt application based on climatic trigger criteria based on how much water has precipitated on the ground, the severity of wetting and drying, temperature fluctuations, relative humidity in the air, etc.

Hourly data is used in the TransChlor model. If the time period were any longer, such as daily, the wetting drying cycle would not be accounted for. A smaller time period, say 15-minutes, could be used which would give even more accuracy to the atmospheric conditions. However, it is very unlikely to acquire a lot of data smaller than 1-hour durations for a long period of time.

Furthermore, precipitation was not separated into rain and snow. Therefore, the simulation can't distinguish between the two, and would cause fewer triggers in the model. This is because the temperature might not be below the critical temperature while there is precipitate and a trigger won't be recorded, where if it was snow, it does not rely on temperature to cause a trigger in the model and would be recorded. As a result, the total amount of triggers in our simulations is lower and the number of interventions is underestimated.

The concrete specification is another input parameter that requires the acquisition of precise data. It is important to know the concrete specifications used in the construction of the structural members since it influences the transport properties. The various specifications, such as w/c, cement content, air content, aggregates, etc., have an effect on the capillary suction and diffusion coefficient of the concrete. Fortunately, specifications are regulated and recorded during the time of construction and, therefore, were easily found for use with the TransChlor model.

However, concrete is in itself a very unpredictable material. Even in the same batch, the concrete can have large differences in constitution and performance. For that reason, the TransChlor model transforms the concrete specifications into diffusion and capillary suction coefficient based on past research and simulations. It takes into account the inherent variability in concrete, and subsequently the diffusion coefficients, by incorporating probabilities in the simulations. Extensive research has been done to determine these distribution functions for the diffusion and capillary suction coefficients. Therefore, by doing so, the inherent variability found in concrete is considered in the model and incorporated in the simulations.

The greatest difficulty in the input parameters was related to the salt estimation and specification. They are the annual chloride ion concentration, the amount spread per intervention and the time between two interventions.

As was mentioned before, the annual chloride ion concentration was the toughest to specify. To obtain this value, calibration of the model was done with data samples taken from a bridge overpass.

The average spread rate of salting trucks is based on government guidelines. The CEPA Priority Substance List Assessment Report recommends salt application rates for each province and major city. The recommended salt application rate for Montreal was used in the TransChlor simulation, which is 300 kg/2-lane km.

The time between salting was not implicitly documented in any report and it was assumed that 8-hours was a sufficient amount of time between salt spreads to minimize risks and be cost effective. It was understood that if the time between passes was too short (2-4 hours), the cost would outweigh the benefits, and if it was too long (10-12 hours), the roads may become unsafe.

In practice salting techniques vary from winter to winter and from storm to storm. Depending on the severity of the storm, the amount of salt and time between interventions may vary greatly. The fluctuation in salting is not accounted for in the TransChlor model simulations. More precise simulations could be obtained if a salt spreading log from spreader trucks was available.

This is advantageous because the amount of interventions is calculated based on the climate and is not directly related to the actual amount of interventions employed. Using a salt spreading data set, there would be no need to base salt application in the simulation on number of estimated interventions, and instead base it on actual interventions.

7.3 Advantages/Disadvantages of TransChlor

Since the majority of the work was done using the TransChlor model, an in-depth discussion on its advantages and disadvantages will be reviewed in this section. TransChlor is a powerful simulation program that models the ingress of chloride ions in the concrete cover. There are several advantages of using TransChlor over other models, which will be explained below.

Chloride ion ingress models have evolved as a function of time. The original models were based on Fick's diffusion law. The TransChlor model is much more sophisticated then its predecessors and includes other transport properties, such as capillary suction, transport of liquid and vapor water, diffusion of water, diffusion of chlorides, and thermal effects. The TransChlor model also accounts for actual concrete specifications and meteorological conditions.

Thermal effects on transport properties are taken into account with data on air temperatures. Water is considered in the model using precipitation data. Relative

humidity has an important role since it affects mist exposure. Solar radiation data, which has an affect on wetting and drying cycles, is incorporated in the simulations as well. Furthermore, the model only triggers salt spread based on interventions that are a function of the climate (i.e. if it rain below freezing point or snows). Therefore, it can be seen that the climate has a big affect on the transport of chloride ions in concrete.

The only disadvantage with the climatic model is that it does not directly take into account the effect of wind. Wind can greatly affect the exposure of concrete elements to deicing salts. The salt can be blown away and not stay on the surface. Less salt on the surface would mean less chloride ions that can penetrate into the concrete cover. Furthermore, mist can be blown away from the structure and not attack it as severely, as is shown in Figure 6.12.

Another advantage the TransChlor model has is that it produces corrosion initiation curves. The corrosion initiation curves takes into account the corrosion resistance of the steel as well as the clear cover depth.

Furthermore, the model takes into account probabilities in its simulation with respect to transport properties, corrosion resistance of steel and depth of steel. This is unique to the TransChlor model.

There are some disadvantages of using the TransChlor model as well. For instance, the model does not take into account advanced chemical changes and the evolution of the concrete composition that affect the transport properties. Also, the chemical balance has a large influence on chloride ion ingress. Furthermore, other chemicals can enter the concrete and may affect the depassivation and corrosion initiation of steel. In the field, chlorides are not the only chemicals that can enter the concrete and this could make the corrosion process a lot more complex. Other chemicals can interact with the concrete or the chlorides or both and may interfere with the

corrosion process, either by accelerating or hindering it. However, on a reinforced concrete bridge deck, deicing salts is generally the only chemical that is found in a large enough quantity to have a significant effect on the reinforcement. TransChlor does take into account basic chemical reactions between the concrete and chloride ions.

Cracking of the concrete is also not taken into account in the model. Cracked concrete can lead to easier ingress of chloride ions, moisture and oxygen. This would cause faster depassivation of the steel and subsequently accelerated corrosion. For example, let's say under normal conditions for sound concrete, steel found at 50 mm depth for direct exposure will initiate corrosion in 10 years. If the concrete were to develop 30 mm deep cracks, it could be assumed that the concrete cover would decrease to 20 mm, and will initiate corrosion in 3 years. This illustrates the detrimental effect of cracking on corrosion protection. On the other hand, for normal sized crack widths (up to roughly 0.4mm), self-healing of cracks being filled and sealed by calcium, dirt or rust products has been frequently observed (CEB 1992). This would hinder the flow of oxygen to the steel and stop corrosion from continuing.

Lastly, the fluctuation in deicing salt use is not taken into account. Higher application rates would be used for larger and more severe storms. Furthermore, bridges would have a higher application rate compared with roads and therefore, should be considered in the simulations. The time interval between salting interventions also changes and may be more frequent in large storms and less frequent in smaller storms.

7.4 Preliminary Analysis

The main objective of the preliminary analysis was to determine the average annual amount of salt spread during each winter. To do so, simple chloride ion profiles were created for various total annual salt spread concentrations and were compared with samples taken from actual bridges. The spread concentrations used were 5, 10, and 20 tons of salt per lane km.

The chloride ion profiles are shown in Figures 6.3 to 6.11. Three graphs were made for each exposure class as a function of time at depths of 25 and 50 mm and as a function of depth at the time of sampling. Comparison of the chloride ion profiles with the samples is shown in Figures 6.13 and 6.14.

To determine the average annual amount of salt spread during each winter, the direct and splash exposures curves were compared with data samples. It was determined that 15 tons per lane-km was the most suitable estimate based on the preliminary analysis.

Comparing all nine graphs for the exposures, one can see that the chloride ion profile increases with an increase in annual concentrations. The chloride ion profile for 20 tons annually per lane-km is greater than the chloride ion profile for 5 tons annually per lane-km and can be seen to be almost double. This increase in graphs is observed for each exposure condition.

The direct and splash exposures are very similar, following the same general trend. They both reach higher concentrations then the mist exposure due to the fact they are in direct contact with liquid water, as opposed to vapor water. This causes a more severe and aggressive ingress of chloride ions into the concrete structure for these two exposure conditions. It is observed that the direct exposure can reach a

higher concentration then splash since it is in constant contact with liquid water, where as splash is only sporadically in contact with liquid water.

Mist exposure is usually less severe because it does not constantly attack the same spot over and over. Mist generally flows in the direction of wind, which can carry the mist particles in every possible direction. On the contrary for overpasses, mist exposure is more severe since the chloride-laden mist travels forward and upwards due to the passage of vehicles, which constantly travel in the same direction and therefore cause the mist to flow in that direction. The mist therefore attacks the same spot on the underside of the bridge. This constant state of mist saturation causes high moisture content that allows easier ingress of chloride ions into the concrete. Since mist is composed of vapor, oxygen can also enter with the mist and provide all the essential ingredients to initiate and progress corrosion.

It is also noted that chloride ion concentrations due to direct and splash exposures are very sporadic and undergo large variations as a function of time close to the concrete surface. This can be observed by comparing the chloride ion profiles at 25mm depth with the chloride ion profiles at 50mm depth for both exposures. To better understand the difference in variations of the chloride ion profile with respect to depth, an illustrative example is shown in Figure 7.1.

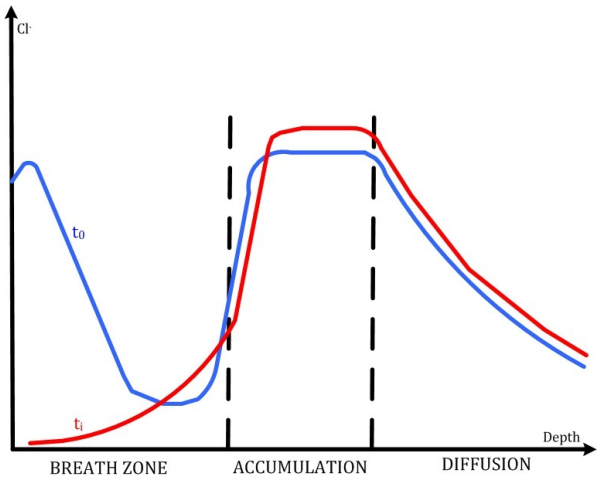

Figure 7.1: Zone Classification with Depth

There are three zone classifications with respect to chloride ion ingress in the concrete cover. The three classifications are the breath zone, the accumulation zone and the diffusion zone. The blue curve in the Figure represents salt being spread on the surface at an initial time and the red curve represents the chlorides progression after a significant amount of time has passed to allow the ions to ingress inwards.

As can be seen, the chloride ion concentration fluctuates a lot more in the breath zone than in the accumulation and diffusion zones. This is due to capillary suction, which is a phenomenon that affects liquid water content. Capillary suction is a quick transport property that only occurs close to the surface. It causes a rapid change in chloride ion content close to the surface. Mist water must condensate to liquid water to be affected by capillary suction and is therefore less susceptible to its action. Therefore, mist exposure does not undergo large fluctuations within shallow depths, as is the case with direct and splash exposures.

The chloride ions in the accumulation and diffusion zones do not vary as much as in the breath zone. These locations are deeper inside the concrete and are governed by diffusion and are not influence by capillary suction. Diffusion is a much slower transport mechanism in comparison with capillary suction. The accumulation zone is the area where chloride ions build up and the diffusion zone is the area where chloride ions from the accumulation zone slowly diffusion deeper into the concrete. The concentration in the accumulation zone increases with time and reaches an equilibrium state only after a few years. Once it reaches equilibrium, the concentration does not vary much with time and stays relatively constant. This is because the rate of chloride ions entering the accumulation zone from the breath zone is balanced with the rate of chlorides diffusing away into the diffusion zone. Hence, direct and splash exposures become much less variable with increased depth.

When comparing all three exposures, it is seen that the mist exposure profiles reaches a similar chloride ion profile as that of direct and splash exposure but is

much less sporadic. This is because Montreal has a very high relative humidity, and when the humidity surpasses a critical humidity in the model, it causes the simulation to trigger a mist exposure. However, in actuality, the mist exposure is not as severe because wind is not taken into account. As a result, the model causes an overestimation of mist attack on bridge structures, since most of the chloride-laden mist is blown away. Nevertheless, the underside of an overpass can be severely damaged by mist attack. The model for mist exposure could be updated to take wind into account by reducing the chloride ion surface concentration when wind occurs for that particular hour.

The TransChlor model was not created to take wind into effect because wind is not severe in Switzerland where this model was originally designed. Hence, mist exposure was more precise since there is little wind and was only dependant on relative humidity, where as here in Montreal, mist exposure is dependant on relative humidity and wind. Further research into mist attack and the effect of wind should be studied.

7.5 Probabilistic Analysis

The majority of the work done in this thesis was geared towards running a probabilistic analysis with the TransChlor model. The model uses a two-point Rosenblueth estimation method using 3 variables. In this section, the probabilistic analysis will be reviewed, as well as the graphs and cumulative distribution curves produced.

The Rosenblueth point estimation method was selected for use in the TransChlor model because it is not as computationally intensive as the Monte Carlo simulation but does produces comparable results. The time to run one simulation with the TransChlor model is roughly 30 to 60 hours. Therefore, the time to run the

TransChlor model with the Rosenblueth point estimation method, which uses 8 simulations in this work, varies from 10 to 20 days.

This time is much shorter than the Monte Carlo simulation because the Monte-Carlo estimate is affected by statistical uncertainty and therefore, contains a random error term. This error term converges to zero only as the number of simulations tends to infinity (Bucher and Frangopol 2006). Thus, many simulations would be needed using the Monte-Carlo simulation technique so that the error term becomes negligible.

The chloride ion profiles obtained by using the Rosenblueth method are shown in Figures 6.18 to 6.29. Four graphs were made for each exposure class, two graphs with respect to time at 25 and 50 mm depth, one with respect to depth at the time of sampling, and one with the mean and standard deviation at the time of sampling. The comparison of the chloride ion profiles with the samples is seen in Figures 6.16 and 6.17.

The difference between graphs for the simple and probabilistic approach is best illustrated by comparing Figures 6.13 and 6.14 with 6.16 and 6.17. In the simple approach, the variation between curves is due to the change in annual chloride ion concentration where as in the probabilistic approach, the change in curves is due to variation in transport properties.

Analyzing the chloride ion samples in Figure 6.16, it confirms that the range of transport properties were appropriate since sample observations fall in between the curves produced. It should be mentioned that the simulation results are skewed towards higher chloride ion profiles. Hence, the annual salt concentration of 15-tons per lane-km is suitable.

Looking at all the graphs, it can be seen that each transport properties affects the amount and rate of chloride ion ingress. It is observed that there are two bands that

are created in the chloride ion profiles from the two values used for the hydraulic transport of water by diffusion, D_{HR}. Using a lower value causes the chloride ion profiles to reach a much higher concentration. This is because the chlorides builds up in the accumulation zone and does not diffuse further into the concrete quickly. This causes the peak chloride ion concentration to become much higher. Within the band, the ionic transport of chlorides, D_{Cl}, determines the magnitude of the peak concentration. A higher value for this parameter causes a larger chloride ion profile since the rate of ingress of the chlorides ions in water is much greater. Lastly, it was found that the hydraulic transport of water by capillary action, D_{CAP}, also has a slight effect on the chloride ion profile, with an increase in this coefficient causing a smaller increase in the profile. As has been mentioned, carbonation was not taken into account because the depth of carbonation does not reach a significant depth after 50 years.

The cumulative distribution curves for the initiation of corrosion are presented in Figures 6.30 to 6.32. It can be seen that the cumulative probability decreases with an increase in depth of steel. Direct exposure is the most severe, followed by splash, and then mist.

Analyzing Figure 6.30 for mist exposure, the probability of corrosion dramatically decreases with depth. It can be seen that the estimated time till corrosion initiation for steel at 25 mm is 4 years (± 2 years), at 50 mm is 15 years (± 3 years), at 75 mm is 32 years (± 3 years), and at 100 mm is 40 years. (± 7 years) These values are determined by integrating the probability distribution function. It is also noted that probability that corrosion has initiated also drastically reduces considering for steel at 25 mm it plateaus at 97%, for steel at 50 mm at 89%, for steel at 75 mm at 59%, and for steel at 100 mm at 2%. The plateau indicates that at a certain point in time, the chloride ion content distribution reaches a steady state and does not surpass the critical chloride ion concentration distribution any further. This is therefore the highest probability that corrosion will initiate.

Examining Figure 6.31 for direct exposure, the probability of corrosion is very high for the first 40 mm and only decreases thereafter. The estimated time till corrosion initiation for steel at 25 mm is roughly in the first year (± ½ year), at 50 mm is 4 years (± 3 years), at 75 mm is 13 years (± 4 years), and at 100 mm is 26 years (± 4 years). The probability that corrosion has initiated also reduces with depth, with steel at 25 mm peaking at 99%, for steel at 50 mm at 98%, for steel at 75 mm at 93%, and for steel at 100 mm at 59%.

Evaluating Figure 6.32 for splash exposure, the probability of corrosion is similar to that of direct exposure but a little less severe. The estimated time till corrosion initiation for steel at 25 mm is also in the first year (± 1½ year), at 50 mm is 5 years (± 3 years), at 75 mm is 17 years (± 6 years), and at 100 mm is 33 years (± 4 years). The probability that corrosion has initiated is also smaller then direct exposure, with steel at 25 mm maxing at 99%, for steel at 50 mm at 95%, for steel at 75 mm at 85%, and for steel at 100 mm at 55%.

It is concluded that the closer the steel is to the surface, the higher the probability that corrosion will occur and at a much faster rate. At the shallower depths, the steel is more susceptible to chloride ion attack. This is even more emphasized in the direct and splash curves. Capillary action causes quick transport in the outer surface, causing steel within the first 30 mm to be really vulnerable to chloride attack and begin corroding.

These results emphasize how essential clear concrete cover is to the protection of reinforcing steel. Steel close to the surface (i.e. 25 mm) can begin corroding very quickly within the first few years, where as steel placed double in depth would take 3 to 5 times longer, tripled would take 10 to 15 times longer, and quadrupled would take 25 to 30 times longer if not more. For that reason, it is important that the minimum specified concrete cover of 75 mm is respected. This will insure that the reinforced concrete structures last as long as possible.

Chapter 8

Conclusions

8.1 General

This dissertation used the TransChlor model to simulate corrosion initiation of reinforcing steel in concrete elements. It is a powerful computer program that produces chloride ion profiles and compares them with steel depth. The benefit of using such a model is the amelioration of structural design and can be used to complement maintenance planning and strategy programs. In this final chapter, the use of TransChlor for maintenance strategies will be discussed. Key points of future work and research on this topic will also be presented.

Initial structural design is based on ultimate strength calculations using intact material and very rarely is design analysis performed with degraded material (i.e. delaminated concrete cover, steel corroded). This type of analysis is only performed once a structure begins to deteriorate and retrofitting is required. However, just like cars are required to have maintenance strategy manuals, structures should be required to have them as well. Considering buildings and bridges cost several times more than cars as well as the enormous cost to repair and replace them, a maintenance strategy and proper planning would be highly advantageous.

A proper maintenance program is one that incorporates a realistic planning schedule that also maximizes resources. This promotes better allocation of time, money, and energy. Using a good maintenance program corrects problems before they can lead into major concerns and thus, serious problem are less likely to occur.

Catching small problems before they can spread lowers resource demands since larger problems tend to require substantially more time, money and energy to fix.

Since the main objective of a maintenance strategy is the planning, inspection and repairs of a structure, it is essential to prediction how a structure will behave during its service life. In this work, modeling of a structure exposed to deicing salt was performed with TransChlor. Therefore, structures exposed to chloride attack can use this model for its structural analysis and maintenance strategies.

At discrete time intervals, chloride ion profiles can be created. These profiles can be compared with the type and depth of steel used to produce corrosion initiation curves and to determine if corrosion has initiated. If corrosion has not initiated, then the structure can be assumed to be at full capacity. On the other hand, if corrosion has begun, a simple corrosion analysis or corrosion propagation model can be used to determine the loss of steel with time for each individual bar.

Using the updated reinforcing area, an in-depth structural analysis can be used against code checks and design criteria. CSA-S6 has a section on how to analyze existing bridges. This should include flexural, shear, and axial capacities, as well as bond strength and crack control. This can be performed with a wide range of structural analysis software.

Using this technique, the estimated dates of inspection and rehabilitations can be determined. Structures are designed with a certain level of safety by using modification and safety factors. To establish when a structure should be retrofitted, the limiting capacity of the structural members should be based on design checks that reaches a utilization factors less than or equal to 1. The critical amount of steel area can thus be determined in this approach. This type of analysis can be performed prior to the simulations to determine the minimum steel area required.

This is just one of many ideas how rehabilitation can be incorporated into the deign process. This is a powerful tool for owners since they can develop exceptionally detailed and structured maintenance programs and also have significantly more control over the structure. Therefore, the guesswork is taken out of maintenance strategies, repairs and replacements (Enright and Frangopol 1998; Akgul and Frangopol 2005; Akgul and Frangopol 2005; Neves and Frangopol 2005; Petcherdchoo, Neves et al. 2008; Biondini and Frangopol 2009).

Maintenance strategies are crucial to our society so that structures remain in safe working condition for as long as possible. Failure of just one overpass can cause significant damage to society. It would require time, money, resources, and energy in fixing the overpass. Furthermore, society is affected as well. Commuters will loose time getting to the desired destination since the route is blocked and will need to be detoured. This will inevitably cause traffic to build elsewhere and cause an added inconvenience to the commune. Employees will tend to be late which cause a loss in wages due to lateness. Businesses will also lose income since the main transport of goods and services, as well as costumer access, is by roads. Water mains, wastepipes, and electrical cables may also be affected due to road failures.

However, the most serious consequence of a road or overpass collapse is the loss of life. It can be extremely dangerous to an individual if an overpass, which has thousands of pounds of concrete and steel, were to fall on them. Although it is an infrequent occurrence, the possibility of a collapse is still present and the loss of time, money and energy is nothing in comparison to the loss of a life. Great care must therefore be taken so that the degradation of a structure never becomes seriously hazardous to the motorist or occupants that use them.

Maintenance and inspection programs can determine the state a structure is in. Depending on the results, the structure can be deemed safe for full loading or even partial loading. It could also avoid and mitigate any inconveniences to society, be

able to catch and stop problems before they become severe and insure the most efficient usage of the structure and limited resources. For this reason, maintenance strategies, repairs, rehabilitation, retrofitting and decommissioning are aspects that should never be forgotten or neglected. The stability of society and the safety of the individuals that use the structures depend on it.

8.2 Recommendations for Future Research

The ongoing strive for knowledge is one that will never cease. With leaps and bounds in technological advancements, new work and research is being created each and every day, each providing new discoveries and conclusions. There is a great opportunity for further development of the various components in this work. In this last section, the potential for further work will be presented below.

- A cost/benefit analysis comparing automatic versus mechanical deicing salt techniques should be investigated. An automatic salt dispenser is a computer-operated mechanism incorporated into the roadway that can spray brine directly on the surface. Some of the expenses would include start up costs, material, training, employment, maintenance of equipment, etc. The benefits would include efficient use of salts by regulating salt rates and monitoring salt spread into the environment, less spending on salt material, less trucks and staff required, less salt attack on reinforced concrete bridge elements since less salt is used, etc. This would further extend the life expectancy of a bridge. Furthermore, automatic deicing salt dispensers can be deployed instantly, with no need for maintenance crews and no delay in getting salt to the section of highway that's of interest. For instance, when a road sensor is triggered, salts applied by automatic dispensers can be sprayed instantly. On the other hand, if salts are applied manually, a truck driver must go to the salt storage site, load the truck, travel to the destination and salt the area. This

requires substantially more time to spread the same amount of salt. During this time, more snow and ice would have accumulated on the roads, rendering the surfaces unsafe for use.

- The inherent variability associated with concrete makes it very challenging to predict its behavior in the environment. Concrete is a highly variable material, which makes it hard to model. This is because there are many different mixtures, with varying aggregate types, cementitious materials, water contents, air contents, etc. Hence, one concrete mixture will not have the same properties as another. In addition, a structure will have large variations since one batch can be different from another batch. Also, chemical composition of concrete changes with time as it cures. Therefore, the concrete material is not the same as it originally started out as. For this reason, the inclusion of a micro model would be beneficial in the modeling of chloride ion in concrete. A micro model, such as Stadium®, would take into account the chemical reactions involved, as well as the concrete phase changes and curing process. It would also take into account the chemical changes when concrete comes into contact with other chemicals, such as sulfates, carbonates, chlorides etc. Additionally, chloride binding to the concrete and free chloride ions is more accurately simulated. The combination of a micro model within TransChlor would be a major improvement.

- The effect of wind was not included in the TransChlor model. It was concluded that mist exposure was affected by such, and thus, future work should be done on this topic. Field studies are needed to determine the correlation between mist exposure and wind.

- The effect of concrete cracking is also not included in the TransChlor model. When the concrete cracks, it is easier for chloride ions, moisture and oxygen

to ingress into the concrete. Thus the time to corrosion initiation is much shorter and this effect should be included in future models.

- The TransChlor model produces cumulative distribution corrosion initiation curves, but does not incorporate corrosion rates once corrosion has begun. Modeling corrosion is seemingly difficult because of the complexity in determining the corrosion rate for a particular concrete and steel. Obtaining corrosion rates for a specific structure can only be obtained by field measurements. Although, average corrosion rates of nearby structures can be taken, they may be irrelevant since there are differences in materials, traffic loading, and exposures. Tests in laboratories have also been done, but once again do not have much relevance because of the perfect conditions in a control room compared with the imperfections and fluctuations in the field. Nevertheless, there are models that simulate corrosion rates with respect to oxygen and moisture availability, which are related to the depth of reinforcing steel and w/c, respectively (Duprat 2007).

- Each bridge is subjected to traffic loads. The intensity and frequency of traffic live loads vary from bridge to bridge. It is important to consider traffic live load because it affects the degradation of the structure, namely the corrosion rate and deterioration of the concrete. Higher stresses in the steel cause faster corrosion rates and increased wheel pounding causes faster abrasion of the concrete surface. A traffic live load stress model would be able to take the effect of load into account. Modeling the degradation due to traffic loading would give even more precision to predicting the service life of the structure.

Combing all the models into one, (i.e. micro model, macro model, corrosion rates, stress loading), would simulate every aspect of the reinforced concrete deterioration process. With more accurate modeling of our structures, designers and owners can better plan for their service life, intended use, maintenance strategies, and

investigations. However, caution is needed since more complicated models allow larger room for errors, inaccuracies, and misinterpretations of what is actually happening in the field. It is therefore very important to verify that the structures are performing as the model predicted. This guarantees a level of safety and confirms the suitability of the model. Nevertheless, combining all the models into a single computer software would give engineers a powerful tool for the design of future structures.

Research still needs to be done in the field and in the laboratory with respect to corrosion. Long-term test and investigations would be a huge asset but they hardly exist because of the large costs and time needed. Companies cannot afford to monitor an entire bridge for its service life. Therefore, government and university-funded programs should continue to perform these research programs.

References

AASHTO. (2009). "Winter Operations and Salt, Sand, and Chemical Management: Stewardship Practices for Reducing Salt and Other Chemical Usage." Center for Environment Excellence, from http://environment.transportation.org/environmental_issues/construct_maint_prac/compendium/manual/8_4.aspx.

Akgul, F. and D. M. Frangopol (2005). "Lifetime Performance Analysis of Existing Reinforced Concrete Bridges. I: Theory." Journal of infrastructure systems / **11**(2): 122.

Akgul, F. and D. M. Frangopol (2005). "Lifetime Performance Analysis of Existing Reinforced Concrete Bridges. II: Application." Journal of infrastructure systems / **11**(2): 129.

Biondini, F. and D. M. Frangopol (2009). "Lifetime reliability-based optimization of reinforced concrete cross-sections under corrosion." Structural safety. **31**(6): 483.

Boyd, A. (2010). CIVE 623 - Durability of Material. McGill University. Montreal, Quebec.

Brink, M. and M. Auen (2004). "Go Light with the Salt, Please: Developing Information Systems for Winter Roadway Safety." TR news.(230): 3.

Bucher, C. and D. M. Frangopol (2006). "Optimization of lifetime maintenance strategies for deteriorating structures considering probabilities of violating safety, condition, and cost thresholds." Probabilistic Engineering Mechanics **21**(1): 1-8.

Canadian Environmental Protection Act. (1999). from http://www.ec.gc.ca/CEPARegistry/the_act/Download/CEPA_Full_e.htm.

CEB (1992). Durable Concrete Structure: Design Guide, Thomas Telford: 121.

City of Toronto (2004). Salt Management Plan. Transportation Services Division. Toronto**:** 17.

Conciatori, D. (2005). Effet du microclimat sur l'initiation de la corrosion des aciers d'armature dans les ouvrages en béton armé. Civil Engineering. Montreal, Ecole Polytechnique fédérale de lausanne. **PhD:** 264.

Conciatori, D., E. Brühwiler, et al. (2009). "Actions microclimatique et environnementale des ouvrages d'art routiers." Canadian Journal of Civil Engineering **36**: 628-638.

Conciatori, D., E. Brühwiler, et al. (2009a). "Calculation of reinforced concrete corrosion initiation probabilities using the Rosenblueth method." Inderscience Enterprises Ltd. **3**(4).

Conciatori, D., F. Laferrière, et al. (2010). "Comprehensive modeling of chloride ion and water ingress into concrete considering thermal and carbonation state for real climate." Cement and Concrete Research **40**(1): 109-118.

Conciatori, D., H. Sadouki, et al. (2008). "Capillary suction and diffusion model for chloride ingress into concrete." Cement and Concrete Research **38**(12): 1401-1408.

Delisle, C. E. and L. Dériger (2000). Caracterisation et élimination des neiges usées: impacts sur l'environnement. Hull, Environment Canada CEPA Priority Substances List Environmental Resource Group on Road Salts, Commercial Chemicals Evaluation Branch.

Duprat, F. (2007). "Reliability of RC beams under chloride-ingress." Construction and Building Materials **21**(8): 1605-1616.

Enright, M. P. and D. M. Frangopol (1998). "Probabilistic analysis of resistance degradation of reinforced concrete bridge beams under corrosion." Engineering structures. **20**(11): 960.

Enright, M. P. and D. M. Frangopol (2000). "Survey and evaluation of damaged concrete bridges." Journal of bridge engineering. **5**(1).

Environment Canada. (2000). "Priority Substances Assessment Report: Road Salts.", from http://www.ec.gc.ca/CEPARegistry/subs_list/PSL2.cfm.

Environment Canada. (2006). "Winter Road Maintenance Activities and the Use of Road Salts in Canada: A Compendium of Costs and Benefits Indicators.", from http://www.ec.gc.ca/nopp/roadsalt/reports/en/winter.cfm.

Environment Canada. (2010). from http://www.ec.gc.ca/.

EPA. (1999). "Storm water management fact sheet minimizing effects from highway deicing." from http://purl.access.gpo.gov/GPO/LPS50757.

Henocq et al. (2007). "Determination of the Chloride Content Threshold to Initiate Steel Corrosion." Proceedings of the 5th International Essen Workshop - Transport in Concrete: Nano to Macrostructure.

Huang, R. and C. C. Yang (1997). "Condition assessment of reinforced concrete beams relative to reinforcement corrosion." Cement & concrete composites. **19**(2): 131.

Jefremczuk, S. (2005). Chloride ingress and transport in cracked concrete. Civil Engineering. Montreal, McGill University. **M.Eng.:** 188.

Ketcham, S. A. and et al. (1996). Manual of Practice for an Effective Anti-Icing Program—A Guide for Highway Winter Maintenance Personnel. U.S. Army Cold Regions Research and Engineering Laboratory Corps of Engineers for the Federal Highway Administration. Hanover, New Hampshire.

Kirkpatrick, T. J., R. E. Weyers, et al. (2002). "Probabilistic model for the chloride-induced corrosion service life of bridge decks." Cement and Concrete Research **32**(12): 1943-1960.

Kirkpatrick, T. J., R. E. Weyers, et al. (2002a). "Impact of specification changes on chloride-induced corrosion service life of bridge decks." Cement and Concrete Research **32**(8): 1189-1197.

Liu, Y., R. E. Weyers, et al. (1996). "Time to cracking for chloride-induced corrosion in reinforced concrete."

Lounis, Z., s. International, et al. (2003). "Probabilistic Modeling of Chloride Contamination and Corrosion of Concrete Bridge Structures."

Morin, D. and M. S. Perchanok (2000). Road salt loadings in Canada. [Ottawa], Commercial Chemicals Evaluation Branch, Environment Canada.

National Cooperative Highway Research Program (2007). Guidelines for the selection of snow and ice control materials to mitigate environmental impacts, Levelton Consultants Limited.

National Research Council (1991). Highway deicing : comparing salt and calcium magnesium acetate. Washington, D.C., Transportation Research Board, National Research Council.

Neves, L. C. and D. M. Frangopol (2005). "Condition, safety and cost profiles for deteriorating structures with emphasis on bridges." Reliability engineering & system safety. **89**(2): 185-198.

NYSDOT (2001). Environmental Handbook for Transportation Operations. New York State Department of Transportation Environmental Analysis Bureau**:** 44.

Oregon Dept. of Transportation (1999). Routine road maintenance : water quality and habitat guide best management practices. Salem, Or., Oregon Dept. of Transportation.

Pakvor, A. (1995). "Repair and Strengthening of Concrete Structures: General Aspects." Structural Engineering International **5**(2).

Petcherdchoo, A., L. A. C. Neves, et al. (2008). "Optimizing Lifetime Condition and Reliability of Deteriorating Structures with Emphasis on Bridges." Journal of structural engineering. **134**(4): 544.

Revie, R. W. (2000). Uhlig's Corrosion Handbook (2nd Edition), John Wiley & Sons.

Roberge, P. R. (1999). "Corrosion Doctors." Atmospheric Corrosion Retrieved July 19, 2010, from http://corrosion-doctors.org/.

Rosenblueth, E. (1975). "Point estimates for probability moments." Proceedings of the National Academy of Sciences of the United States of America **72**(10): 3812-3814.

Rush, D. K. (2009). "Deicing Montreal." Ecoengineering Retrieved july 19, 2010, from http://eco-eng.blogspot.com/2009/11/deicing-montreal-proposal.html.

Salt Institute. (2009). from http://www.saltinstitute.org/.

Stewart, M. G. (2003). Temporal and Spatial Aspects of Probabilistic Corrosion Models. Third IABMAS Workshop on Life-Cycle Cost Analysis and Design of Civil Infrastructure Systems and the JCSS Workshop on Probabilistic Modeling of Deterioration Processes in Concrete Structures**:** 10.

Stewart, M. G. and A. Al-Harthy (2008). "Pitting corrosion and structural reliability of corroding RC structures: Experimental data and probabilistic analysis." Reliability engineering & system safety. **93**(3): 373-382.

Stewart, M. G. and D. V. Rosowsky (1998). "Time-dependent reliability of deteriorating reinforced concrete bridge decks." Structural safety. **20**(1): 91.

Tikalsky, P. J., D. Pustka, et al. (2005). "Statistical Variations in Chloride Diffusion in Concrete Bridges." ACI structural journal. **102**(3): 481.

Transport Québec. (1994). "System for Storing and Loading Deicing Salt." from http://www1.mtq.gouv.qc.ca/en/projet_recherche/description.asp?NO_PROJ=E031.1P1.

Transportation Association of Canada (2003). Syntheses of best practices. Road salt management. Ottawa, Canada, Transportation Association of Canada.

U.S. Roads. (1997). "Using Salt and Sand for Winter Road Maintenance." Road Management Journal, from http://www.usroads.com/journals/p/rmj/9712/rm971202.htm.

Val, D. V. and M. G. Stewart (2005). "Decision analysis for deteriorating structures." Reliability engineering & system safety. **87**(3): 377-385.

Val, D. V., M. G. Stewart, et al. (1998). "Effect of reinforcement corrosion on reliability of highway bridges." Engineering structures. **20**(11): 1010.

Vu, K. A. T. and M. G. Stewart (2000). "Structural reliability of concrete bridges including improved chloride-induced corrosion models." Structural safety. **22**(4): 313.

Wegner, W. and M. Yagi (2001) "Environmental Impacts of Road Salt and Alternatives in the New York City Watershed." Stormwater.